

Shape-Adaptive Conditional Calibration for Conformal Prediction via Minimax Optimization

Yajie Bao^{1*}, Chuchen Zhang^{1*}, Zhaojun Wang¹, Haojie Ren², and Changliang Zou¹

¹ School of Statistics and Data Science, Nankai University

² School of Mathematical Sciences, Shanghai Jiao Tong University

March 25, 2026

Abstract

Achieving valid conditional coverage in conformal prediction is challenging due to the theoretical difficulty of satisfying pointwise constraints in finite samples. Building upon the characterization of conditional coverage through marginal moment restrictions, we introduce Minimax Optimization Predictive Inference (MOPI), a framework that generalizes prior work by optimizing over a flexible class of set-valued mappings during the calibration phase, rather than simply calibrating a fixed sublevel set. This minimax formulation effectively circumvents the structural constraints of predefined score functions, achieving superior shape adaptivity while maintaining a principled connection to the minimization of mean squared coverage error. Theoretically, we provide non-asymptotic oracle inequalities and show that the convergence rate of the coverage error attains the optimal order under regular conditions. The MOPI also enables valid inference conditional on sensitive attributes that are available during calibration but unobserved at test time. Empirical results on complex, non-standard conditional distributions demonstrate that MOPI produces more efficient prediction sets than existing baselines.

Keywords: Conditional validity; Geometric shape; Mean squared coverage error; Prediction set; Set-valued mapping.

*The first two authors contributed equally to this work and are listed in alphabetical order.

1 Introduction

Predictive inference aims to construct a prediction set for an unknown label based on a machine learning model, ensuring that the prediction set covers the true label with a pre-specified confidence level. This statistical guarantee is essential in high-stakes applications, such as medical diagnosis (Vazquez and Facelli, 2022), safe planning in autonomous systems (Lindemann et al., 2023), and robust decision-making under uncertainty (Johnstone and Cox, 2021), where reliable and uncertainty-aware predictions can enhance decision safety.

Conformal prediction (Vovk et al., 2005) is a distribution-free and model-agnostic tool in predictive inference. Given the test covariate $X \in \mathcal{X}$, it can issue an $(1 - \alpha)$ -level prediction set $C(X)$ for the unobserved label $Y \in \mathcal{Y}$ by using the collected labeled data and a machine learning model. Suppose the labeled data and the test data (X, Y) are independent and identically distributed (i.i.d.) or exchangeable, then the conformal prediction set satisfies the *marginal coverage* property $\mathbb{P}\{Y \in C(X)\} \geq 1 - \alpha$, see Lei et al. (2018). Although marginal coverage offers a simple and attractive validity guarantee, it may fail to provide uniform reliability across individuals or under heterogeneous data distributions. For example, certain subgroups or regions of the covariate space may experience systematic under-coverage. To overcome this limitation, a more stringent and relevant objective is the *test-conditional coverage*: $\mathbb{P}\{Y \in C(X) \mid X\} \geq 1 - \alpha$ almost surely.

Previous work has shown that achieving exact test-conditional coverage is impossible in a distribution-free setting without resorting to trivial prediction sets of infinite expected size (Vovk, 2012; Lei et al., 2013). Consequently, various conformal prediction methods have been proposed to achieve approximate or asymptotic conditional coverage by either modifying the calibration step (Guan, 2023; Hore and Barber, 2025; Gibbs et al., 2025) or using different score functions (Romano et al., 2019; Chernozhukov et al., 2021).

Consider a generalized notion for conditional predictive inference:

$$\mathbb{P}\{Y \in C(X) \mid Z = z\} = 1 - \alpha, \quad \forall z \in \mathcal{Z}, \quad (1)$$

where $Z \in \mathcal{Z}$ is an *arbitrary* conditioning variable. The formulation in (1) encapsulates several important cases: test-conditional coverage when $Z = X$; group-conditional coverage when $Z = \mathbb{1}\{X \in G\}$ where G is a specific group in the covariate domain \mathcal{X} ; the equalized coverage in Romano et al. (2020) when Z represents a sensitive attribute, e.g., gender, race. To achieve this conditional coverage, a natural strategy is the “conditional-to-marginal” relaxation, which transforms the conditional constraint into a set of marginal moment restrictions (Andrews and Shi, 2013):

$$\mathbb{E}[f(Z)(\mathbb{1}\{Y \notin C(X)\} - \alpha)] = 0, \quad \forall f \in \mathcal{F}, \quad (2)$$

where \mathcal{F} is a “weight” function class defined on the conditioning domain \mathcal{Z} . When \mathcal{F} includes all measurable functions, the conditional coverage target (1) is equivalent to the marginal relation (2). A seminal approach leveraging this relaxation is the *conditional calibration* framework proposed by Gibbs et al. (2025), which considers the prediction set of the sublevel form:

$$C(X, Z) = \{y \in \mathcal{Y} : s(X, y) \leq f(Z)\},$$

where s is a fixed score pretrained on a separate dataset and $f \in \mathcal{F}$ is a threshold function to be determined. In this context, finding a prediction set that satisfies (2) can be recast as solving the functional quantile regression problem: $\min_{f \in \mathcal{F}} \mathbb{E}[\ell_\alpha(s(X, Y), f(Z))]$, where $\ell_\alpha(u, v) = (u - v)(\mathbb{1}\{u - v > 0\} - \alpha)$ is the pinball loss.

While computationally tractable, this formulation inherently restricts the predictive region to the sublevel sets of a fixed score function. It can only adjust the volume of the set

in the calibration phase but fails to rotate the shape or alter its aspect ratio to capture local correlations among output variables. This *geometric rigidity* is especially pronounced in multivariate regression with vector-valued labels. Although recent efforts have focused on designing efficient scores during the training phase (Johnstone and Cox, 2021; Thurin et al., 2025), the resulting predictive sets still lack the flexibility to adapt to local distributional heteroscedasticity during calibration. Furthermore, this paradigm typically requires the threshold $f(\cdot)$ to be a direct mapping from observed features. Consequently, it struggles to handle scenarios where Z represents sensitive attributes that can be masked at test time (Zafar et al., 2017). In such cases, a threshold function learned solely on X cannot effectively incorporate the necessary conditioning information from Z during calibration.

1.1 A snapshot of our ideas and contributions

To break these constraints, we introduce *Minimax Optimization Predictive Inference* (MOPI), a novel framework that reformulates conditional predictive inference as a minimax problem. We consider a general and structured set-valued function class:

$$\mathfrak{C} = \left\{ C(x; h) = \{y \in \mathcal{Y} : T(h(x), y) \leq 0\} : h \in \mathcal{H} \right\}, \quad (3)$$

where $T(\cdot, \cdot)$ is a fixed function, $h(x)$ can be a vector or matrix-valued function encoding the geometric structure (e.g., mean $\mu(x)$ or covariance $\Sigma(x)$), and \mathcal{H} is a function class in the covariate domain \mathcal{X} . Assuming \mathcal{F} is symmetric (i.e., $-f \in \mathcal{F}$ whenever $f \in \mathcal{F}$), the deviation of the left-hand side of (2) from zero can be quantified by the maximum quantity $\max_{f \in \mathcal{F}} \mathbb{E}[f(Z)(\mathbb{1}\{Y \in C(X)\} - (1 - \alpha))]$. Hence, we can construct the desired prediction set by *minimizing this maximum quantity* over all set-valued functions $C \in \mathfrak{C}$, leading naturally to a minimax optimization problem (Dikkala et al., 2020):

$$\min_{C \in \mathfrak{C}} \max_{f \in \mathcal{F}} \mathbb{E}[f(Z)(\mathbb{1}\{Y \notin C(X)\} - \alpha) - f^2(Z)],$$

where the term $f^2(Z)$ is used for normalization (see Section 2.2 for details). This framework offers two fundamental advantages. First, by optimizing $C \in \mathfrak{C}$, MOPI can dynamically “reshape” the prediction set through finding the optimal $h \in \mathcal{H}$ in (3), such as adjusting the aspect ratio of a box or the orientation of an ellipsoid, to match local heteroscedasticity. Second, MOPI is inherently suited for masked conditioning variables. By decoupling the coverage enforcement (inner maximization depending on Z) from the predictive mapping (outer minimization depending on X), our framework allows information from Z to guide the construction of prediction set $C(X)$ during the calibration phase without requiring Z at prediction time.

The main contributions of this paper are summarized as follows:

- (1) The MOPI generalizes Gibbs et al. (2025)’s conditional calibration principle by allowing the prediction set’s geometry to co-evolve with the local data density. Moreover, unlike existing conditional conformal methods, which typically require the conditioning variable Z to be a subset of the test covariates (i.e., $Z \subseteq X$), MOPI allows Z to be distinct from X . This decoupling enables our framework to enforce valid conditional coverage on sensitive attributes or latent groups that are available during calibration but masked at test time.
- (2) We demonstrate that the MOPI objective possesses a rigorous statistical interpretation: under mild expressiveness conditions on the weight function class \mathcal{F} , it is equivalent to minimizing the *Mean Squared Coverage Error* (MSCE), defined as $\text{MSCE}(C) = \mathbb{E}[(\mathbb{P}\{Y \notin C(X) \mid Z\} - \alpha)^2]$. We further establish non-asymptotic oracle inequalities for the MSCE of the empirical MOPI predictor. Our analysis provides specific convergence rates for both finite-dimensional and RKHS function classes, matching the optimal order up to logarithmic factors in the group-conditional coverage case.
- (3) We provide a principled guide for choosing the weight function class \mathcal{F} in (2) according

to the cardinality of the conditioning domain \mathcal{Z} . Under practical choices of \mathcal{F} , the inner maximization of the minimax problem admits a closed form, which greatly facilitates the overall optimization process. To solve the empirical problem, we replace the miscoverage indicator with a smooth surrogate, and the corresponding MSCE bound is also established.

- (4) We evaluate MOPI on extensive synthetic and real-world datasets, including those with multi-dimensional labels and masked sensitive attributes. The results demonstrate that MOPI produces more compact prediction sets while maintaining robust conditional coverage performance.

1.2 Related works

Several studies have examined how to achieve test-conditional coverage in the asymptotic regime, typically by designing improved nonconformity scores or by reweighting labeled data. For example, [Romano et al. \(2019\)](#) proposed a conformalized quantile regression score that leverages quantile regression to capture local distributional characteristics of the label. [Chernozhukov et al. \(2021\)](#) introduced a nonconformity score based on joint distribution modeling. More recently, [Guan \(2023\)](#) developed a localized conformal prediction approach that assigned similarity-based weights to calibration scores, which ensured finite-sample marginal coverage and asymptotic conditional coverage under mild distributional assumptions. Building on this framework, [Hore and Barber \(2025\)](#) proposed a randomly localized conformal prediction method that offers relaxed local coverage and marginal validity under certain covariate shifts. Further examples and developments can also be found in [Györfi and Walk \(2019\)](#), [Sesia and Romano \(2021\)](#), and [Kiyani et al. \(2024a\)](#).

Another line of work has focused on approximate notions of test-conditional coverage. [Lei and Wasserman \(2014\)](#) proposed partitioning the covariate space into disjoint bins and constructing prediction sets using only calibration points within the same bin, thereby

achieving group-conditional coverage within each bin of these partitions. [Barber et al. \(2021\)](#) studied the problem of obtaining approximate conditional coverage over every regular subset of the covariate space. Drawing on the idea of multiaccuracy from algorithmic fairness ([Hébert-Johnson et al., 2018](#)), [Jung et al. \(2023\)](#) developed a multivalid conformal prediction method that asymptotically guarantees conditional coverage over any user-specified finite collection of (possibly overlapping) groups. Notably, [Gibbs et al. \(2025\)](#) introduced a conditional calibration (abbreviated as **CC**) framework via functional quantile regression. For the finite-dimensional case, their method provides a finite-sample group-conditional coverage guarantee and maintains marginal validity under a class of covariate shifts. In the infinite-dimensional setting, they characterized relaxed conditional coverage by bounding the absolute deviation in (2). In contrast, our work establishes an oracle inequality for the MSCE, which offers a more direct quantification of conditional coverage.

For vector-valued responses, recent studies have increasingly moved towards parameterized scoring functions that aim to better approximate non-standard prediction set geometries. [Johnstone and Cox \(2021\)](#) and [Messoudi et al. \(2022\)](#) proposed norm-based scores that restrict prediction regions to box or ellipsoidal shapes. [Feldman et al. \(2023\)](#) employed a latent-space representation learning approach to enable non-convex set. [Thurin et al. \(2025\)](#) leveraged optimal transport to define a ranking of multivariate scores, thereby allowing prediction regions beyond predefined geometric families. [Braun et al. \(2025\)](#) studied the volume minimization problem over a class of arbitrary norm-based sets. However, these approaches focus primarily on the design of nonconformity scores within the split conformal prediction framework, rather than adapting the shape of prediction sets during the calibration, and they do not explicitly address conditional coverage for shape-adaptive prediction sets.

The minimax formulations for moment-restriction problems have been explored in several related contexts, including solving nonparametric regression problems ([Dikkala et al., 2020](#)),

the estimation of generalized average causal effects in causal inference (Kallus et al., 2021), off-policy evaluation in reinforcement learning (Shi et al., 2022), and parameter estimation under conditional moment constraints (Bennett and Kallus, 2023). In contrast, these prior works focused on learning point-prediction models. In the context of conformal prediction, Kiyani et al. (2024b) studied the length minimization for sublevel sets of a pretrained score while ensuring the group-conditional validity, and transformed the constrained optimization problem to a minimax formulation. However, both the motivation and objective in Kiyani et al. (2024b) differ from ours, and the theoretical analysis is fundamentally distinct.

Notations The following notations will be used throughout the paper. For domains \mathcal{X} , \mathcal{Y} , and \mathcal{Z} , we use $d_{\mathcal{X}}$, $d_{\mathcal{Y}}$, and $d_{\mathcal{Z}}$, respectively, to denote the corresponding dimension if they are Euclidean spaces. When \mathcal{Z} is finite, we write $|\mathcal{Z}|$ for its cardinality. For a Euclidean vector $u \in \mathbb{R}^d$, we write $\|u\| = \sqrt{\sum_{j=1}^d u_j^2}$ and $\|u\|_{\infty} = \max_{1 \leq j \leq d} |u_j|$. For a function $g : \mathcal{X} \times \mathcal{Y} \times \mathcal{Z} \rightarrow \mathbb{R}$, we denote the L_2 -norm as $\|g\|_{L_2} = \sqrt{\mathbb{E}[g^2(X, Y, Z)]}$. For two positive sequences a_n and b_n for $n \geq 1$, we write $a_n \lesssim b_n$ if there exists a constant $C > 0$ such that $a_n \leq Cb_n$ holds for sufficiently large n .

2 Minimax Optimization for Conditional Coverage

2.1 Problem setup

Let $(X, Y) \in \mathcal{X} \times \mathcal{Y}$ be a data pair drawn from an unknown distribution, and let $C(\cdot) : \mathcal{X} \rightarrow 2^{\mathcal{Y}}$ denote a measurable set-valued function that assigns to each covariate X a *prediction set* $C(X) \subseteq \mathcal{Y}$. In particular, given a conditioning variable $Z \in \mathcal{Z}$, our goal is to find a prediction set $C(X)$ satisfying the conditional coverage property in (1). The conditioning variable Z typically depends on (X, Y) and determines the scope of coverage enforcement, representing various forms of contextual, structural, or latent information about the data. Below, we provide several representative examples with different types of Z .

Example 2.1 (Test-conditional coverage). *The most popular form of conditional coverage validity arises when $Z = X$, which is also referred to as test-conditional coverage in the conformal prediction literature (Angelopoulos et al., 2024). In this case, the target (1) reduces to: $\mathbb{P}\{Y \in C(X) \mid X = x\} = 1 - \alpha$, $\forall x \in \mathcal{X}$. Another practical case is that Z is a part of the covariate X , representing special features of interest.*

Example 2.2 (Group-conditional coverage). *Let $\{G_1, \dots, G_K\}$ be a finite collection of groups, where each $G_k \subseteq \mathcal{X}$ defines a subset of the covariate space. The groups can be disjoint or overlap. The goal of group-conditional coverage (Jung et al., 2023; Gibbs et al., 2025) is to ensure coverage within each group: $\mathbb{P}\{Y \in C(X) \mid X \in G_k\} = 1 - \alpha$, $\forall 1 \leq k \leq K$, which is a special case of the target (1) by $Z = (\mathbb{1}\{X \in G_1\}, \dots, \mathbb{1}\{X \in G_K\})^\top$.*

Example 2.3 (Equalized coverage on sensitive attributes). *In the context of fairness, the conditioning variable Z can represent sensitive attributes, and we require coverage parity of the prediction set $C(X)$ across different values of the sensitive attribute Z (Romano et al., 2020). In particular, the target (1) allows the case where the variable Z is masked in the test data (the prediction set depends only on the covariate X), which aligns with the requirement of algorithmic fairness literature (Zafar et al., 2017; Zhang et al., 2018).*

2.2 A minimax optimization framework

Given a set-valued function C , recall from (2) that the conditional coverage (1) is equivalent to requiring $\Phi(C, f) := \mathbb{E}[f(Z)(\mathbb{1}\{Y \notin C(X)\} - \alpha)] = 0$ for all measurable f . Then, when the exact conditional coverage holds, and the weight function class \mathcal{F} is symmetric, we have $\max_{f \in \mathcal{F}} \Phi(C, f) = 0$. This motivates us to construct the desired prediction set by solving the following minimax problem:

$$\min_{C \in \mathfrak{C}} \max_{f \in \mathcal{F}} \mathbb{E}[f(Z)(\mathbb{1}\{Y \notin C(X)\} - \alpha)],$$

where \mathfrak{C} is the general class of set-valued functions defined in (3). To make the optimization problem well-defined, the inner maximization domain (i.e., the function class \mathcal{F}) must typically be bounded (Nemirovski, 2004). To remove the dependence on the scale of f , we may add an L_2 norm constraint $\|f\|_{L_2} \leq 1$ when taking the maximum on $\Phi(C, f)$ over $f \in \mathcal{F}$. To further facilitate optimization, we consider the following L_2 penalized objective:

$$\Psi(C, f) := \mathbb{E} \left[f(Z)(\mathbb{1}\{Y \notin C(X)\} - \alpha) - f^2(Z) \right], \quad (4)$$

and define the *minimax optimization predictive inference (MOPI)* set as the solution

$$C^* = \arg \min_{C \in \mathfrak{C}} \max_{f \in \mathcal{F}} \Psi(C, f). \quad (5)$$

The L_2 penalty makes the objective $\Psi(C, f)$ strongly concave in f , and the corresponding minimax problem is easier to tackle; see Lin et al. (2020) and Rafique et al. (2022).

Remark 2.1. In the previous works such as Dikkala et al. (2020), the objective function includes a tuning parameter $\lambda > 0$ for the L_2 penalty, taking the form $\Psi_\lambda(C, f) := \mathbb{E}[f(Z)(\mathbb{1}\{Y \notin C(X)\} - \alpha) - \lambda f^2(Z)]$ in our case. In fact, under the mild condition that $\lambda f \in \mathcal{F}$ for all $f \in \mathcal{F}$, the choice of λ does not affect the resulting optimizer. This can be seen from the relation: $\lambda \max_{f \in \mathcal{F}} \Psi_\lambda(C, f) = \max_{f \in \mathcal{F}} \{\lambda f(Z)(\mathbb{1}\{Y \notin C(X)\} - \alpha) - \lambda^2 f^2(Z)\} = \max_{f \in \mathcal{F}} \Psi(C, f)$. This allows us to simply set $\lambda = 1$ without additional tuning. See Appendix A.1 for a more detailed discussion. \square

2.2.1 Mean squared coverage error of minimax solution

Given any set-valued function C , we denote by $\alpha(Z; C) := \mathbb{P}\{Y \notin C(X) \mid Z\}$ the conditional miscoverage probability and recall the definition of MSCE:

$$\text{MSCE}(C) = \mathbb{E} \left[(\alpha(Z; C) - \alpha)^2 \right].$$

This metric quantifies the average conditional coverage error. Next, we establish the theoretical connection between the minimax objective (4) and the $\text{MSCE}(C)$, providing a rigorous justification for the statistical optimality of the MOPI framework.

In fact, note that the conditional coverage (1) can also be pursued by minimizing the *oracle* least-squares problem

$$C^{\text{ora}} = \arg \min_{C \in \mathfrak{C}} \text{MSCE}(C). \quad (6)$$

The term ‘‘oracle’’ indicates that the conditional miscoverage probability $\alpha(Z; C)$ cannot be computed if the conditional distribution is unknown. The oracle set-valued function C^{ora} is the optimal element within the class \mathfrak{C} , achieving the smallest MSCE, and the $\text{MSCE}(C^{\text{ora}})$ can be interpreted as the approximation error of the class \mathfrak{C} . The next proposition connects the MSCEs of the minimax solution C^* in (5) and the oracle solution C^{ora} .

Proposition 2.1. *If $\alpha(\cdot; C) - \alpha \in \mathcal{F}$ for any $C \in \mathfrak{C}$, we have $\max_{f \in \mathcal{F}} \Psi(C, f) = \text{MSCE}(C)/4$ for any $C \in \mathfrak{C}$ and $\text{MSCE}(C^*) = \text{MSCE}(C^{\text{ora}})$.*

This result implies that if \mathcal{F} is expressive enough to include the miscoverage error function $\alpha(\cdot; C) - \alpha$, then solving the minimax problem (5) is equivalent to solving (6). Proposition 2.1 also sheds light on a principled way to choose the weight function class \mathcal{F} based on the domain of the conditioning variable Z .

- *Finite-dimensional \mathcal{F} .* When the domain \mathcal{Z} contains only finite elements, i.e., $|\mathcal{Z}| < \infty$, the function $\alpha(\cdot; C)$ is a $|\mathcal{Z}|$ -dimensional function. To meet the condition of Proposition 2.1, we can take a parametric function class $\mathcal{F} = \{\sum_{z \in \mathcal{Z}} \beta_z \mathbb{1}\{Z = z\} : \beta_z \in \mathbb{R}, z \in \mathcal{Z}\}$. For the group-conditional coverage in Example 2.2, it can be seen that $|\mathcal{Z}| = K$ for the disjoint groups and $|\mathcal{Z}| \leq 2^K$ for the overlap groups. In Example 2.3, the parametric class \mathcal{F} remains applicable when the sensitive attribute Z is a categorical variable.

- *Infinite-dimensional \mathcal{F} .* When the domain \mathcal{Z} contains infinite points, e.g., \mathcal{Z} is a subset of the Euclidean space, we can choose \mathcal{F} as a reproducing kernel Hilbert space (RKHS). This choice is suitable for the test-conditional coverage in Example 2.1 and the continuous sensitive variable in Example 2.3.

By adjusting the weight function class \mathcal{F} to the conditioning variable Z , the MOPI framework can be tailored to enforce local or groupwise coverage, as well as fairness constraints.

2.2.2 Structured set-valued function class

Structured set-valued function class \mathfrak{C} in (3) provides a flexible and expressive formulation of prediction sets, and can meet most downstream requirements. Now, we present two common examples of \mathfrak{C} .

Sublevel set of pretrained score function. This class is widely used in the conformal prediction literature (Vovk et al., 2005; Lei et al., 2018). Given a pretrained score function $s(x, y)$, the sublevel prediction set takes the form

$$\mathfrak{C}_{\text{sublevel}} = \{C(x; h) = \{y \in \mathcal{Y} : s(x, y) \leq h(x)\} : h \in \mathcal{H}\}, \quad (7)$$

where $h : \mathcal{X} \rightarrow \mathbb{R}$ is a one-dimensional threshold function. Let $T(h(x), y) = s(x, y) - h(x)$ in (3), then $\mathfrak{C}_{\text{sublevel}}$ is a special case. In this formulation, the pretrained function s fixes the geometric structure of $C(x; h)$, leaving only the threshold $h(x)$ to be optimized.

Remark 2.2. For test-conditional coverage with $Z = X$, the population quantile regression in the CC method sets $\mathcal{H} = \mathcal{F}$ in (7), yielding the prediction set $C^{\text{qr}}(X) := \{y \in \mathcal{Y} : s(X, y) \leq f^{\text{qr}}(X)\}$. Here, $f^{\text{qr}} = \arg \min_{f \in \mathcal{F}} \mathbb{E}[\ell_\alpha(s(X, Y), f(X))]$ is the minimizer of the expected pinball loss. In addition, let $q(x) = \inf\{t \in \mathbb{R} : \mathbb{P}(s(X, Y) \leq t \mid X = x) \geq 1 - \alpha\}$ be the ground truth conditional quantile function. If $q \in \mathcal{F}$, the prediction set $C^{\text{qr}}(X)$ achieves zero MSCE, as well as for the minimax solution C^* under the condition of Proposition

2.1. If $q \notin \mathcal{F}$, the first conclusion of Proposition 2.1 guarantees that $C^*(X)$ achieves lower MSCE than $C^{\text{qr}}(X)$. Hence, MOPI exhibits better performance in terms of MSCE. We defer more theoretical discussions to Appendix B. \square

Geometrically structured prediction sets. In some downstream tasks, e.g., the robust optimization problems (Ben-Tal et al., 2009; Johnstone and Cox, 2021), the geometric structure of prediction sets in the multi-dimensional label space $\mathcal{Y} \subseteq \mathbb{R}^{d_{\mathcal{Y}}}$ is critical to the decision making. Let us consider the following two commonly used set classes:

- (i) Let $h = (\mu, \sigma)$ with mean function $\mu : \mathcal{X} \rightarrow \mathbb{R}^{d_{\mathcal{Y}}}$ and variance function $\sigma : \mathcal{X} \rightarrow \mathbb{R}^{d_{\mathcal{Y}}}$, the box set-valued function class takes the form

$$\mathfrak{C}_{\text{box}} = \left\{ C(x; h) = \left\{ y \in \mathbb{R}^{d_{\mathcal{Y}}} : \|(y - \mu(x))/\sigma(x)\|_{\infty} \leq 1 \right\} : h \in \mathcal{H} \right\},$$

where “/” denotes element-wise division of vectors. By setting $T(h(x), y) = \|(y - \mu(x))/\sigma(x)\|_{\infty} - 1$ in (3), we recover the box class $\mathfrak{C}_{\text{box}}$.

- (ii) Let $h = (\mu, \Sigma)$ with mean function $\mu : \mathcal{X} \rightarrow \mathbb{R}^{d_{\mathcal{Y}}}$ and covariance function $\Sigma : \mathcal{X} \rightarrow \mathbb{R}^{d_{\mathcal{Y}} \times d_{\mathcal{Y}}}$, the ellipsoidal set-valued function class takes the form

$$\mathfrak{C}_{\text{ell}} = \left\{ C(x; h) = \left\{ y \in \mathbb{R}^{d_{\mathcal{Y}}} : (y - \mu(x))^{\top} \Sigma^{-1}(x) (y - \mu(x)) \leq 1 \right\} : h \in \mathcal{H} \right\}.$$

This corresponds to the choice $T(h(x), y) = (y - \mu(x))^{\top} \Sigma^{-1}(x) (y - \mu(x)) - 1$ in (3).

Remark 2.3. It is also possible to construct a sublevel prediction set of the form (7) with geometric structures described above using a pretrained score. For example, Johnstone and Cox (2021) and Sun et al. (2023) built an ellipsoidal sublevel set via the score $s(x, y) = (y - \mu_0(x))^{\top} \Sigma_0^{-1} (y - \mu_0(x))$, where $\mu_0(x)$ is a regression model and Σ_0 is the covariance matrix obtained on a separate dataset. However, given such a score function, the CC method cannot further adjust the covariance matrix with respect to the conditioning variable. To

embed the pretrained information into a more flexible structure, we may consider setting $T(h(x), y) = \tilde{y}^\top \Sigma^{-1}(x) \tilde{y}$ in (3) where $\tilde{y} = \Sigma_0^{-1/2}(y - \mu_0(x))$ and $h(x) = \Sigma(x)$. This enables MOPI to adaptively refine the shape model $\Sigma(x)$ during calibration, leading to more accurate conditional coverage. \square

3 Empirical Minimax Optimization Problem

Suppose we have i.i.d. labeled data $\mathcal{D}_n := \{(X_i, Y_i, Z_i)\}_{i=1}^n$. The goal of this section is to construct MOPI sets by solving the empirical version of the minimax problem (5).

3.1 Empirical minimax problem

Formally, we consider the following sample averaging approximation to the population objective function $\Psi(C, f)$ defined in (4),

$$\hat{\Psi}(C, f) := \frac{1}{n} \sum_{i=1}^n [f(Z_i) (\mathbb{1}\{Y_i \notin C(X_i)\} - \alpha) - f^2(Z_i)].$$

We assume the set-valued function class \mathfrak{C} is finite-dimensional, and defer the infinite-dimensional case to Appendix D. Suppose the weight function class \mathcal{F} is equipped with a norm $\|\cdot\|_{\mathcal{F}}$, which measures the complexity of \mathcal{F} . Accordingly, we output the empirical MOPI prediction set by solving the following minimax optimization problem:

$$\hat{C} = \arg \min_{C \in \mathfrak{C}} \max_{f \in \mathcal{F}} \left\{ \hat{\Psi}(C, f) - \gamma \|f\|_{\mathcal{F}}^2 \right\}, \quad (8)$$

where $\gamma \geq 0$ acts as a regularization parameter when \mathcal{F} is an infinite-dimensional function class. We can simply set $\gamma = 0$ when \mathcal{F} is finite-dimensional.

In Section 2.2.1, we discussed how to choose the weight function class \mathcal{F} according to the cardinality of the conditioning domain \mathcal{Z} . Now, we show that the inner maximization

of the empirical problem (8) admits a closed form under two practical choices of \mathcal{F} .

Lemma 3.1. *Let $\mathcal{F} = \{\sum_{z \in \mathcal{Z}} \beta_z \mathbb{1}\{Z = z\} : \beta_z \in \mathbb{R}, z \in \mathcal{Z}\}$ when $|\mathcal{Z}| < \infty$. The inner maximization in the problem (8) with $\gamma = 0$ is:*

$$\max_{f \in \mathcal{F}} \widehat{\Psi}(C, f) = \sum_{z \in \mathcal{Z}} \frac{\left(\sum_{i=1}^n \mathbb{1}\{Z_i = z\} (\mathbb{1}\{Y_i \notin C(X_i)\} - \alpha)\right)^2}{4n \sum_{i=1}^n \mathbb{1}\{Z_i = z\}}.$$

Lemma 3.2. *Let \mathcal{F} be a RKHS equipped with a kernel function $\mathcal{K}(\cdot, \cdot) : \mathcal{Z} \times \mathcal{Z} \rightarrow \mathbb{R}$. Denote $\boldsymbol{\varphi}_n(C) = (\varphi_1(C), \dots, \varphi_n(C))^\top$ where $\varphi_i(C) = \frac{1}{n}(\mathbb{1}\{Y_i \notin C(X_i)\} - \alpha)$ for $i = 1, \dots, n$ and $\mathbf{K}_n = (\mathcal{K}(Z_i, Z_j))_{i,j=1}^n$ be the empirical kernel matrix. Let \mathbf{I}_n be an $n \times n$ identity matrix. The inner maximization in the problem (8) is:*

$$\max_{f \in \mathcal{F}} \left\{ \widehat{\Psi}(C, f) - \gamma \|f\|_{\mathcal{F}}^2 \right\} = \frac{1}{4} \boldsymbol{\varphi}_n(C)^\top \mathbf{K}_n \left(\frac{1}{n} \mathbf{K}_n + \gamma \mathbf{I}_n \right)^{-1} \boldsymbol{\varphi}_n(C).$$

Using the two lemmas above, we transform the corresponding empirical minimax problems (8) into empirical risk *minimization* problems.

3.2 Implementation of MOPI by smoothing

Since the objective function $\widehat{\Psi}(C, f)$ contains the non-differentiable miscoverage indicator $\mathbb{1}\{Y_i \notin C(X_i)\} = \mathbb{1}\{T(h(X_i), Y_i) > 0\}$ for $C(X_i) = \{y \in \mathcal{Y} : T(h(X_i), Y_i) \leq 0\}$ as defined in (3), direct optimization is infeasible. To overcome this non-differentiability, we can replace the indicator $\mathbb{1}\{u > 0\}$ with a smooth surrogate, such as the Sigmoid function $\tilde{\mathbb{1}}\{u > 0\} = (1 + \exp(-u/r))^{-1}$ or the Gaussian error function $\tilde{\mathbb{1}}\{u > 0\} = \frac{1}{2} \left(1 + \operatorname{erf}\left(\frac{u}{\sqrt{2}r}\right)\right)$, where $\operatorname{erf}(x) = \frac{2}{\sqrt{\pi}} \int_0^x e^{-t^2} dt$ and $r > 0$ is the smoothing parameter. The smoothing strategy has been widely used in recent optimization works on conformal prediction, see e.g. [Bai et al. \(2022\)](#), [Kiyani et al. \(2024b\)](#), and [Wu et al. \(2025\)](#).

Denote the smoothed miscoverage indicator as $\tilde{\mathbb{1}}\{Y \notin C(X)\} := \tilde{\mathbb{1}}\{T(h(X), Y) > 0\}$.

Then we have the following smoothed objective function:

$$\tilde{\Psi}(C, f) := \frac{1}{n} \sum_{i=1}^n [f(Z_i) (\tilde{\mathbb{1}}\{Y_i \notin C(X_i)\} - \alpha) - f^2(Z_i)].$$

Accordingly, the smoothed empirical MOPI prediction set can be obtained by solving the minimax problem

$$\tilde{C} := \arg \min_{C \in \mathfrak{C}} \max_{f \in \mathcal{F}} \{ \tilde{\Psi}(C, f) - \gamma \|f\|_{\mathcal{F}}^2 \}. \quad (9)$$

Similar to Lemmas 3.1 and 3.2, we can obtain the closed form of the inner maximization $\max_{f \in \mathcal{F}} \{ \tilde{\Psi}(C, f) - \gamma \|f\|_{\mathcal{F}}^2 \}$ by replacing miscoverage indicators. Then we can solve the resulting empirical risk minimization problem through gradient-based methods, such as stochastic gradient descent. In Appendix B.2, we discuss and compare the computational efficiency of MOPI via the smoothed minimax optimization (9) and the quantile regression in the CC method (Gibbs et al., 2025).

4 Theoretical Results

In this section, we first establish an upper bound for the MSCE of the empirical MOPI set (8), and then derive specific convergence rates for examples discussed in Section 2.1. After that, we analyze the MSCE of the MOPI set obtained by the smoothed problem (9).

4.1 Oracle inequality for MOPI

We begin with the following two assumptions on the weight function class \mathcal{F} .

Assumption 1. *There exists a constant $U > 0$ such that $\sup_{f \in \mathcal{F}_U} \sup_{z \in \mathcal{Z}} |f(z)| \leq 1$, where $\mathcal{F}_U := \{f \in \mathcal{F} : \|f\|_{\mathcal{F}}^2 \leq U\}$. In addition, \mathcal{F}_U is star-shaped around zero, i.e., $tf \in \mathcal{F}_U$ whenever $f \in \mathcal{F}_U$ for any $t \in [0, 1]$.*

Assumption 2. For any $C \in \mathfrak{C}$, the projection error of f_C satisfies $\mathbb{E}[(f_C(Z) - \{\alpha(Z; C) - \alpha(Z; C^{\text{ora}})\})^2] \leq \eta^2$, where $f_C := \arg \min_{f \in \mathcal{F}_U} \mathbb{E} \left[\left(f(Z) - \{\alpha(Z; C) - \alpha(Z; C^{\text{ora}})\} \right)^2 \right]$ and C^{ora} is defined in (6).

In Assumption 1, \mathcal{F}_U is a ball with radius U in the function class \mathcal{F} , and the conditions are quite mild and can be satisfied for both a parametric function class and an RKHS. In Assumption 2, the function $f_C(\cdot)$ is a projection of the conditional miscoverage probability difference $\alpha(\cdot; C) - \alpha(\cdot; C^{\text{ora}})$ onto the function class \mathcal{F} , and η is an upper bound for the projection error. If the assumption of Proposition 2.1 holds, that is $\alpha(\cdot; C) - \alpha \in \mathcal{F}$ for any $C \in \mathfrak{C}$, we have $\eta = 0$; see the corollaries in Section 4.3.

To characterize the excess risk of the empirical objective relative to the population objective, we introduce the following function class:

$$\mathcal{G} := \left\{ (x, y, z) \mapsto f_C(z) [\mathbb{1}\{y \notin C(x)\} - \mathbb{1}\{y \notin C^{\text{ora}}(x)\}] : C \in \mathfrak{C} \right\},$$

which depends on the set-valued class \mathfrak{C} . Given $\delta > 0$, define localized Rademacher complexities (Bartlett et al., 2005) as $\overline{\mathcal{R}}_n(\delta; \mathcal{G}) := \mathbb{E} \left[\sup_{g \in \mathcal{G}, \|g\|_{L_2} \leq \delta} \left| n^{-1} \sum_{i=1}^n \varepsilon_i g(X_i, Y_i, Z_i) \right| \right]$, where $\{\varepsilon_i\}_{i=1}^n$ are i.i.d. Rademacher random variables taking values in $\{-1, +1\}$ with equal probability. The *critical radius* of \mathcal{G} is any positive solution to $\overline{\mathcal{R}}_n(\delta; \mathcal{F}_U) \leq \delta^2$. The critical radius of \mathcal{F}_U is defined similarly. The next theorem gives a non-asymptotic upper bound for the MSCE of the empirical MOPI in (8).

Theorem 4.1 (Oracle inequality). *Suppose Assumptions 1-2 hold. Let $\delta_{n, \mathcal{F}_U}$ and $\delta_{n, \mathcal{G}}$ be the critical radius of \mathcal{F}_U and \mathcal{G} , respectively. (i) For finite-dimensional \mathcal{F} , we choose the hyperparameter $\gamma = 0$ in (8); (ii) For infinite-dimensional \mathcal{F} , we choose the hyperparameter γ in (8) such that $\gamma \|f\|_{\mathcal{F}}^2 \leq \|f\|_{L_2}^2$. For any $\zeta \in (0, 1)$, if $\left(\delta_{n, \mathcal{F}_U} + \sqrt{\frac{\log(1/\zeta)}{n}} \right) \|f\|_{\mathcal{F}} \lesssim \sqrt{U} \|f\|_{L_2}$*

holds all $f \in \mathcal{F}$, with probability at least $1 - 4\zeta$, we have:

$$\mathbb{E} \left[\left(\alpha(Z; \hat{C}) - \alpha \right)^2 \mid \mathcal{D}_n \right] \lesssim \text{MSCE}(C^{\text{ora}}) + \eta^2 + \delta_{n, \mathcal{F}_U}^2 + \delta_{n, \mathcal{G}}^2 + \frac{\log(\log_2(1/\delta_{n, \mathcal{G}})/\zeta)}{n}.$$

In general, the approximation error $\text{MSCE}(C^{\text{ora}})$ is small if the capacity of \mathfrak{C} is large enough. Moreover, the projection error η can be negligible when \mathcal{F} is expressive enough. The critical values $\delta_{n, \mathcal{F}_U}$ and $\delta_{n, \mathcal{G}}$ decrease as the sample size n grows, and their scales also depend on the complexities of \mathcal{F} and \mathfrak{C} .

4.2 Upper bound for the approximation error

Next, we investigate how the relationship between the covariate X and the conditioning variable Z influences the approximation error.

Assumption 3. Suppose \mathcal{H} is a class including functions that map from \mathcal{X} to \mathbb{R}^m for some $m \geq 1$. (i) There exist measurable functions $w(\cdot)$ and $l(\cdot, \cdot)$ such that for any $u_1, u_2 \in \mathbb{R}^m$,

$$|\mathbb{P}\{T(u_1, Y) \leq 0 \mid w(X), Z\} - \mathbb{P}\{T(u_2, Y) \leq 0 \mid w(X), Z\}| \leq l(w(X), Z) \|u_1 - u_2\|,$$

where $\mathbb{E}[l^2(w(X), Z)] \leq \kappa^2$ for some constant $\kappa > 0$. (ii) There exists a measurable function $H^0(\cdot, \cdot)$ such that $\mathbb{P}\{T(H^0(w(X), Z), Y) \leq 0 \mid w(X), Z\} = 1 - \alpha$. (iii) The conditional expectation $h^0(w(X)) := \mathbb{E}[H^0(w(X), Z) \mid w(X)]$ belongs to \mathcal{H} .

Assumption 3 (i) requires Lipschitz continuity of the conditional miscoverage probability with respect to the geometric parameter, which is a standard regularity condition. Assumption 3 (ii) and (iii) impose the realizability condition for the conditional coverage. Let us consider the group-conditional coverage in Example 2.2 and assume \mathfrak{C} is the sublevel prediction set (7) of the pretrained score s . Recalling that $Z = (\mathbb{1}\{X \in G_1\}, \dots, \mathbb{1}\{X \in G_K\})^\top$, we take $w(X) = Z$ in this case. Let $H^0(w(X), Z) = \sum_{z \in \mathcal{Z}} q_z \mathbb{1}\{Z = z\}$, where

$q_z = \inf\{t : \mathbb{P}(s(X, Y) \leq t \mid Z = z) \geq 1 - \alpha\}$ is the $(1 - \alpha)$ conditional quantile given $Z = z$. Then, we can guarantee $h^0 \in \mathcal{H}$ by choosing $\mathcal{H} = \{\sum_{z \in \mathcal{Z}} \beta_z \mathbb{1}\{Z = z\} : \beta_z \in \mathbb{R}, z \in \mathcal{Z}\}$ since $h^0(w(X)) = H^0(w(X), Z)$.

Theorem 4.2 (Approximation error). *Let $\rho^2 = \frac{\text{Tr}(\text{Cov}\{h^0(w(X))\})}{\text{Tr}(\text{Cov}\{H^0(w(X), Z)\})}$. Under Assumption 3, we have*

$$\text{MSCE}(C^{\text{ora}}) \leq \kappa^2(1 - \rho^2) \text{Tr}(\text{Cov}\{H^0(w(X), Z)\}).$$

In particular, $\text{MSCE}(C^{\text{ora}}) = 0$ if $Z = w(X)$ for some measurable function $w(\cdot)$.

As shown in Theorem 4.2, the approximation error is largely determined by the proportion of the variance of H^0 captured by h^0 , which is quantified by ρ . When h^0 captures a large proportion of variance, it can approximately achieve conditional coverage. Specifically, if Z is a function of X , then h^0 has the same variance as H^0 , leading to the perfect conditional coverage, i.e., $\text{MSCE}(C^{\text{ora}}) = 0$. This case corresponds to the test-conditional coverage with $Z = X$ in Example 2.1 and group-conditional coverage in Example 2.2. For Example 2.3, the approximation error would depend on the degree of correlation between covariate X and the sensitive attribute Z .

4.3 Convergence rates of MSCE

In what follows, we derive the specific convergence rates of the MSCE under the following Vapnik–Chervonenkis (VC) complexity assumption on the set-valued class \mathfrak{C} , which is satisfied by basic linear models (Wainwright, 2019) and deep neural networks (Bartlett et al., 2019). For infinite-dimensional class \mathfrak{C} , since VC-based arguments are no longer applicable, we establish the corresponding convergence rate using a different technique; the details are deferred to Appendix D.

Assumption 4. *The function class $\{(x, y) \mapsto T(h(x), y) : h \in \mathcal{H}\}$ has a VC-dimension $d_{\mathfrak{C}}$.*

4.3.1 Convergence rate when \mathcal{F} is finite-dimensional

In the following analysis, we upper bound the MSCE when the domain \mathcal{Z} is finite. In this case, one can consider the parametric function class \mathcal{F} , which naturally satisfies Assumption 1. In addition, given any $C \in \mathfrak{C}$, the function $\alpha(z; C)$ takes at most $|\mathcal{Z}|$ distinct values. Consequently, $\alpha(z; C) \in \mathcal{F}$ and we have $\eta = 0$ in Assumption 2.

Theorem 4.3. *Suppose $|\mathcal{Z}| < \infty$ and Assumption 4 hold for the set-valued class \mathfrak{C} in (3). Choosing $\mathcal{F} = \{\sum_{z \in \mathcal{Z}} \beta_z \mathbb{1}\{Z = z\} : \beta_z \in \mathbb{R}, \forall z \in \mathcal{Z}\}$ and setting $\gamma = 0$ in the optimization problem (8), then we have*

$$\mathbb{E} \left[\left(\alpha(Z; \hat{C}) - \alpha \right)^2 \right] \lesssim \text{MSCE}(C^{\text{ora}}) + \frac{d_{\mathfrak{C}} + |\mathcal{Z}|}{n} \log \left(\frac{n}{d_{\mathfrak{C}} + |\mathcal{Z}|} \right).$$

In particular, we can obtain the group-conditional coverage guarantee in Example 2.2 based on Theorem 4.3. Let $\{G_1, \dots, G_K\}$ be a collection of groups in \mathcal{X} , and we recall the conditioning variable $Z = (\mathbb{1}\{X \in G_1\}, \dots, \mathbb{1}\{X \in G_K\})^\top$. The choice of Z implies that $\rho = 1$ in Theorem 4.2, and hence $\text{MSCE}(C^{\text{ora}}) = 0$. By choosing the function class $\mathcal{H} = \mathcal{F}$ in the set-valued class \mathfrak{C} , we have the following corollary.

Corollary 4.1. *Considering Example 2.2, we let $Z = (\mathbb{1}\{X \in G_1\}, \dots, \mathbb{1}\{X \in G_K\})^\top$ and choose $\mathcal{H} = \mathcal{F} = \{\sum_{z \in \mathcal{Z}} \beta_z \mathbb{1}\{Z = z\} : \beta_z \in \mathbb{R}, \forall z \in \mathcal{Z}\}$. Suppose the conditions (i) and (ii) in Assumption 3 hold for $w(X) = Z$, then for any $k \in [K]$*

$$\left| \mathbb{P} \left\{ Y \in \hat{C}(X) \mid X \in G_k \right\} - (1 - \alpha) \right| \lesssim \sqrt{\frac{d_{\mathfrak{C}} + |\mathcal{Z}|}{n \cdot \mathbb{P}(X \in G_k)} \log \left(\frac{n}{d_{\mathfrak{C}} + |\mathcal{Z}|} \right)}.$$

For the sublevel set class (7) under the choice of \mathcal{H} in Corollary 4.1, we have $d_{\mathfrak{C}} = O(|\mathcal{Z}|)$. Then the upper bound significantly improves the dependence on sample size from $n^{-1/4}$ in Jung et al. (2023) to $n^{-1/2}$, and matches the optimal convergence rate in Areces et al. (2024) up to a logarithmic factor.

Next, we provide equalized coverage guarantee for Example 2.3.

Corollary 4.2. *Considering Example 2.3 with $|\mathcal{Z}| < \infty$, suppose the conditions (i)–(iii) in Assumption 3 hold for some $w(X)$, then for any $z \in \mathcal{Z}$,*

$$\left| \mathbb{P} \left\{ Y \in \widehat{C}(X) \mid Z = z \right\} - (1 - \alpha) \right| \lesssim \sqrt{\frac{1 - \rho^2}{\mathbb{P}(Z = z)}} + \sqrt{\frac{d_{\mathfrak{C}} + |\mathcal{Z}|}{n \cdot \mathbb{P}(Z = z)} \log \left(\frac{n}{d_{\mathfrak{C}} + |\mathcal{Z}|} \right)},$$

where ρ^2 is defined in Theorem 4.2.

4.3.2 Convergence rate when \mathcal{F} is RKHS

We now establish upper bounds for the MSCE when the domain \mathcal{Z} is infinite. For simplicity, let us consider a bounded Euclidean domain $\mathcal{Z} = [0, 1]^{d_{\mathcal{Z}}}$, where $d_{\mathcal{Z}}$ is the dimension. In this case, we choose \mathcal{F} as the RKHS equipped with a Gaussian kernel $\mathcal{K}(z, z') = \exp\left(-\frac{1}{2\vartheta^2}\|z - z'\|^2\right)$ with the bandwidth ϑ . Then Assumption 1 holds with $U = 1$ since $\sup_{z \in \mathcal{Z}} |f(z)| \leq \sup_{z \in \mathcal{Z}} \sqrt{\mathcal{K}(z, z)} \|f\|_{\mathcal{F}} \leq 1$ for any $f \in \mathcal{F}_U$.

Theorem 4.4. *Suppose Assumptions 2 and 4 hold for the set-valued class \mathfrak{C} in (3). If the hyperparameter γ in optimization problem (8) is chosen such that $\gamma \|f\|_{\mathcal{F}}^2 \leq \|f\|_{L_2}^2$ for all $f \in \mathcal{F}$, then we have*

$$\mathbb{E} \left[\left(\alpha(Z; \widehat{C}) - \alpha \right)^2 \right] \lesssim \text{MSCE}(C^{\text{ora}}) + \eta^2 + \frac{d_{\mathfrak{C}} \log(n/d_{\mathfrak{C}})}{n} + \frac{d_{\mathcal{Z}} \log^{d_{\mathcal{Z}}+1}(n/d_{\mathcal{Z}})}{n}.$$

Combining Theorems 4.2 and 4.4, we have the following corollary for the test-conditional coverage in Example 2.1.

Corollary 4.3. *Consider Example 2.1 with $Z = X$. Suppose the conditions (i)–(iii) in Assumption 3 hold with $w(X) = X$, and Assumptions 2 and 4 hold for \mathfrak{C} . If $\alpha(Z; C) - \alpha \in \mathcal{F}_U$*

with $U = 1$ for any $C \in \mathfrak{C}$, then

$$\mathbb{E} \left[\left(\alpha(X; \hat{C}) - \alpha \right)^2 \right] \lesssim \frac{d_{\mathfrak{C}} \log(n/d_{\mathfrak{C}})}{n} + \frac{d_{\mathcal{Z}} \log^{d_{\mathcal{Z}}+1}(n/d_{\mathcal{Z}})}{n}.$$

4.4 Oracle inequality for MOPI via smoothed optimization

Since the miscoverage indicator is replaced by the smooth surrogate in the objective (9), we define a new function class as $\tilde{\mathcal{G}} := \left\{ (x, y, z) \mapsto f_C(z) [\tilde{\mathbb{I}}\{y \notin C(x)\} - \tilde{\mathbb{I}}\{y \notin C^{\text{ora}}(x)\}] : C \in \mathfrak{C} \right\}$ to get the bound of the corresponding excess risk. In the following, we focus on the Gaussian error function as the smooth surrogate: $\tilde{\mathbb{I}}\{y \notin C(x)\} = \frac{1}{2} \left(1 + \text{erf} \left\{ T(h(x), y) / \sqrt{2}r \right\} \right)$ for $C(x) = \{y \in \mathcal{Y} : T(h(x), y) \leq 0\}$, where $r > 0$ is the smoothing parameter.

The next theorem provides the oracle inequality for the MOPI set (9). Compared with Theorem 4.1, there will be an additional error regarding the smoothing bias, which depends on the scale of the smoothing parameter r .

Theorem 4.5. *Suppose Assumptions 1-2 hold. Assume the density of $T(h(X), Y) \mid Z$ is upper bounded for all $h \in \mathcal{H}$, and $\sup_{f \in \mathcal{F}} \sup_{z \in \mathcal{Z}} |f(z)|$ is also upper bounded. Under the same choice of γ in Theorem 4.1, if $\left(\delta_{n, \mathcal{F}_U} + \sqrt{\frac{\log(1/\zeta)}{n}} \right) \|f\|_{\mathcal{F}} \lesssim \sqrt{U} \|f\|_{L_2}$ holds for any $f \in \mathcal{F}$, with probability at least $1 - 4\zeta$, we have:*

$$\begin{aligned} \mathbb{E} \left[\left(\alpha(Z; \tilde{C}) - \alpha \right)^2 \mid \mathcal{D}_n \right] &\lesssim \text{MSCE}(C^{\text{ora}}) + \eta^2 + \delta_{n, \mathcal{F}_U}^2 + \delta_{n, \tilde{\mathcal{G}}}^2 \\ &\quad + \frac{r^2}{\left(\delta_{n, \mathcal{F}_U} + \sqrt{\log(1/\zeta)/n} \right)^2} + \frac{\log(\log_2(1/\delta_{n, \tilde{\mathcal{G}}})/\zeta)}{n}, \end{aligned}$$

where $\delta_{n, \mathcal{F}_U}$ and $\delta_{n, \tilde{\mathcal{G}}}$ are critical radius of \mathcal{F}_U and $\tilde{\mathcal{G}}$, respectively.

According to the result of Theorem 4.5, the MSCE will be dominated by complexities of \mathcal{F} and \mathfrak{C} provided that the smoothing parameter is chosen such that $r \lesssim \min\{\delta_{n, \mathcal{F}_U}^2, \log n/n\}$. Similar to Section 4.3, we can get specific coverage rates on MSCE for different choices

of classes \mathcal{F} and \mathfrak{C} . In Appendix A.2, we conduct an empirical sensitivity analysis on the choice of r , indicating that the performance of MOPI is stable as long as r is not too large.

5 Simulation Results

We conduct simulations on synthetic data to compare the performance of our proposed MOPI with split conformal prediction (SCP) in Vovk et al. (2005) and Lei et al. (2018), the conditional calibration (CC) in Gibbs et al. (2025), and randomly-localized conformal prediction (RLCP) in Hore and Barber (2025). For MOPI, we replace the indicator function $\mathbb{1}\{u > 0\}$ with a sigmoid smoothing surrogate $\tilde{\mathbb{1}}\{u > 0\} = (1 + \exp(-u/r))^{-1}$, with the smoothing parameter set to $r = 0.1$. The nominal coverage level is set to $1 - \alpha = 90\%$, and all simulation results are averaged over 100 replications. In each replication, we independently generate three datasets from the same distribution: pretraining set $\{(X_i, Y_i, Z_i)\}_{i \in \mathcal{D}_{\text{pre}}}$, calibration set $\{(X_i, Y_i, Z_i)\}_{i \in \mathcal{D}_{\text{cal}}}$ and test set $\{(X_i, Y_i, Z_i)\}_{i \in \mathcal{D}_{\text{test}}}$. We provide additional simulation results in Appendix F.

5.1 Geometrically structured sets for multi-dimensional label

For a multivariate label Y , we design a simulation setting involving cross-dimensional dependence, in which the strength of heterogeneity varies across dimensions. Let $X \sim U(0, 5)$, the multi-dimensional label is generated as follows: $Y \mid X \sim N(\mu^*(X), \Sigma^*(X))$, where $\mu_j^*(X) = \sin(X + j) + 0.3j$ and $\Sigma_{jj}^*(X) = (0.05 + 1.5\sqrt{j} \cdot |\sin(X + 2j)|)^{\sqrt{j}}$ for $j = 1, \dots, d_Y$ and $\Sigma_{12}^*(X) = \Sigma_{21}^*(X) = 0.6\sqrt{\Sigma_{11}^*(X)\Sigma_{22}^*(X)}$, while all other entries of $\Sigma^*(X)$ are zero. In this simulation, we set the sample size of test data as $|\mathcal{D}_{\text{test}}| = 10,000$.

Test-conditional coverage. In this experiment, we focus on the test-conditional coverage ($Z = X$) for ellipsoid-shaped sets. The baseline methods (SCP, CC, and RLCP) rely on a score function $s(x, y)$ fitted on the pretraining set to construct the sublevel set (7).

The score takes the form $s(x, y) = (y - \mu_0(x))^\top \Sigma_0^{-1} (y - \mu_0(x))$ for ellipsoidal prediction sets. Here, $\mu_0(x)$ is a pretrained random forest model and Σ_0 is the constant empirical covariance matrix computed from the pretraining set with size $|\mathcal{D}_{\text{pre}}| = 1,500$. Using this score function $s(x, y)$, baseline methods use calibration data to obtain thresholds for the sublevel sets. To make a fair comparison and incorporate the pretrained models $\mu_0(x)$ and Σ_0 , the MOPI first normalizes y as $\tilde{y} = \Sigma_0^{-1/2} (y - \mu_0(x))$ for ellipsoidal sets. It then constructs structured prediction sets by instantiating the general form in (3) as $\mathfrak{C}_{\text{ell}} = \{C(x; \Sigma) = \{y \in \mathbb{R}^{d_y} : \tilde{y}^\top \Sigma^{-1}(x) \tilde{y} \leq 1\} : \Sigma \in \mathcal{H}\}$, where \mathcal{H} is a class of neural networks that maps the covariate to covariance matrices.

For MOPI and CC, we choose the function class \mathcal{F} to be the RKHS on \mathcal{X} equipped with a Gaussian kernel. RLCP also employs the same Gaussian kernel for its localization. To evaluate the performance of different methods, we compute the following metrics:

- (i) Marginal Coverage (*Marginal*): $|\mathcal{D}_{\text{test}}|^{-1} \sum_{i \in \mathcal{D}_{\text{test}}} \mathbb{1}\{Y_i \in \hat{C}(X_i)\}$.
- (ii) Root of MSCE ($\sqrt{\text{MSCE}}$): $\left\{ |\mathcal{J}|^{-1} \sum_{J \in \mathcal{J}} \left(n_J^{-1} \sum_{i \in \mathcal{D}_{\text{test}}} \mathbb{1}\{X_i \in J, Y_i \notin \hat{C}(X_i)\} - \alpha \right)^2 \right\}^{1/2}$, where \mathcal{J} is the set of equidistant partition sets of \mathcal{X} and $n_J = \sum_{i \in \mathcal{D}_{\text{test}}} \mathbb{1}\{X_i \in J\}$.
- (iii) Worst-case conditional coverage (*Worst-case*): $\min_{B \in \mathcal{B}} n_B^{-1} \sum_{i \in \mathcal{D}_{\text{test}}} \mathbb{1}\{X_i \in B, Y_i \in \hat{C}(X_i)\}$, where $n_B = \sum_{i \in \mathcal{D}_{\text{test}}} \mathbb{1}\{X_i \in B\}$, and \mathcal{B} denotes a collection of balls in \mathcal{X} . Specifically, each ball is centered at a randomly selected test point, and its radius is drawn independently from a uniform distribution on the interval (0.1, 0.25).
- (iv) Set volume: $\text{Median}\{|\hat{C}(X_i)| : i \in \mathcal{D}_{\text{test}}\}$, which serves as a robust empirical proxy for the expected set volume $\mathbb{E}[|\hat{C}(X)|]$, since RLCP may produce sets with infinite volume.

We first evaluate the competing methods by varying the calibration sample size. The results in Figure 1 show that, compared to the baseline methods, MOPI achieves worst-case coverage rates closest to the nominal 90% level across all calibration set sizes, while consistently attaining a lower MSCE. Moreover, during the calibration stage, our method

can adapt the shape of the prediction sets via the learned $\Sigma(x)$, whereas the baseline methods are limited to simply rescaling the pretrained sets by adjusting a scalar quantile. Consequently, MOPI produces substantially smaller prediction sets. As shown in Table 1, we further compare four methods across different label-space dimensions $d_y \in \{2, 4, 6\}$ and different nominal coverage levels $1 - \alpha \in \{95\%, 90\%, 85\%\}$. The results indicate that MOPI consistently outperforms the baselines in both conditional coverage metrics and set volumes.

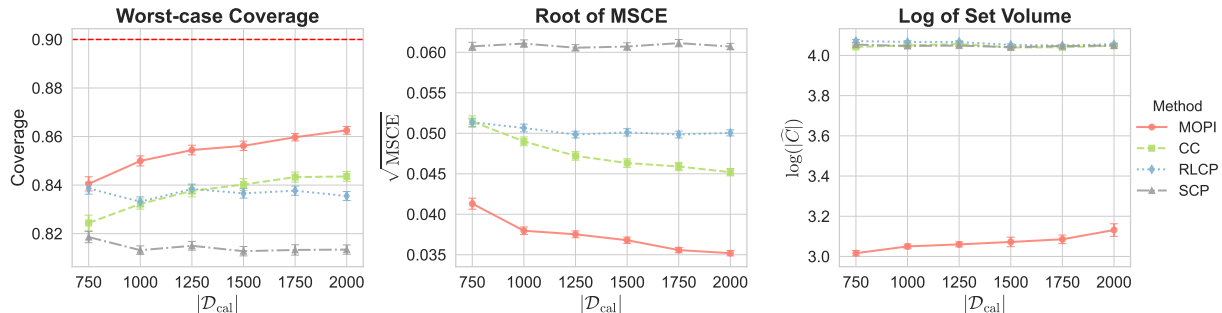


Figure 1: Conditional coverage metrics and log of set volumes (denoted by $\log|\hat{C}|$) versus sample sizes of calibration set under *ellipsoidal* sets and $d_y = 2$. The error bars represent the standard deviation of the metrics over 100 replications.

Table 1: Coverage metrics and log of set volumes (denoted by $\log|\hat{C}|$) for *ellipsoidal* prediction sets under different label-space dimensions and nominal coverage levels.

Methods	$d_y = 2$				$d_y = 4$				$d_y = 6$			
	<i>Marginal</i>	<i>Worst-case</i>	$\sqrt{\text{MSCE}}$	$\log \hat{C} $	<i>Marginal</i>	<i>Worst-case</i>	$\sqrt{\text{MSCE}}$	$\log \hat{C} $	<i>Marginal</i>	<i>Worst-case</i>	$\sqrt{\text{MSCE}}$	$\log \hat{C} $
$1 - \alpha = 95\%$												
MOPI	0.952	0.918	0.026	3.301	0.955	0.920	0.027	7.752	0.953	0.914	0.027	13.311
CC	0.948	0.905	0.034	4.393	0.947	0.907	0.032	10.228	0.948	0.905	0.033	18.845
RLCP	0.952	0.908	0.034	4.431	0.951	0.892	0.040	10.248	0.952	0.900	0.036	18.844
SCP	0.950	0.892	0.040	4.414	0.950	0.858	0.054	10.177	0.951	0.872	0.047	18.718
$1 - \alpha = 90\%$												
MOPI	0.903	0.856	0.037	3.072	0.902	0.856	0.035	7.301	0.902	0.853	0.037	12.714
CC	0.897	0.840	0.046	4.040	0.898	0.847	0.044	9.636	0.898	0.844	0.045	17.960
RLCP	0.901	0.837	0.050	4.052	0.901	0.817	0.059	9.586	0.902	0.828	0.054	17.865
SCP	0.900	0.813	0.061	4.041	0.900	0.767	0.083	9.500	0.900	0.787	0.073	17.722
$1 - \alpha = 85\%$												
MOPI	0.853	0.799	0.044	2.901	0.853	0.801	0.042	7.064	0.852	0.795	0.043	12.313
CC	0.846	0.780	0.056	3.780	0.848	0.788	0.053	9.204	0.848	0.785	0.053	17.320
RLCP	0.850	0.774	0.061	3.777	0.850	0.751	0.073	9.117	0.851	0.764	0.066	17.188
SCP	0.849	0.746	0.074	3.759	0.850	0.692	0.103	9.020	0.850	0.713	0.092	16.992

Group-conditional coverage. We now investigate group-conditional coverage for the box-shaped prediction sets, where the groups are defined as $G_k = [k - 1, k)$ for $k =$

1, \dots, 5. Let $Z = (\mathbb{1}\{X \in G_1\}, \dots, \mathbb{1}\{X \in G_5\})$. For this experiment, we choose \mathcal{F} and \mathcal{H} in MOPI, \mathcal{F} in CC, to be the same parametric function class $\{\beta^\top z : \beta \in \mathbb{R}^5\}$. Let $\sigma_{0,k}$ be the empirical standard deviation of pretraining labels $\{Y_i : X_i \in G_k\}_{i \in \mathcal{D}_{\text{pre}}}$ for $k = 1, \dots, 5$, where $|\mathcal{D}_{\text{pre}}| = 1,500$. For baseline methods, the score function is defined as $s(X, y) = \|(y - \mu_0(X))/\sigma_0(X)\|_\infty$, where $\mu_0(X)$ is a pretrained random forest model and $\sigma_0(X) = \sum_{k=1}^5 \sigma_{0,k} \mathbb{1}\{X \in G_k\}$ is a piecewise constant function derived from the pretraining set. Following the same normalization as in the previous experiment, MOPI first computes $\tilde{y} = (y - \mu_0(X))/\sigma_0(X)$. It then constructs structured prediction sets by instantiating the general form in (3) as $\mathfrak{C}_{\text{box}} = \{C(x; \sigma) = \{y \in \mathbb{R}^{d_y} : \|\tilde{y}/\sigma(x)\|_\infty \leq 1\} : \sigma \in \mathcal{H}\}$. We evaluate each method by computing the group-conditional coverage rates: $(\sum_{i \in \mathcal{D}_{\text{test}}} \mathbb{1}\{X_i \in G_k\})^{-1} \sum_{i \in \mathcal{D}_{\text{test}}} \mathbb{1}\{X_i \in G_k, Y_i \in \hat{C}(X_i)\}$ for $k = 1, \dots, 5$. The simulation results are reported in Figure 2, where the sample size of calibration set is $|\mathcal{D}_{\text{cal}}| = 1,500$. Overall, MOPI achieves group-conditional coverage rates that are closer to the nominal level than those of the baseline methods. Moreover, MOPI yields box prediction regions with consistently smaller sizes across groups than the baselines.

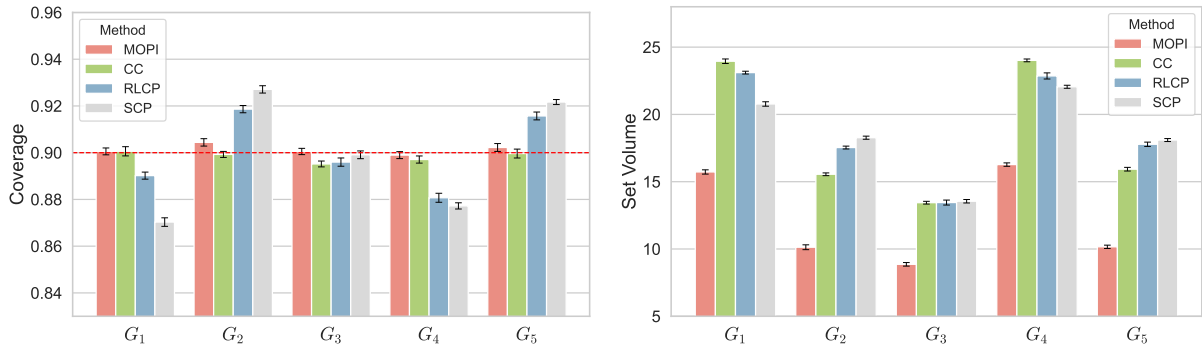


Figure 2: Group-conditional coverage rates and set sizes under *box* sets and $d_y = 2$. The error bars represent the standard deviation of the metrics over 100 replications.

5.2 Sublevel sets for equalized coverage on sensitive attributes

In this subsection, we consider the equalized coverage problem described in Example 2.3, where the sensitive attribute Z is unobserved in the test data. We construct prediction

sets using the sublevel set formulation in (7) based on a pretrained score function $s(x, y)$. Here, we use a pretraining set with size $|\mathcal{D}_{\text{pre}}| = 3,000$ to fit a linear model $\mu(x)$ and adopt the absolute residual score function $s(x, y) = |y - \mu(x)|$. Then, using the calibration set with size $|\mathcal{D}_{\text{cal}}| = 1,500$, we construct the prediction sets for all methods based on the same pretrained score. The size of test data is $|\mathcal{D}_{\text{test}}| = 500$. The data are generated from a heteroscedastic regression model $Y = \mu^*(X, Z) + \varepsilon(X, Z)$ with $\varepsilon(X, Z) \sim \text{N}(0, \sigma^*(X, Z)^2)$ and $X = (X_1, \dots, X_{11})^\top$, where X_1 is independently drawn from $\text{Unif}(0, 5)$, and X_2, \dots, X_{11} are independently drawn from $\text{N}(0, 1)$. We consider the following two settings:

- **Setting 1:** $\mu^*(X, Z) = \sum_{j=1}^{11} \frac{1}{\sqrt{11}} X_j + 0.5Z$ and $\sigma^*(X, Z)^2 = 1 + Z^2 + 0.5 \times \sin(\sum_{j=2}^{11} X_j)$ with $Z = \mathbb{1}\{X_1 \leq 2.5\}$ and $\mathcal{Z} = \{0, 1\}$.
- **Setting 2:** $\mu^*(X, Z) = \mu_Z^*(X)$ and $\sigma^*(X, Z) = \sigma_Z^*(X)$ for $Z \in \mathcal{Z} = \{1, 2, 3, 4\}$, where $Z | X \sim \text{Cat}(\pi_1^*(X), \dots, \pi_4^*(X))$, and $\text{Cat}(\cdot, \dots, \cdot)$ denotes the categorical distribution. The functions $\{\mu_z^*(X), \sigma_z^*(X), \pi_z^*(X)\}_{z=1}^4$ are given in Appendix F.2.

For MOPI, we take the weight function class as $\mathcal{F} = \{\sum_{z \in \mathcal{Z}} \beta_z \mathbb{1}\{Z = z\} : \beta_z \in \mathbb{R}\}$. For the comparison, we let \mathcal{H} in MOPI and \mathcal{F} in CC be the same RKHS on \mathcal{X} equipped with a Gaussian kernel. We report the conditional coverage rate for each sensitive attribute value $z \in \mathcal{Z}$, which should reach the nominal level $1 - \alpha = 90\%$.

The experiment results are reported in Figure 3. We can see that MOPI attains the best equalized coverage in both settings, again without sacrificing marginal coverage. In **Setting 1**, where Z is a deterministic function of X , both CC and RLCP show moderate improvements in equalized coverage over SCP. However, in **Settings 2**, where Z is correlated with X but not a deterministic function of it, CC and RLCP largely fail to leverage the information in Z to improve equalized coverage. This limitation arises because these methods cannot incorporate information about Z during the calibration stage. In contrast, MOPI effectively utilizes the available calibration-stage information about Z , thereby achieving

substantially better equalized coverage.

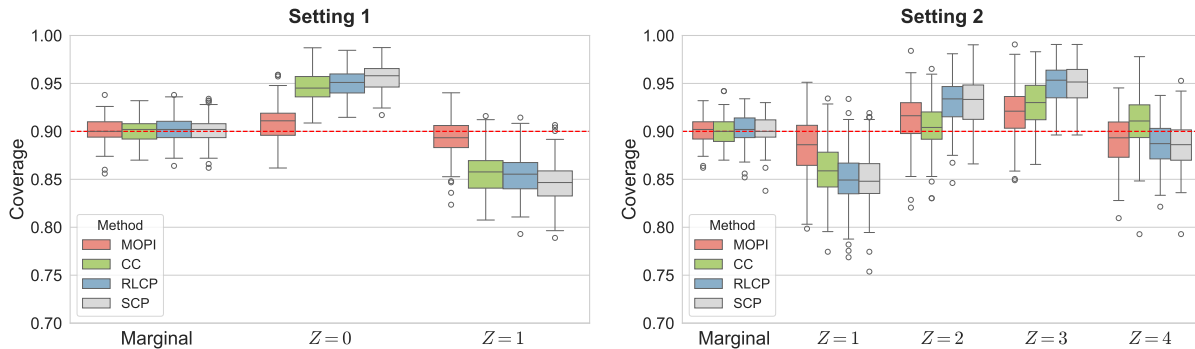


Figure 3: Marginal coverage rate and conditional coverage rates on sensitive attributes.

Now, we empirically investigate the impact of the dependence between X and Z on conditional coverage performance under the following setting.

- **Setting 1'**: $\mu^*(X, Z)$ and $\sigma^*(X, Z)^2$ are the same as **Setting 1**, where $Z = \mathbb{1}\{\rho^*X_1 + (1 - \rho^*)V \leq 2.5\rho^*\}$, where $V \sim N(0, 1)$ and $\rho^* \in \{0, 0.25, 0.5, 0.75, 1\}$.

The dependence between the conditioning variable Z and the covariate X increases monotonically with ρ^* , which plays a similar role to ρ^2 in Theorem 4.2. When $\rho^* = 1$, Z is a deterministic function of X ; when $\rho^* = 0$, Z is independent of X . As shown in Figure 4, for all values of ρ^* , the proposed MOPI method consistently achieves better conditional coverage than the three baseline approaches. The simulation results are consistent with the theoretical insight in Theorem 4.2 and Corollary 4.2 that a larger correlation of Z and X leads to smaller MSCE and conditional coverage gap.

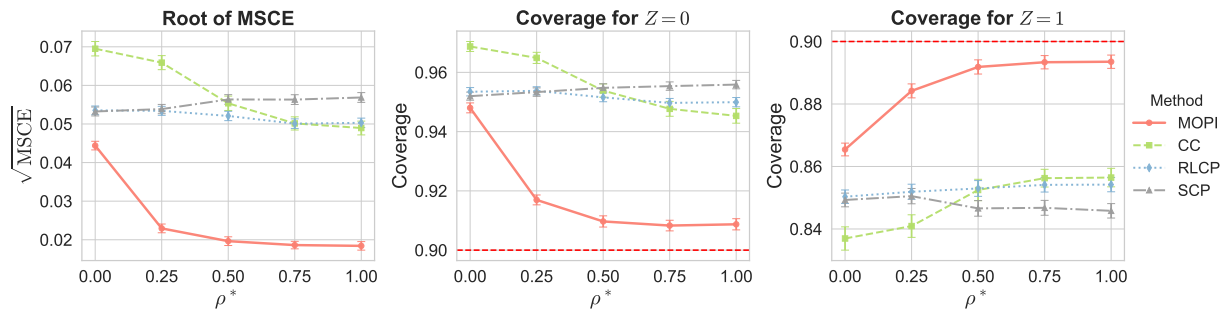


Figure 4: Root of MSCE and conditional coverage rates under **Setting 1'** as ρ^* varies. The error bars represent the standard deviation of the metrics over 100 replications.

6 Real Data Analysis

In this section, we examine the performance of MOPI and three baseline methods on two real-world datasets. The additional experiment results are deferred to Appendix G.

6.1 Households dataset

In this subsection, we consider the Households Dataset, a multivariate response dataset previously analyzed in Dheur et al. (2025). The response dimension is $d_y = 2$, corresponding to expenditures on housing and health. The covariates include five household characteristics, expenditures on transportation, entertainment, food, utilities, and household income. The full dataset consists of 7,207 observations. Due to the wide numerical ranges, we apply a logarithmic transformation to both the labels and the covariates.

In this experiment, we focus on constructing ellipsoidal prediction sets. In each repetition, we split the dataset into three parts: pretraining set with size $|\mathcal{D}_{\text{pre}}| = 3,460$, calibration set with size $|\mathcal{D}_{\text{cal}}| = 2,307$, and test set with size $|\mathcal{D}_{\text{test}}| = 1,440$. The experiment is repeated 100 times with random splits, and the target coverage level is $1 - \alpha = 90\%$. The baseline methods use the score function $s(x, y) = (y - \mu_0(x))^\top \Sigma_0^{-1}(x)(y - \mu_0(x))$, where $\mu_0(x)$ is a random forest predictor and $\Sigma_0(x)$ is a neural network fitted on the pretraining data. The detailed formulation of the pretraining loss is provided in Appendix G.1. For CC, the function space is chosen to be an RKHS with a Gaussian kernel, and RLCP is implemented using the same Gaussian kernel. For MOPI, we take \mathcal{F} to be an RKHS equipped with a Gaussian kernel, and \mathcal{H} to be the class of neural networks with the same architecture used to estimate $\Sigma_0(x)$.

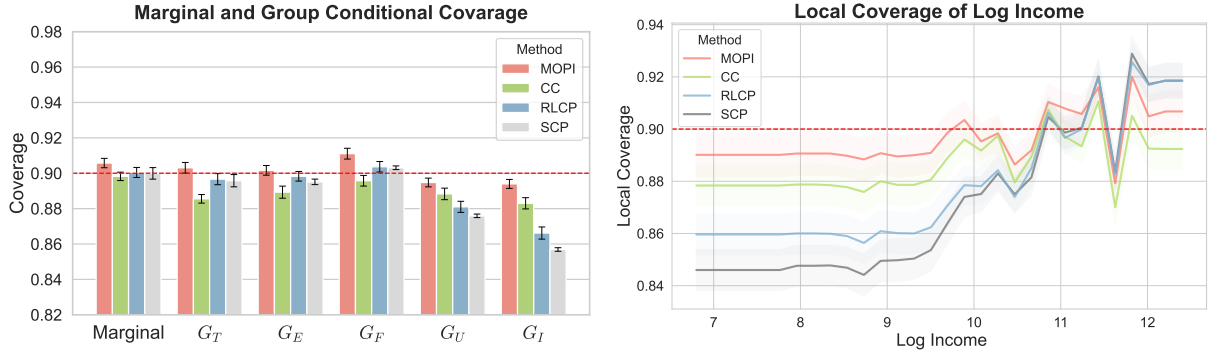


Figure 5: Coverage comparison for the Households dataset. The error bars (left) show the standard deviation, and the confidence bands (right) represent approximate 95% normal confidence intervals, both computed over 100 replications.

We evaluate two metrics to assess test-conditional coverage. (i) *Group-conditional coverage*: we consider subpopulations corresponding to low expenditure or income levels across five covariates described above. Specifically, for each covariate, we define the “low” group as those observations whose value falls below the 10th percentile of that covariate over the full sample, denoted by $\{G_T, G_E, G_F, G_U, G_I\}$, where the subscripts denote the initials of the five covariates described above, respectively. (ii) *Local coverage of log income*: we partition the range of the household income into 30 evenly spaced grid points and compute the coverage rate at each point using the nearest 5% of test samples. From Figure 5, we observe that MOPI achieves coverage that is generally close to the nominal level across most groups while maintaining marginal validity. Moreover, the local coverage of log income shows that MOPI provides more uniform coverage across income levels.

6.2 Communities and Crime dataset

In this subsection, we focus on the Communities and Crime dataset (Redmond and Baveja, 2002), in which the objective is to predict each community’s per-capita violent crime rate from its demographic and socioeconomic characteristics. Following Gibbs et al. (2025), we consider a concise set of explanatory variables, including population size, unemployment rate, median household income, percentage of residents with limited English

proficiency, racial composition (the proportions of Black, White, Asian, and Hispanic categories, denoted as $X_{\%Black}$, $X_{\%White}$, $X_{\%Asian}$, and $X_{\%Hispanic}$, respectively), and age structure (the shares of individuals aged 12–21 and those over 65). Let X^{all} denote the collection of all covariates listed above, and define the racial composition variables as $X^{\text{racial}} = (X_{\%Black}, X_{\%White}, X_{\%Asian}, X_{\%Hispanic})$. This vector X^{racial} serves as the conditioning variable Z . In this experiment, we consider the sublevel sets defined in (7) with the pretrained score $s(x, y) = |y - \mu_0(x)|$, where μ_0 is fitted on the pretraining set. The experiment is repeated 100 times with random splits. In each repetition, we split the original dataset into three parts: a pretraining set of size $|\mathcal{D}_{\text{pre}}| = 650$, a calibration set of size $|\mathcal{D}_{\text{cal}}| = 650$, and a test set of size $|\mathcal{D}_{\text{test}}| = 694$.

We set both \mathcal{H} and \mathcal{F} in MOPI to be the same RKHS with Gaussian kernels. RLCP is implemented using the same Gaussian kernel. We compute the linear re-weighting coverage of each racial group (Gibbs et al., 2025) defined as $\sum_{i \in \mathcal{D}_{\text{test}}} \frac{X_{i,j}^{\text{racial}}}{\sum_{i \in \mathcal{D}_{\text{test}}} X_{i,j}^{\text{racial}}} \mathbb{1}\{Y_i \in \hat{C}(X_i)\}$, $j = 1, \dots, 4$, where $X_{i,j}^{\text{racial}}$ denotes the proportion of racial group j in community i . We consider two experimental settings. In the *unmasked* case, both the calibration and test datasets contain the full set of covariates, including racial and demographic attributes. This corresponds to the case $X = X^{\text{all}}$ and $Z = X^{\text{racial}}$. In this case, we implement CC under the same configuration as in Gibbs et al. (2025). Specifically, we choose the function class $\mathcal{F} = \{\beta_0 + Z^\top \beta + f(X) : f \in \mathbb{H}, \beta_0 \in \mathbb{R}, \beta \in \mathbb{R}^4\}$, where \mathbb{H} is an RKHS equipped with a Gaussian kernel. In the *masked* case, the sensitive attribute is unobserved at test time. This corresponds to the scenario where $X = X^{\text{all}} \setminus X^{\text{racial}}$ and $Z = X^{\text{racial}}$. Since Z is unobserved in test data, we adopt the function class $\mathcal{F} = \{\beta_0 + f(X) : f \in \mathbb{H}, \beta_0 \in \mathbb{R}\}$ for CC. The hyperparameters of each method are selected via cross-validation on the calibration data by minimizing the linearly reweighted coverage error, meaning that baseline methods can also leverage information from sensitive attributes during calibration.

The experiment results are reported in Figure 6. In the unmasked case, both MOPI

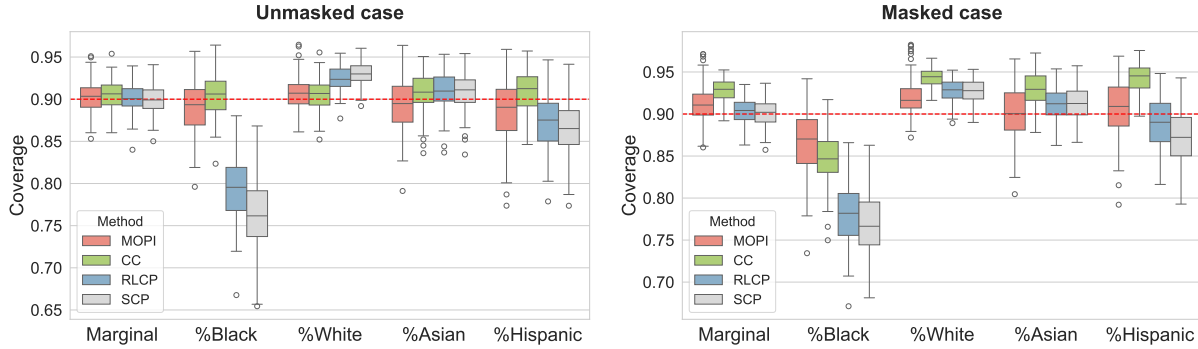


Figure 6: Marginal and linear re-weighting coverage for the Communities and Crime dataset. The box plots are obtained from 100 replications with random data splits.

and CC successfully achieve the target coverage level across all four racial groups. In the masked case, the baseline methods fail to maintain the desired coverage across different racial subgroups. By contrast, since MOPI can leverage Z during the minimax optimization phase, it achieves better and more balanced coverage across racial groups than baselines.

7 Concluding Remarks

Two promising directions remain for future work. First, the miscoverage indicator in objective (8) results in a nonconvex optimization problem; it would thus be meaningful to explore convex surrogate losses and analyze the corresponding theoretical properties, as has been done in classification contexts (Bartlett et al., 2006). Second, while the prediction sets in this paper are constructed to satisfy Z -conditional coverage, a challenging open problem is how to simultaneously optimize the efficiency of a downstream task under the same conditional coverage constraint, such as volume efficiency (Braun et al., 2025) and decision efficiency (Bao et al., 2025).

SUPPLEMENTARY MATERIAL

The supplementary material contains the implementation details of MOPI, more comparisons with the conditional calibration method, proofs of theoretical results, and additional

experimental results.

References

- Andrews, D. W. and Shi, X. (2013), “Inference based on conditional moment inequalities,” *Econometrica*, 81, 609–666.
- Angelopoulos, A. N., Barber, R. F., and Bates, S. (2024), “Theoretical foundations of conformal prediction,” *arXiv preprint arXiv:2411.11824*.
- Areces, F., Cheng, C., Duchi, J., and Rohith, K. (2024), “Two fundamental limits for uncertainty quantification in predictive inference,” in *The Thirty Seventh Annual Conference on Learning Theory*, PMLR, pp. 186–218.
- Bai, Y., Mei, S., Wang, H., Zhou, Y., and Xiong, C. (2022), “Efficient and differentiable conformal prediction with general function classes,” in *International Conference on Learning Representations*.
- Bao, Y., Hu, Y., Ren, H., Zhao, P., and Zou, C. (2025), “Optimal model selection for conformalized robust optimization,” *arXiv preprint arXiv:2507.04716*.
- Barber, R. F., Candès, E. J., Ramdas, A., and Tibshirani, R. J. (2021), “The limits of distribution-free conditional predictive inference,” *Information and Inference: A Journal of the IMA*, 10, 455–482.
- Bartlett, P. L., Bousquet, O., and Mendelson, S. (2005), “Local Rademacher complexities,” *The Annals of Statistics*, 33, 1497 – 1537.
- Bartlett, P. L., Harvey, N., Liaw, C., and Mehrabian, A. (2019), “Nearly-tight VC-dimension and pseudodimension bounds for piecewise linear neural networks,” *Journal of Machine Learning Research*, 20, 1–17.
- Bartlett, P. L., Jordan, M. I., and McAuliffe, J. D. (2006), “Convexity, classification, and risk bounds,” *Journal of the American Statistical Association*, 101, 138–156.
- Ben-Tal, A., Ghaoui, L., and Nemirovski, A. (2009), *Robust Optimization*, Princeton Series in Applied Mathematics, Princeton University Press.
- Bennett, A. and Kallus, N. (2023), “The variational method of moments,” *Journal of the Royal Statistical Society Series B: Statistical Methodology*, 85, 810–841.
- Braun, S., Aolaritei, L., Jordan, M. I., and Bach, F. (2025), “Minimum volume conformal sets for multivariate regression,” *arXiv preprint arXiv:2503.19068*.
- Chernozhukov, V., Wüthrich, K., and Zhu, Y. (2021), “Distributional conformal prediction,” *Proceedings of the National Academy of Sciences*, 118, e2107794118.
- Dheur, V., Fontana, M., Estievenart, Y., Desobry, N., and Ben Taieb, S. (2025), “A Unified Comparative Study with Generalized Conformity Scores for Multi-Output Conformal Regression,” in *International Conference on Machine Learning*, PMLR, vol. 267, pp. 13444–13485.
- Dikkala, N., Lewis, G., Mackey, L., and Syrgkanis, V. (2020), “Minimax estimation of conditional moment models,” *Advances in Neural Information Processing Systems*, 33, 12248–12262.

- Feldman, S., Bates, S., and Romano, Y. (2023), “Calibrated multiple-output quantile regression with representation learning,” *Journal of Machine Learning Research*, 24, 1–48.
- Gibbs, I., Cherian, J. J., and Candès, E. J. (2025), “Conformal prediction with conditional guarantees,” *Journal of the Royal Statistical Society Series B: Statistical Methodology*, 87, 1100–1126.
- Guan, L. (2023), “Localized conformal prediction: A generalized inference framework for conformal prediction,” *Biometrika*, 110, 33–50.
- Györfi, L. and Walk, H. (2019), “Nearest neighbor based conformal prediction,” *Annales de l’ISUP*, 63, 173–190.
- Hébert-Johnson, U., Kim, M., Reingold, O., and Rothblum, G. (2018), “Multicalibration: Calibration for the (computationally-identifiable) masses,” in *International Conference on Machine Learning*, PMLR, pp. 1939–1948.
- Hore, R. and Barber, R. F. (2025), “Conformal prediction with local weights: randomization enables robust guarantees,” *Journal of the Royal Statistical Society Series B: Statistical Methodology*, 87, 549–578.
- Johnstone, C. and Cox, B. (2021), “Conformal uncertainty sets for robust optimization,” in *Conformal and Probabilistic Prediction and Applications*, PMLR, pp. 72–90.
- Jung, C., Noarov, G., Ramalingam, R., and Roth, A. (2023), “Batch multivald conformal prediction,” in *International Conference on Learning Representations*.
- Kallus, N., Mao, X., and Uehara, M. (2021), “Causal inference under unmeasured confounding with negative controls: A minimax learning approach,” *arXiv preprint arXiv:2103.14029*.
- Kiyani, S., Pappas, G. J., and Hassani, H. (2024a), “Conformal prediction with learned features,” in *International Conference on Machine Learning*, PMLR, pp. 24749–24769.
- (2024b), “Length optimization in conformal prediction,” *Advances in Neural Information Processing Systems*, 37, 99519–99563.
- Koltchinskii, V. and Panchenko, D. (2002), “Empirical margin distributions and bounding the generalization error of combined classifiers,” *The Annals of Statistics*, 30, 1–50.
- Lei, J., G’Sell, M., Rinaldo, A., Tibshirani, R. J., and Wasserman, L. (2018), “Distribution-free predictive inference for regression,” *Journal of the American Statistical Association*, 113, 1094–1111.
- Lei, J., Robins, J., and Wasserman, L. (2013), “Distribution-free prediction sets,” *Journal of the American Statistical Association*, 108, 278–287.
- Lei, J. and Wasserman, L. (2014), “Distribution-free prediction bands for non-parametric regression,” *Journal of the Royal Statistical Society Series B: Statistical Methodology*, 76, 71–96.
- Lin, T., Jin, C., and Jordan, M. (2020), “On gradient descent ascent for nonconvex-concave minimax problems,” in *International Conference on Machine Learning*, PMLR, pp. 6083–6093.
- Lindemann, L., Cleaveland, M., Shim, G., and Pappas, G. J. (2023), “Safe planning in dynamic environments using conformal prediction,” *IEEE Robotics and Automation Letters*, 8, 5116–5123.

- Mason, L., Bartlett, P. L., and Baxter, J. (2000), “Improved generalization through explicit optimization of margins,” *Machine Learning*, 38, 243–255.
- Messoudi, S., Destercke, S., and Rousseau, S. (2022), “Ellipsoidal conformal inference for multi-target regression,” in *Conformal and Probabilistic Prediction with Applications*, PMLR, pp. 294–306.
- Nemirovski, A. (2004), “Prox-method with rate of convergence $O(1/t)$ for variational inequalities with Lipschitz continuous monotone operators and smooth convex-concave saddle point problems,” *SIAM Journal on Optimization*, 15, 229–251.
- Rafique, H., Liu, M., Lin, Q., and Yang, T. (2022), “Weakly-convex-concave min-max optimization: provable algorithms and applications in machine learning,” *Optimization Methods and Software*, 37, 1087–1121.
- Romano, Y., Barber, R. F., Sabatti, C., and Candès, E. (2020), “With malice toward none: Assessing uncertainty via equalized coverage,” *Harvard Data Science Review*, 2, <https://hdsr.mitpress.mit.edu/pub/qedrwcz3>.
- Romano, Y., Patterson, E., and Candès, E. (2019), “Conformalized quantile regression,” *Advances in Neural Information Processing Systems*, 32, 1–11.
- Sesia, M. and Romano, Y. (2021), “Conformal prediction using conditional histograms,” *Advances in Neural Information Processing Systems*, 34, 6304–6315.
- Shi, C., Uehara, M., Huang, J., and Jiang, N. (2022), “A minimax learning approach to off-policy evaluation in confounded partially observable markov decision processes,” in *International Conference on Machine Learning*, PMLR, pp. 20057–20094.
- Sun, C., Liu, L., and Li, X. (2023), “Predict-then-calibrate: A new perspective of robust contextual lp,” *Advances in Neural Information Processing Systems*, 36, 17713–17741.
- Thurin, G., Nadjahi, K., and Boyer, C. (2025), “Optimal transport-based conformal prediction,” *arXiv preprint arXiv:2501.18991*.
- Vazquez, J. and Facelli, J. C. (2022), “Conformal prediction in clinical medical sciences,” *Journal of Healthcare Informatics Research*, 6, 241–252.
- Vovk, V. (2012), “Conditional validity of inductive conformal predictors,” in *Asian Conference on Machine Learning*, PMLR, pp. 475–490.
- Vovk, V., Gammerman, A., and Shafer, G. (2005), *Algorithmic Learning in A Random World*, vol. 29, Springer.
- Wainwright, M. J. (2019), *High-Dimensional Statistics: A Non-Asymptotic Viewpoint*, vol. 48, Cambridge University Press.
- Wu, J., Hu, D., Bao, Y., Xia, S.-T., and Zou, C. (2025), “Error-quantified conformal inference for time series,” in *International Conference on Learning Representations*.
- Zafar, M. B., Valera, I., Ródriguez, M. G., and Gummadi, K. P. (2017), “Fairness constraints: Mechanisms for fair classification,” in *International Conference on Artificial Intelligence and Statistics*, PMLR, pp. 962–970.
- Zhang, B. H., Lemoine, B., and Mitchell, M. (2018), “Mitigating unwanted biases with adversarial learning,” in *Proceedings of the 2018 AAAI/ACM Conference on AI, Ethics, and Society*, pp. 335–340.

Supplementary Material for “Shape-Adaptive Conditional Calibration for Conformal Prediction via Minimax Optimization”

A Implementation of MOPI

A.1 The effect of L_2 penalty coefficient

In this section, we consider a more general form of (4):

$$\Psi_\lambda(C, f) := \mathbb{E} \left[f(Z)(\mathbb{1}\{Y \notin C(X)\} - \alpha) - \lambda f^2(Z) \right], \quad (\text{A.1})$$

and therefore (4) is a special case of (A.1) with $\lambda = 1$. Depending on the cardinality of \mathcal{Z} , we choose different \mathcal{F} and admit close forms of $\max_{f \in \mathcal{F}} \Psi_\lambda(C, f)$.

Lemma A.1. *If the cardinality of \mathcal{Z} is finite and $\mathcal{F} = \{\sum_{z \in \mathcal{Z}} \beta_z \mathbb{1}\{Z = z\} : \beta_z \in \mathbb{R}, z \in \mathcal{Z}\}$, then for any $C \in \mathfrak{C}$ we have*

$$\max_{f \in \mathcal{F}} \Psi_\lambda(C, f) = \sum_{z \in |\mathcal{Z}|} \frac{\left(\mathbb{E} \left[\mathbb{1}\{Z = z\}(\mathbb{1}\{Y \notin C(X)\} - \alpha) \right] \right)^2}{4\lambda \mathbb{P}(Z = z)}.$$

Lemma A.2. *If the cardinality of \mathcal{Z} is infinite and $\mathcal{F} = \mathbb{K}$ as the RKHS with the kernel function $\mathcal{K}(\cdot, \cdot) : \mathcal{Z} \times \mathcal{Z} \rightarrow \mathbb{R}$. For $u, v, h \in \mathbb{K}$, let $\langle u(\cdot), v(\cdot) \rangle_{\mathbb{K}}$ be the inner product in RKHS and define $(u \otimes v)(h) = \langle h, v \rangle_{\mathbb{K}} u$. Suppose $\alpha(\cdot; C) - \alpha \in \mathcal{F}$ for all $C \in \mathfrak{C}$, then we have*

$$\max_{f \in \mathcal{F}} \Psi_\lambda(C, f) = \frac{1}{4\lambda} \left\langle \mathbb{E}[\mathcal{K}(\cdot, Z)\{\alpha(Z; C) - \alpha\}], \mathcal{T}^{-1} \mathbb{E}[\mathcal{K}(\cdot, Z)\{\alpha(Z; C) - \alpha\}] \right\rangle_{\mathbb{K}},$$

where $\mathcal{T}(\cdot) = \mathbb{E}[\mathcal{K}(\cdot, Z) \otimes \mathcal{K}(\cdot, Z)]$.

From the two lemmas above, we see that when the function class \mathcal{F} is restricted to a finite-

dimensional space or an RKHS according to the cardinality of \mathcal{Z} , the inner maximization problem admits a closed-form solution. Moreover, the parameter λ only rescales the objective function and does not affect the optimizer.

Align with (A.1), consider the following empirical objective function:

$$\widehat{\Psi}_\lambda(C, f) = \frac{1}{n} \sum_{i=1}^n f(Z_i) (\mathbb{1}\{Y_i \notin C(X)\} - \alpha) - \frac{\lambda}{n} \sum_{i=1}^n f^2(Z_i),$$

where $\lambda > 0$ is a hyperparameter. The empirical minimax optimization problem can be written as:

$$\arg \min_{C \in \mathfrak{C}} \max_{f \in \mathcal{F}} \left\{ \widehat{\Psi}_\lambda(C, f) - \gamma \|f\|_{\mathcal{F}}^2 \right\}. \quad (\text{A.2})$$

Hence, problem (8) is a special case of (A.2) by letting $\lambda = 1$. For finite dimensional \mathcal{F} , we let $\gamma = 0$ and $\mathcal{F} = \{\sum_{z \in \mathcal{Z}} \beta_z \mathbb{1}\{Z = z\} : \beta_z \in \mathbb{R}, z \in \mathcal{Z}\}$, by Lemma C.2, the (A.2) can be rewritten as:

$$\arg \min_{C \in \mathfrak{C}} \left\{ \sum_{z \in \mathcal{Z}} \frac{\left(\sum_{i=1}^n \mathbb{1}\{Z_i = z\} (\mathbb{1}\{Y_i \notin C(X_i)\} - \alpha) \right)^2}{4\lambda n \sum_{i=1}^n \mathbb{1}\{Z_i = z\}} \right\}.$$

Since λ only acts as a multiplicative scaling factor in the objective, its value does not affect the optimizer. Similarly, For $\mathcal{F} = \mathbb{K}$ is a RKHS, by Lemma C.3, the (A.2) can be rewritten as:

$$\arg \min_{C \in \mathfrak{C}} \left\{ \frac{1}{4\lambda} \varphi_n(C)^\top \mathbf{K}_n \left(\frac{1}{n} \mathbf{K}_n + \underbrace{\gamma/\lambda \mathbf{I}_n}_{:=\tilde{\gamma}} \right)^{-1} \varphi_n(C) \right\}.$$

Thus, by reparameterizing γ as $\tilde{\gamma} = \gamma/\lambda$, the parameter λ still only rescales the objective function and does not affect the resulting optimal solution. Consequently, throughout this paper we set $\lambda = 1$ both theoretically and empirically.

A.2 Sensitive analysis of smoothing parameter

To study the effect of the smoothing parameter r on the resulting prediction sets, we consider **Setting 1**(x) and apply the sigmoid surrogate with different values of r . The experimental setup is identical to that in Section F.3.

As shown in Figure A.1, the Root of MSCE decreases rapidly as r decreases and attains its minimum around $r = 0.1$. At the same time, both the marginal coverage and the worst-case conditional coverage decrease from over-coverage to values close to the nominal level. As r is further reduced, the Root of MSCE increases slowly with a mild slope, and the changes in marginal and worst-case conditional coverage remain limited. Moreover, the error bars indicate that smaller values of r lead to larger variability in coverage. This is expected, since a smaller r shrinks the region where the smooth surrogate has non-negligible gradients, which in turn makes the optimization more unstable.

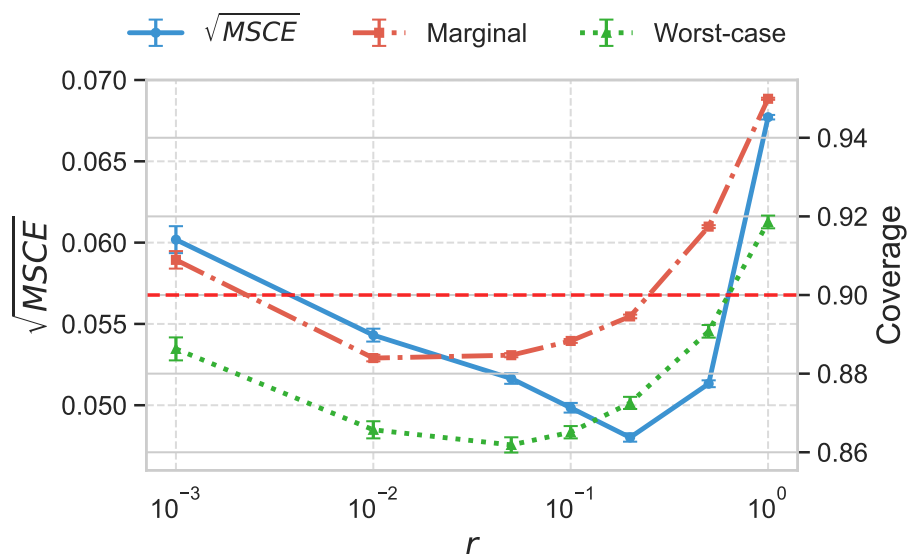


Figure A.1: Root of MSCE, Marginal coverage and Worst-case conditional coverage as smoothing parameter r varies. Dots and error bars represent the means and confidence intervals over 300 trials.

Overall, these results suggest that in practice one should choose a relatively small—but not excessively small—smoothing parameter, depending on the available labeled sample

size. Moreover, MOPI appears to be reasonably robust to the choice of r over a moderate range, without requiring precise tuning of the optimal value.

B More Comparison with Conditional Calibration

B.1 Theoretical comparison under sublevel sets

In this section, we compare the MSCE performance of the quantile regression approach and MOPI. For test-conditional coverage with $Z = X$ consider the sublevel set (7), and set $\mathcal{H} = \mathcal{F}$ in MOPI for a fair comparison. For a sufficiently large \mathcal{F} such that $\alpha(X, C) - \alpha \in \mathcal{F}$ for all $C \in \mathfrak{C} = \{C(X; f) = \{y : s(X, y) \leq f(X)\}, f \in \mathcal{F}\}$, by proposition 2.1, we have $\max_{f \in \mathcal{F}} \Psi(C, f) = \text{MSCE}(C)/4$. Therefore,

$$C^* := \arg \min_{C \in \mathfrak{C}} \max_{f \in \mathcal{F}} \Psi(C, f) = \arg \min_{C \in \mathfrak{C}} \frac{1}{4} \text{MSCE}(C) := C^{\text{ora}}.$$

On the other hand, the quantile regression predictor is given by $C^{\text{qr}}(X) := \{y \in \mathcal{Y} : s(X, y) \leq f^{\text{qr}}(X)\}$ where $f^{\text{qr}} = \arg \min_{f \in \mathcal{F}} \mathbb{E}[\ell_\alpha(s(X, Y), f(X))]$. By the optimality of C^{ora} , it follows that

$$\text{MSCE}(C^*) = \text{MSCE}(C^{\text{ora}}) \leq \text{MSCE}(C^{\text{qr}}).$$

Therefore, the minimax solution C^* achieves lower MSCE compared with C^{qr} . Let $q(x) = \inf\{t \in \mathbb{R} : \mathbb{P}(s(X, Y) \leq t \mid X = x) \geq 1 - \alpha\}$ be the ground truth quantile function. Next, we investigate when the MSCE of C^* and C^{qr} equals zero. If $q \in \mathcal{F}$, by the definition of q , we have $\text{MSCE}(C(X; q)) = 0$. Hence, under the condition of proposition 2.1:

$$0 \leq \text{MSCE}(C^*) = \text{MSCE}(C^{\text{ora}}) \leq \text{MSCE}(C(X; q)) = 0.$$

Let $f_x = f(x)$ for any fixed $x \in \mathcal{X}$. Note that $\mathbb{E}[\ell_\alpha(s(X, Y), f(X)) \mid X = x] = \mathbb{E}[\ell_\alpha(s(X, Y), f_x) \mid X = x]$, consider the following point-wise optimization:

$$\min_{f_x \in \mathbb{R}} \mathbb{E}[\ell_\alpha(s(X, Y), f_x) \mid X = x].$$

Then, the first order condition of above optimization problem is

$$\frac{\partial}{\partial f_x} \mathbb{E}[\ell_\alpha(s(X, Y), f_x) \mid X = x] = \mathbb{P}\{s(X, Y) < f_x \mid X = x\} - (1 - \alpha) = 0,$$

Hence, the optimal solution is $q(x)$ for a fixed $x \in \mathcal{X}$ by the definition of $q(x)$. If $q \in \mathcal{F}$, note that

$$\begin{aligned} \min_{f \in \mathcal{F}} \mathbb{E}[\ell_\alpha(s(X, Y), f(X))] &\leq \mathbb{E}[\ell_\alpha(s(X, Y), q(X))] \\ &= \mathbb{E}_X [\mathbb{E}[\ell_\alpha(s(X, Y), q(x)) \mid X = x]] \\ &= \mathbb{E}_X \left[\min_{f_x \in \mathbb{R}} \mathbb{E}[\ell_\alpha(s(X, Y), f_x) \mid X = x] \right]. \end{aligned}$$

On the other hand, $\mathbb{E}[\ell_\alpha(s(X, Y), f_x) \mid X = x] \geq \mathbb{E}[\ell_\alpha(s(X, Y), q(x)) \mid X = x]$, by the optimality of $q(x)$. Taking expectation on both side and minimize over $f \in \mathcal{F}$, we have

$$\min_{f \in \mathcal{F}} \mathbb{E}[\ell_\alpha(s(X, Y), f(X))] \geq \mathbb{E}[\ell_\alpha(s(X, Y), q(X))].$$

Therefore, $f^{\text{qr}}(x) = q(x)$ a.s. for all $x \in \mathcal{X}$. Thus, when $q \in \mathcal{F}$, $\text{MSCE}(C^*) = \text{MSCE}(C^{\text{qr}}) = 0$.

B.2 Computational efficiency of MOPI

In this section, we study the computational efficiency of MOPI. We focus on **Setting 1**, with experimental configurations following Section 5.2.

We consider two variants of CC: CC(full) and CC(non-full). The CC(full) variant follows Gibbs et al. (2025) exactly, solving quantile regression jointly over \mathcal{D}_{cal} and each test point. In contrast, CC(non-full) estimates the score quantile using only \mathcal{D}_{cal} via quantile regression. Both CC(non-full) and MOPI are optimized using the Adam algorithm with the same learning rate and number of iterations. All experiments are conducted on a MacBook Pro equipped with an M4 Pro CPU and 24GB of RAM.

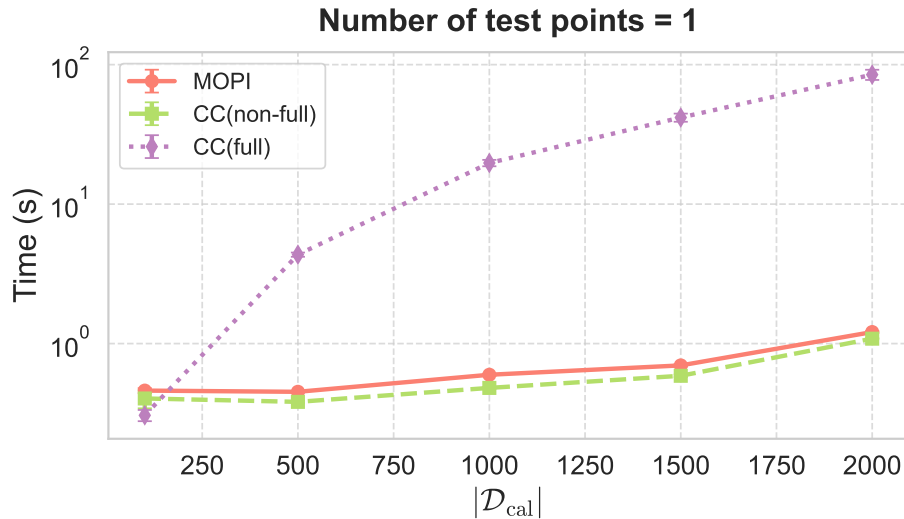


Figure B.1: Comparison of the computational efficiency of MOPI and CC with a single test point. Dots and error bars show means and confidence intervals from 100 trials.

As shown in Figure B.1, the computational time of MOPI is comparable to that of CC(non-full), since both methods solve an optimization problem solely on the calibration dataset. In contrast, CC(full), as a full conformal method, requires solving the optimization problem jointly over the calibration data and each test point, resulting in a computational cost that is several times higher—typically $10\times$ to $100\times$ that of MOPI and CC(non-full). This observation is broadly consistent with the simulation findings reported in Duchi (2025).

C Proofs of Main Results

C.1 Proof of Proposition 2.1

Proposition 2.1 is the special case of Lemma C.1 with $\lambda = 1$.

Lemma C.1. *Let $\Psi_\lambda(C, f) = \mathbb{E}[f(Z)(\mathbb{1}\{Y \notin C(X)\} - \alpha) - \lambda f^2(Z)]$. Then we have $\Psi_\lambda(C, f) \leq \frac{1}{4\lambda} \mathbb{E}[(\alpha(Z; C) - \alpha)^2]$. If for any $C \in \mathfrak{C}$, there exists some $f^* \in \mathcal{F}$ such that $\alpha(Z; C) - \alpha = 2\lambda f^*(Z)$, then it holds that $\max_{f \in \mathcal{F}} \Psi_\lambda(C, f) = \frac{1}{4\lambda} \mathbb{E}[(\alpha(Z; C) - \alpha)^2]$ for any $C \in \mathfrak{C}$. In addition, we also have*

$$\text{MSCE}(C^*) = \text{MSCE}(C^{\text{ora}}). \quad (\text{C.1})$$

Proof. By the definition of Ψ_λ , we have

$$\begin{aligned} \max_{f \in \mathcal{F}} \Psi_\lambda(C, f) &= \max_{f \in \mathcal{F}} \mathbb{E} \left[f(Z)(\mathbb{1}\{Y \notin C(X)\} - \alpha) - \lambda f^2(Z) \right] \\ &= \max_{f \in \mathcal{F}} \mathbb{E} \left[f(Z)(\alpha(Z; C) - \alpha) - \lambda f^2(Z) \right] \\ &= \frac{1}{4\lambda} \mathbb{E} \left[(\alpha(Z; C) - \alpha)^2 \right] - \frac{1}{\lambda} \min_{f \in \mathcal{F}} \mathbb{E} \left[\left(\frac{1}{2}(\alpha(Z; C) - \alpha) - \lambda f(Z) \right)^2 \right] \end{aligned} \quad (\text{C.2})$$

According to the assumption, we know for any $C \in \mathfrak{C}$, $\exists f^* \in \mathcal{F}$ such that $\alpha(Z; C) - \alpha = 2\lambda f^*(Z)$. Therefore,

$$0 \leq \min_{f \in \mathcal{F}} \mathbb{E} \left[(\alpha(Z; C) - \alpha - \lambda f(Z))^2 \right] \leq \mathbb{E} \left[(\alpha(Z; C) - \alpha - \lambda f^*(Z))^2 \right] = 0.$$

Hence by (C.2) we have $\max_{f \in \mathcal{F}} \Psi_\lambda(C, f) = \frac{1}{4\lambda} \mathbb{E}[(\alpha(Z; C) - \alpha)^2]$ for all $C \in \mathfrak{C}$. Taking arg min on both side w.r.t. C ,

$$C^* := \arg \min_{C \in \mathfrak{C}} \max_{f \in \mathcal{F}} \Psi_\lambda(C, f) = \arg \min_{C \in \mathfrak{C}} \frac{1}{4\lambda} \mathbb{E}[(\alpha(Z; C) - \alpha)^2] =: C^{\text{ora}},$$

which indicate $\text{MSCE}(C^*) = \text{MSCE}(C^{\text{ora}})$. \square

C.2 Proof of Lemma 3.1 and 3.2

We consider the empirical minimax problem (A.2) and state the following two Lemmas.

Lemma 3.1 and 3.2 is a special case with $\lambda = 1$.

Lemma C.2. *Let $\mathcal{F} = \{\sum_{z \in \mathcal{Z}} \beta_z \mathbb{1}\{Z = z\} : \beta_z \in \mathbb{R}, z \in \mathcal{Z}\}$. The inner maximization in the problem (A.2) with $\gamma = 0$ is:*

$$\max_{f \in \mathcal{F}} \widehat{\Psi}_\lambda(C, f) = \sum_{z \in \mathcal{Z}} \frac{\left(\sum_{i=1}^n \mathbb{1}\{Z_i = z\} (\mathbb{1}\{Y_i \notin C(X_i)\} - \alpha) \right)^2}{4\lambda n \sum_{i=1}^n \mathbb{1}\{Z_i = z\}}.$$

Lemma C.3. *Let $\mathcal{F} = \mathbb{K}$, where \mathbb{K} is a RKHS equipped with a kernel function $\mathcal{K}(\cdot, \cdot) : \mathcal{Z} \times \mathcal{Z} \rightarrow \mathbb{R}$. Denote $\boldsymbol{\varphi}_n(C) = (\varphi_1(C), \dots, \varphi_n(C))^\top$ where $\varphi_i(C) = \frac{1}{n} (\mathbb{1}\{Y_i \notin C(X_i)\} - \alpha)$ for $i = 1, \dots, n$ and $\mathbf{K}_n = (\mathcal{K}(Z_i, Z_j))_{i,j=1}^n$ be the empirical kernel matrix. Then inner maximization in the problem (A.2) reduces to:*

$$\max_{f \in \mathcal{F}} \left\{ \widehat{\Psi}_\lambda(C, f) - \gamma \|f\|_{\mathcal{F}}^2 \right\} = \frac{1}{4\lambda} \boldsymbol{\varphi}_n(C)^\top \mathbf{K}_n \left(\frac{1}{n} \mathbf{K}_n + \gamma / \lambda \mathbf{I}_n \right)^{-1} \boldsymbol{\varphi}_n(C),$$

where \mathbf{I}_n is an $n \times n$ identity matrix.

Proof of Lemma C.2. Since $\mathcal{F} = \{\sum_{z \in \mathcal{Z}} \beta_z \mathbb{1}\{Z = z\} : \beta_z \in \mathbb{R}, z \in \mathcal{Z}\}$, let $\boldsymbol{\beta} = (\beta_1, \dots, \beta_{|\mathcal{Z}|})^\top$, $\mathbf{1}(Z) = (\mathbb{1}\{Z = z_1\}, \dots, \mathbb{1}\{Z = z_{|\mathcal{Z}|}\})^\top$ and $\varphi_i(C) = \frac{1}{n} (\mathbb{1}\{Y_i \notin C(X_i)\} - \alpha)$, then by choosing $\gamma = 0$ we can rewrite the inner problem of (8) as:

$$\begin{aligned} \sup_{f \in \mathcal{F}} \widehat{\Psi}_\lambda(C, f) &= \sup_{\boldsymbol{\beta} \in \mathbb{R}^{|\mathcal{Z}|}} \frac{1}{n} \sum_{i=1}^n \left[\boldsymbol{\beta}^\top \mathbf{1}(Z_i) n \varphi_i(C) - \lambda \boldsymbol{\beta}^\top \mathbf{1}(Z_i) \mathbf{1}(Z_i)^\top \boldsymbol{\beta} \right] \\ &:= \sup_{\boldsymbol{\beta} \in \mathbb{R}^{|\mathcal{Z}|}} \boldsymbol{\beta}^\top \left(\sum_{i=1}^n \mathbf{1}(Z_i) \varphi_i(C) \right) - \lambda \boldsymbol{\beta}^\top \left(\frac{1}{n} \sum_{i=1}^n \mathbf{1}(Z_i) \mathbf{1}(Z_i)^\top \right) \boldsymbol{\beta}, \end{aligned}$$

which is a quadratic form w.r.t. $\boldsymbol{\beta}$. Moreover, since for $z, z' \in \mathcal{Z}$, $z \neq z'$, we have

$\mathbb{1}\{Z = z\} \cdot \mathbb{1}\{Z = z'\} = 0$. Hence,

$$\frac{1}{n} \sum_{i=1}^n \mathbf{1}(Z_i) \mathbf{1}(Z_i)^\top = \text{Diag} \left(\frac{1}{n} \sum_{i=1}^n \mathbb{1}\{Z_i = z_1\}, \dots, \frac{1}{n} \sum_{i=1}^n \mathbb{1}\{Z_i = z_{|\mathcal{Z}|}\} \right).$$

Assume n is sufficiently large such that $\sum_{i=1}^n \mathbb{1}\{Z_i = z\} > 0$ for all $z \in \mathcal{Z}$. Taking the first order condition, we have the optimizer:

$$\boldsymbol{\beta}^* = \frac{1}{2\lambda} \left(\frac{1}{n} \sum_{i=1}^n \mathbf{1}(Z_i) \mathbf{1}(Z_i)^\top \right)^{-1} \left(\sum_{i=1}^n \mathbf{1}(Z_i) \varphi_i(C) \right)$$

Thus,

$$\begin{aligned} \sup_{f \in \mathcal{F}} \widehat{\Psi}(C, f) &= \sup_{\boldsymbol{\beta} \in \mathbb{R}^{|\mathcal{Z}|}} \boldsymbol{\beta}^\top \left(\sum_{i=1}^n \mathbf{1}(Z_i) \varphi_i(C) \right) - \lambda \boldsymbol{\beta}^\top \left(\frac{1}{n} \sum_{i=1}^n \mathbf{1}(Z_i) \mathbf{1}(Z_i)^\top \right) \boldsymbol{\beta} \\ &= \sum_{z \in \mathcal{Z}} \frac{\left(\sum_{i=1}^n \mathbb{1}\{Z_i = z\} \varphi_i(C) \right)^2}{4\lambda \left(\frac{1}{n} \sum_{i=1}^n \mathbb{1}\{Z_i = z\} \right)} \\ &= \sum_{z \in \mathcal{Z}} \frac{\left(\sum_{i=1}^n \mathbb{1}\{Z_i = z\} (\mathbb{1}\{Y_i \notin C(X_i)\} - \alpha) \right)^2}{4\lambda n \sum_{i=1}^n \mathbb{1}\{Z_i = z\}} \end{aligned}$$

□

Proof of Lemma C.3. Since we let $\mathcal{F} = \mathbb{K}$ and the inner maximization of (A.2) takes form

$$\sup_{f \in \mathcal{F}} \widehat{\Psi}_\lambda(C, f) - \gamma \|f\|_{\mathcal{F}}^2.$$

By the generalized representer theorem (E.g., Schölkopf et al. (2001), Theorem 1), the optimal solution of the inner maximization of (A.2) takes form

$$f^*(z) = \sum_{i=1}^n \alpha_i^* \mathcal{K}(Z_i, z)$$

for some weight $\boldsymbol{\alpha}^* \in \mathbb{R}^n$. Let $\mathbf{K}_n = (\mathcal{K}(Z_i, Z_j))_{i,j=1}^n$ be the empirical kernel matrix. For

any $\boldsymbol{\alpha} = (\alpha_1, \dots, \alpha_n)^\top \in \mathbb{R}^n$, consider a function $f(z) = \sum_{i=1}^n \alpha \mathcal{K}(Z_i, z)$, then we have $\|f\|_{\mathbb{K}}^2 = \boldsymbol{\alpha}^\top \mathbf{K}_n \boldsymbol{\alpha}$, $f(Z_i) = \mathbf{e}_i^\top \mathbf{K}_n \boldsymbol{\alpha}$, where $\mathbf{e}_i \in \{0, 1\}^n$ is the vector with a 1 in the i -th position and 0 elsewhere. Then

$$\frac{1}{n} \sum_{i=1}^n f(Z_i) = \frac{1}{n} \sum_{i=1}^n \boldsymbol{\alpha}^\top \mathbf{K}_n \mathbf{e}_i \mathbf{e}_i^\top \mathbf{K}_n \boldsymbol{\alpha} = \frac{1}{n} \boldsymbol{\alpha}^\top \mathbf{K}_n^2 \boldsymbol{\alpha}.$$

Let $\boldsymbol{\varphi}_n(C) = (\varphi_1(C), \dots, \varphi_n(C))^\top$ where $\varphi_i(C) = \frac{1}{n} (\mathbb{1}\{Y_i \notin C(X_i)\} - \alpha)$ for $i = 1, \dots, n$.

Then we can rewrite the inner problem of (A.2) as:

$$\sup_{f \in \mathcal{F}} \widehat{\Psi}_\lambda(C, f) - \gamma \|f\|_{\mathcal{F}}^2 = \sup_{\boldsymbol{\alpha} \in \mathbb{R}^n} \boldsymbol{\varphi}_n^\top(C) \mathbf{K}_n \boldsymbol{\alpha} - \boldsymbol{\alpha}^\top \mathbf{K}_n \left(\frac{\lambda}{n} \mathbf{K}_n + \gamma \mathbf{I}_n \right) \boldsymbol{\alpha}.$$

Taking the first order condition, we have the optimizer:

$$\boldsymbol{\alpha}^* = \frac{1}{2} \left(\frac{\lambda}{n} \mathbf{K}_n + \gamma \mathbf{I}_n \right)^{-1} \boldsymbol{\varphi}_n(C),$$

and the optimal value:

$$\frac{1}{4} \boldsymbol{\varphi}_n(C)^\top \mathbf{K}_n \left(\frac{\lambda}{n} \mathbf{K}_n + \gamma \mathbf{I}_n \right)^{-1} \boldsymbol{\varphi}_n(C) = \frac{1}{4\lambda} \boldsymbol{\varphi}_n(C)^\top \mathbf{K}_n \left(\frac{1}{n} \mathbf{K}_n + \gamma/\lambda \mathbf{I}_n \right)^{-1} \boldsymbol{\varphi}_n(C).$$

□

C.3 Proof of Theorem 4.1

In the following, we denote $\epsilon^2 := \text{MSCE}(C^{\text{ora}})$, $\widehat{\Psi}_\gamma(C, f) = \widehat{\Psi}(C, f) - \gamma \|f\|_{\mathcal{F}}$. Consider $\mathfrak{C} = \{C(x; h) : h \in \mathcal{H}\}$ be the structure prediction set (3) and a more general minimax problem with the penalty $\|C\|_{\mathcal{H}} = \|h\|_{\mathcal{H}}$, Eq. (D.1), we rewrite it here for convenience.

$$\widehat{C} := \arg \min_{C \in \mathfrak{C}} \max_{f \in \mathcal{F}} \left\{ \widehat{\Psi}_\gamma(C, f) + \nu \|C\|_{\mathcal{H}} \right\}. \quad (\text{C.3})$$

Thus, the Eq. (8) is the special case of (C.3) with $\mu = 0$ and Theorem 4.1 is the special case of the following Theorem C.1.

Theorem C.1. *Suppose the Assumptions 1, 2 holds. Furthermore, assume the constant U satisfies $\sup_{f \in \mathcal{F}_U} \|f\|_\infty \leq 1$. Let $\delta_{n, \mathcal{F}_U}$ and $\delta_{n, \mathcal{G}}$ be the critical radius of \mathcal{F}_U and \mathcal{G} , respectively. For any $\zeta \in (0, 1)$, let $\tilde{\delta}_{n, \mathcal{F}} := \delta_{n, \mathcal{F}_U} + \sqrt{\frac{\log(c_1/\zeta)}{c_2 n}}$ for some positive constants c_1 and c_2 .*

- *For finite-dimensional \mathcal{F} , let the hyperparameter $\gamma = 0$ in (C.3). Then, for sufficiently large n , such that $\tilde{\delta}_{n, \mathcal{F}}^2 \|f\|_{\mathcal{F}}^2 \leq \frac{U}{2} \|f\|_{L_2}^2$ for any $f \in \mathcal{F}$, conditioning on the labeled data \mathcal{D}_n , with probability at least $1 - 4\zeta$, we have:*

$$\begin{aligned} \mathbb{E} \left[\left(\alpha(Z; \hat{C}) - \alpha \right)^2 \mid \mathcal{D}_n \right] &\lesssim \epsilon^2 + \eta^2 + \delta_{n, \mathcal{F}_U}^2 + \delta_{n, \mathcal{G}}^2 \\ &\quad + \frac{\log(\log_2(1/\delta_{n, \mathcal{G}})/\zeta)}{n} + \frac{\nu^2 \|C^{\text{ora}}\|_{\mathcal{H}}^4}{\delta_{n, \mathcal{F}}^2}. \end{aligned}$$

- *For infinite-dimensional \mathcal{F} , if we choose the hyperparameter γ in (C.3) such that $\gamma \|f\|_{\mathcal{F}}^2 \leq \|f\|_{L_2}^2$, then for sufficiently large n , such that $\tilde{\delta}_{n, \mathcal{F}}^2 \|f\|_{\mathcal{F}}^2 \leq \frac{U}{2} \|f\|_{L_2}^2$ for any $f \in \mathcal{F}$, conditioning on the labeled data \mathcal{D}_n , with probability at least $1 - 4\zeta$, we have:*

$$\begin{aligned} \mathbb{E} \left[\left(\alpha(Z; \hat{C}) - \alpha \right)^2 \mid \mathcal{D}_n \right] &\lesssim \epsilon^2 + \eta^2 + \delta_{n, \mathcal{F}_U}^2 + \delta_{n, \mathcal{G}}^2 \\ &\quad + \frac{\log(\log_2(1/\delta_{n, \mathcal{G}})/\zeta)}{n} + \frac{\nu^2 \|C^{\text{ora}}\|_{\mathcal{H}}^4}{\delta_{n, \mathcal{F}}^2}. \end{aligned}$$

Proof of Theorem C.1. Let $\hat{C} = \arg \min_{C \in \mathcal{C}} \max_{f \in \mathcal{F}} \hat{\Psi}_\gamma(C, f) + \nu \|C\|_{\mathcal{H}}$. Notice that

$$\mathbb{E} \left[\left(\alpha(Z; \hat{C}) - \alpha \right)^2 \right] \leq 2\epsilon^2 + 2 \mathbb{E} \left[\left(\alpha(Z; \hat{C}) - \alpha(Z; C^{\text{ora}}) \right)^2 \right], \quad (\text{C.4})$$

where $\mathbb{E}[(\alpha(Z; C^{\text{ora}}) - \alpha)^2] = \epsilon^2$. Let $\mathcal{F}_U = \{f \in \mathcal{F} : \|f\|_{\mathcal{F}}^2 \leq U\}$ and $\delta_{n, \mathcal{F}_U}$ be the critical radius of \mathcal{F}_U . Let $Pf^2 := \|f\|_{L_2}^2 = \mathbb{E}_P[f^2(Z)]$, $P_n f^2 := \|f\|_{L_2, n}^2 = \frac{1}{n} \sum_{i=1}^n f^2(Z_i)$. By

Lemma E.6 and our assumption $\sup_{f \in \mathcal{F}_U} \|f\|_\infty \leq 1$, for any $t \geq \delta_{n, \mathcal{F}_U}$, we have

$$\mathbb{P} \left(\forall f \in \mathcal{F}_U, |P_n f^2 - P f^2| \leq \frac{P f^2}{2} + \frac{t^2}{2} \right) \geq 1 - c_1 e^{-c_2 n t^2},$$

where $c_1, c_2 > 0$ are universal constants. For $f \notin \mathcal{F}_U$, we apply the same exponential inequality to $\sqrt{U}f/\|f\|_{\mathcal{F}}$, then we have

$$\mathbb{P} \left(\forall f \in \mathcal{F}_U, |P_n f^2 - P f^2| \leq \frac{P f^2}{2} + \frac{t^2 \|f\|_{\mathcal{F}}^2}{2U} \right) \geq 1 - c_1 e^{-c_2 n t^2}.$$

Combining the results above and taking $t = \delta_{n, \mathcal{F}_U} + \sqrt{\frac{\log(c_1/\zeta)}{c_2 n}}$ for any $\zeta > 0$, we have w.p. $1 - \zeta$,

$$\forall f \in \mathcal{F}, |P_n f^2 - P f^2| \leq \frac{P f^2}{2} + \frac{1 \vee (\|f\|_{\mathcal{F}}^2/U)}{2} \left(\delta_{n, \mathcal{F}_U} + \sqrt{\frac{\log(c_1/\zeta)}{c_2 n}} \right)^2.$$

Since we choose $\tilde{\delta}_{n, \mathcal{F}} = \delta_{n, \mathcal{F}_U} + \sqrt{\frac{\log(c_1/\zeta)}{c_2 n}}$, and assume $\tilde{\delta}_{n, \mathcal{F}}^2 \|f\|_{\mathcal{F}}^2 \leq \frac{U}{2} \|f\|_{L_2}^2$, then w.p. $1 - \zeta$:

$$\begin{aligned} \forall f \in \mathcal{F} : \gamma \|f\|_{\mathcal{F}}^2 + \|f\|_{L_{2,n}}^2 &\geq \gamma \|f\|_{\mathcal{F}}^2 + \left(\frac{\|f\|_{L_2}^2}{2} - \left(1 \vee \frac{\|f\|_{\mathcal{F}}^2}{U} \right) \frac{\tilde{\delta}_{n, \mathcal{F}}^2}{2} \right) \\ &\geq \gamma \|f\|_{\mathcal{F}}^2 + \frac{1}{4} \|f\|_{L_2}^2 - \frac{\tilde{\delta}_{n, \mathcal{F}}^2}{2}, \end{aligned} \quad (\text{C.5})$$

and

$$\begin{aligned} \forall f \in \mathcal{F} : \gamma \|f\|_{\mathcal{F}}^2 + \|f\|_{L_{2,n}}^2 &\leq \gamma \|f\|_{\mathcal{F}}^2 + \left(\frac{3\|f\|_{L_2}^2}{2} + \left(1 \vee \frac{\|f\|_{\mathcal{F}}^2}{U} \right) \frac{\tilde{\delta}_{n, \mathcal{F}}^2}{2} \right) \\ &\leq \gamma \|f\|_{\mathcal{F}}^2 + \frac{7}{4} \|f\|_{L_2}^2 + \frac{\tilde{\delta}_{n, \mathcal{F}}^2}{2}. \end{aligned} \quad (\text{C.6})$$

For $f \in \mathcal{F}, C \in \mathfrak{C}$, we denote the function

$$\psi(C, f) = f(Z) (\mathbb{1}\{Y \notin C(X)\} - \alpha),$$

Since $\psi(C, f)$ is 1-Lipschitz w.r.t. f , using Lemma 14 in [Foster and Syrgkanis \(2023\)](#), then w.p. $1 - \zeta$,

$$\forall f \in \mathcal{F}, |(P_n - P)\psi(C^{\text{ora}}, f)| \leq 18 \left(\tilde{\delta}_{n, \mathcal{F}} \|f\|_{L_2} + \left(1 \vee \frac{\|f\|_{\mathcal{F}}}{\sqrt{U}}\right) \tilde{\delta}_{n, \mathcal{F}}^2 \right). \quad (\text{C.7})$$

Note that $\Psi_\lambda(C, f) = P\psi(C, f) - \lambda P f^2$ and $\hat{\Psi}_\gamma(C, f) = P_n\psi(C, f) - P_n f^2 - \gamma \|f\|_{\mathcal{F}}^2$ for any $C \in \mathfrak{C}, f \in \mathcal{F}$. By the optimality of \hat{C} ,

$$\sup_{f \in \mathcal{F}} \hat{\Psi}_\gamma(\hat{C}, f) \leq \sup_{f \in \mathcal{F}} \hat{\Psi}_\gamma(C^{\text{ora}}, f) + \nu \left(\|C^{\text{ora}}\|_{\mathcal{H}}^2 - \|\hat{C}\|_{\mathcal{H}}^2 \right) \quad (\text{C.8})$$

Combining [\(C.5\)](#) and [\(C.7\)](#), for $\gamma \geq 0$, we can get w.p. $1 - 2\zeta$:

$$\begin{aligned} \sup_{f \in \mathcal{F}} \hat{\Psi}_\gamma(C^{\text{ora}}, f) &= \sup_{f \in \mathcal{F}} \left\{ P_n\psi(C^{\text{ora}}, f) - P_n f^2 - \gamma \|f\|_{\mathcal{F}}^2 \right\} \\ &\leq \sup_{f \in \mathcal{F}} \left\{ P_n\psi(C^{\text{ora}}, f) - \left(\gamma \|f\|_{\mathcal{F}}^2 + \frac{1}{4} \|f\|_{L_2}^2 - \frac{\tilde{\delta}_{n, \mathcal{F}}^2}{2} \right) \right\} \\ &\leq \sup_{f \in \mathcal{F}} \left\{ P\psi(C^{\text{ora}}, f) + 18 \left(\tilde{\delta}_{n, \mathcal{F}} \|f\|_{L_2} + \left(1 \vee \frac{\|f\|_{\mathcal{F}}}{\sqrt{U}}\right) \tilde{\delta}_{n, \mathcal{F}}^2 \right) - \left(\gamma \|f\|_{\mathcal{F}}^2 + \frac{1}{4} \|f\|_{L_2}^2 - \frac{\tilde{\delta}_{n, \mathcal{F}}^2}{2} \right) \right\} \\ &\stackrel{(i)}{\leq} \sup_{f \in \mathcal{F}} \left\{ P\psi(C^{\text{ora}}, f) + 18 \left(2\tilde{\delta}_{n, \mathcal{F}} \|f\|_{L_2} + \tilde{\delta}_{n, \mathcal{F}}^2 \right) - \left(\frac{1}{4} \|f\|_{L_2}^2 - \frac{\tilde{\delta}_{n, \mathcal{F}}^2}{2} \right) \right\} \\ &\leq \sup_{f \in \mathcal{F}} \left\{ P\psi(C^{\text{ora}}, f) - \frac{1}{8} P f^2 \right\} + \sup_{f \in \mathcal{F}} \left\{ 36\tilde{\delta}_{n, \mathcal{F}} \|f\|_{L_2} - \frac{1}{8} \|f\|_{L_2}^2 \right\} + 18\tilde{\delta}_{n, \mathcal{F}}^2 + \frac{\tilde{\delta}_{n, \mathcal{F}}^2}{2} \\ &\stackrel{(ii)}{\leq} \sup_{f \in \mathcal{F}} \Psi_{\frac{1}{8}}(C^{\text{ora}}, f) + 2 \cdot 36^2 \tilde{\delta}_{n, \mathcal{F}}^2 + 18\tilde{\delta}_{n, \mathcal{F}}^2 + \frac{\tilde{\delta}_{n, \mathcal{F}}^2}{2} \\ &\leq \sup_{f \in \mathcal{F}} \Psi_{\frac{1}{8}}(C^{\text{ora}}, f) + 2611\tilde{\delta}_{n, \mathcal{F}}^2, \end{aligned} \quad (\text{C.9})$$

where (i) we used the assumption $\tilde{\delta}_{n, \mathcal{F}} \|f\|_{\mathcal{F}} \leq \sqrt{\frac{U}{2}} \|f\|_{L_2}$ and $\gamma \geq 0$, and (ii) we used the fact $\sup_{f \in \mathcal{F}} (a\|f\| - b\|f\|^2) \leq \frac{a^2}{4b}$ for any norm $\|\cdot\|$ and $a, b > 0$. In addition, we also have the lower bound

$$\sup_{f \in \mathcal{F}} \hat{\Psi}_\gamma(\hat{C}, f) = \sup_{f \in \mathcal{F}} \left\{ P_n\psi(\hat{C}, f) - P_n\psi(C^{\text{ora}}, f) + P_n\psi(C^{\text{ora}}, f) - P_n f^2 - \gamma \|f\|_{\mathcal{F}}^2 \right\}$$

$$\begin{aligned}
&\geq \sup_{f \in \mathcal{F}} \left\{ P_n \psi(\widehat{C}, f) - P_n \psi(C^{\text{ora}}, f) - 2 \left(P_n f^2 + \gamma \|f\|_{\mathcal{F}}^2 \right) \right\} \\
&\quad + \inf_{f \in \mathcal{F}} \left\{ P_n \psi(C^{\text{ora}}, f) + P_n f^2 + \gamma \|f\|_{\mathcal{F}}^2 \right\} \\
&= \sup_{f \in \mathcal{F}} \left\{ P_n \psi(\widehat{C}, f) - P_n \psi(C^{\text{ora}}, f) - 2 \left(P_n f^2 + \gamma \|f\|_{\mathcal{F}}^2 \right) \right\} - \sup_{f \in \mathcal{F}} \widehat{\Psi}_\gamma(C^{\text{ora}}, f),
\end{aligned}$$

where we used the fact that \mathcal{F} is symmetric. It follows that w.p. $1 - 2\zeta$:

$$\begin{aligned}
&\sup_{f \in \mathcal{F}} \left\{ P_n \psi(\widehat{C}, f) - P_n \psi(C^{\text{ora}}, f) - 2 \left(P_n f^2 + \gamma \|f\|_{\mathcal{F}}^2 \right) \right\} \\
&\leq \left\{ \sup_{f \in \mathcal{F}} \widehat{\Psi}_\gamma(\widehat{C}, f) + \sup_{f \in \mathcal{F}} \widehat{\Psi}_\gamma(C^{\text{ora}}, f) \right\} \\
&\stackrel{(i)}{\leq} 2 \sup_{f \in \mathcal{F}} \widehat{\Psi}_\gamma(C^{\text{ora}}, f) + \nu \left(\|C^{\text{ora}}\|_{\mathcal{H}}^2 - \|\widehat{C}\|_{\mathcal{H}}^2 \right) \\
&\stackrel{(ii)}{\leq} 2 \sup_{f \in \mathcal{F}} \Psi_{\frac{1}{8}}(C^{\text{ora}}, f) + 2 \cdot 2611 \tilde{\delta}_{n, \mathcal{F}}^2 + \nu \left(\|C^{\text{ora}}\|_{\mathcal{H}}^2 - \|\widehat{C}\|_{\mathcal{H}}^2 \right) \\
&\stackrel{(iii)}{\leq} 4\epsilon^2 + 2 \cdot 2611 \tilde{\delta}_{n, \mathcal{F}}^2 + \nu \|C^{\text{ora}}\|_{\mathcal{H}}^2, \tag{C.10}
\end{aligned}$$

where (i) holds due to (C.8), (ii) holds due to (C.9) and (iii) holds due to Lemma C.1 and $\mathbb{E}[(\alpha(Z; C^{\text{ora}}) - \alpha)^2] = \epsilon^2$.

For any $C \in \mathfrak{C}$, we define

$$f_C = \arg \min_{f \in \mathcal{F}_U} \mathbb{E} \left[(f(Z) - (\alpha(Z; C) - \alpha(Z; C^{\text{ora}})))^2 \right]. \tag{C.11}$$

By the assumption $\mathbb{E} [(f_C(Z) - (\alpha(Z; C) - \alpha(Z; C^{\text{ora}})))^2] \leq \eta^2$ for any $C \in \mathfrak{C}$, we have

$$\begin{aligned}
P\psi(C, f_C) - P\psi(C^{\text{ora}}, f_C) &= \mathbb{E} [f_C(Z)(\alpha(Z; C) - \alpha(Z; C^{\text{ora}}))] \\
&= \mathbb{E} [f_C^2(Z)] + \mathbb{E} [f_C(Z)(\alpha(Z; C) - \alpha(Z; C^{\text{ora}}) - f_C(Z))] \\
&\geq \|f_C\|_{L_2}^2 - \|f_C\|_{L_2} \|\alpha(C) - \alpha(C^{\text{ora}}) - f_C\|_{L_2} \\
&\geq \|f_C\|_{L_2}^2 - \|f_C\|_{L_2} \eta,
\end{aligned}$$

where the first inequality follows from Cauchy's inequality. It follows that

$$\frac{P\psi(C, f_C) - P\psi(C^{\text{ora}}, f_C)}{\|f_C\|_{L_2}} \geq \|f_C\|_{L_2} - \eta \geq \|\alpha(C) - \alpha(C^{\text{ora}})\|_{L_2} - 2\eta. \quad (\text{C.12})$$

Let $r \in [0, 1]$, then $rf_{\hat{C}} \in \mathcal{F}_U$ since \mathcal{F}_U is star-shaped. Let $v^2(C, C^{\text{ora}}) := \mathbb{E}[|\alpha(Z; C) - \alpha(Z; C^{\text{ora}})|^2]$ and define the function class

$$\mathcal{G} = \{(x, z, y) \mapsto f_C(z)(\mathbb{1}\{y \notin C(x)\} - \mathbb{1}\{y \notin C^{\text{ora}}(x)\}) : C \in \mathfrak{C}\}. \quad (\text{C.13})$$

Then we have w.p. $1 - 2\zeta$:

$$\begin{aligned} & \sup_{f \in \mathcal{F}} \left\{ P_n\psi(\hat{C}, f) - P_n\psi(C^{\text{ora}}, f) - 2 \left(P_n f^2 + \gamma \|f\|_{\mathcal{F}}^2 \right) \right\} \\ & \geq r P_n\psi(\hat{C}, f_{\hat{C}}) - r P_n\psi(C^{\text{ora}}, f_{\hat{C}}) - 2r^2 \left(P_n f_{\hat{C}}^2 + \gamma \|f_{\hat{C}}\|_{\mathcal{F}}^2 \right) \\ & \stackrel{\text{(i)}}{\geq} r P_n\psi(\hat{C}, f_{\hat{C}}) - r P_n\psi(C^{\text{ora}}, f_{\hat{C}}) - 2r^2 \left(\gamma \|f_{\hat{C}}\|_{\mathcal{F}}^2 + \frac{7}{4} \|f_{\hat{C}}\|_{L_2}^2 + \frac{\tilde{\delta}_{n, \mathcal{F}}^2}{2} \right) \\ & \stackrel{\text{(ii)}}{\geq} r \left\{ P\psi(\hat{C}, f_{\hat{C}}) - P\psi(C^{\text{ora}}, f_{\hat{C}}) - v(\hat{C}, C^{\text{ora}}) \left(4\delta_{n, \mathcal{G}} + 2\sqrt{\frac{2 \log(R_n/\zeta)}{n}} \right) - \frac{\log(R_n/\zeta)}{3n} \right\} \\ & \quad - 2r^2 \left(\gamma \|f_{\hat{C}}\|_{\mathcal{F}}^2 + \frac{7}{4} \|f_{\hat{C}}\|_{L_2}^2 + \frac{\tilde{\delta}_{n, \mathcal{F}}^2}{2} \right) \\ & \stackrel{\text{(iii)}}{\geq} r \left\{ (v(\hat{C}, C^{\text{ora}}) - 2\eta) \|f_{\hat{C}}\|_{L_2} - v(\hat{C}, C^{\text{ora}}) \left(4\delta_{n, \mathcal{G}} + 2\sqrt{\frac{2 \log(R_n/\zeta)}{n}} \right) - \frac{\log(R_n/\zeta)}{3n} \right\} \\ & \quad - 2r^2 \left(\gamma \|f_{\hat{C}}\|_{\mathcal{F}}^2 + \frac{7}{4} \|f_{\hat{C}}\|_{L_2}^2 + \frac{\tilde{\delta}_{n, \mathcal{F}}^2}{2} \right), \end{aligned} \quad (\text{C.14})$$

where (i) use (C.6); (ii) holds due to Lemma E.8; and (iii) holds due to (C.12). $R_n = \lceil \log_2(1/\delta_{n, \mathcal{G}}) \rceil + 1$. If $4\delta_{n, \mathcal{G}} + 2\sqrt{\frac{2 \log(R_n/\zeta)}{n}} \geq \|f_{\hat{C}}\|_{L_2}/2$, we have

$$v(\hat{C}, C^{\text{ora}}) \leq \|f_{\hat{C}}\|_{L_2} + \eta \lesssim \delta_{n, \mathcal{G}} + \sqrt{\frac{\log(R_n/\zeta)}{n}} + \eta.$$

Otherwise, i.e., $4\delta_{n, \mathcal{G}} + 2\sqrt{\frac{2 \log(R_n/\zeta)}{n}} \leq \|f_{\hat{C}}\|_{L_2}/2$, combining (C.14) and (C.10), w.p. $1 - 4\zeta$,

we get

$$\begin{aligned} v(\widehat{C}, C^{\text{ora}}) &\leq \frac{2}{r\|f_{\widehat{C}}\|_{L_2}} \left(4\epsilon^2 + 2 \cdot 2611\tilde{\delta}_{n,\mathcal{F}}^2 + \nu\|C^{\text{ora}}\|_{\mathcal{H}}^2 \right) + 2\eta \\ &\quad + \frac{2\log(R_n/\zeta)}{3n\|f_{\widehat{C}}\|_{L_2}} + \frac{4r}{\|f_{\widehat{C}}\|_{L_2}} \left(\gamma\|f_{\widehat{C}}\|_{\mathcal{F}}^2 + \frac{7}{4}\|f_{\widehat{C}}\|_{L_2}^2 + \frac{\tilde{\delta}_{n,\mathcal{F}}^2}{2} \right). \end{aligned}$$

If $\|f_{\widehat{C}}\|_{L_2} \geq \tilde{\delta}_{n,\mathcal{F}} \geq \sqrt{\frac{\log(c_1/\zeta)}{c_2n}}$, choosing $r = \max\{\epsilon, \tilde{\delta}_{n,\mathcal{F}}\}/\|f_{\widehat{C}}\|_{L_2}$, by $\gamma\|f\|_{\mathcal{F}}^2 \leq \|f\|_{L_2}^2$, we have

$$\begin{aligned} v(\widehat{C}, C^{\text{ora}}) &\lesssim \epsilon + \tilde{\delta}_{n,\mathcal{F}} + \frac{\nu\|C^{\text{ora}}\|_{\mathcal{H}}^2}{\tilde{\delta}_{n,\mathcal{F}}} + \eta + \sqrt{\frac{\log(R_n/\zeta)}{n}} + \tilde{\delta}_{n,\mathcal{F}} + \tilde{\delta}_{n,\mathcal{F}} + \tilde{\delta}_{n,\mathcal{F}} \\ &\lesssim \epsilon + \tilde{\delta}_{n,\mathcal{F}} + \frac{\nu\|C^{\text{ora}}\|_{\mathcal{H}}^2}{\tilde{\delta}_{n,\mathcal{F}}} + \eta + \sqrt{\frac{\log(R_n/\zeta)}{n}}. \end{aligned}$$

Therefore,

$$v(\widehat{C}, C^{\text{ora}}) \lesssim \epsilon + \tilde{\delta}_{n,\mathcal{F}} + \eta + \sqrt{\frac{\log(R_n/\zeta)}{n}} + \frac{\nu\|C^{\text{ora}}\|_{\mathcal{H}}^2}{\tilde{\delta}_{n,\mathcal{F}}}. \quad (\text{C.15})$$

Otherwise, i.e. $\|f_{\widehat{C}}\|_{L_2} \leq \tilde{\delta}_{n,\mathcal{F}}$, we have

$$v(\widehat{C}, C^{\text{ora}}) \leq \|f_{\widehat{C}}\|_{L_2} + \eta \lesssim \tilde{\delta}_{n,\mathcal{F}} + \eta.$$

Combining the relations above, we can conclude that

$$v(\widehat{C}, C^{\text{ora}}) \lesssim \epsilon + \delta_{n,\mathcal{F}_U} + \delta_{n,\mathcal{G}} + \eta + \frac{\nu\|C^{\text{ora}}\|_{\mathcal{H}}^2}{\tilde{\delta}_{n,\mathcal{F}}} + \sqrt{\frac{\log(R_n/\zeta)}{n}}, \quad (\text{C.16})$$

where we used the definition of $\tilde{\delta}_{n,\mathcal{F}}$. □

C.4 Proof of Theorem 4.2

Proof. By Assumption 3, there exist $H^0(w(X), Z)$ such that $\mathbb{P}\{T(H^0(w(X), Z), Y) \leq 0 \mid w(X), Z\} = 1 - \alpha$ and for any $\mathbf{u}_1, \mathbf{u}_2 \in \mathbb{R}^m$, there exist $l(x, z)$ such that $\mathbb{E}[l^2(w(X), Z)] = \kappa^2 < \infty$,

$$|\mathbb{P}\{T(\mathbf{u}_1, Y) \leq 0 \mid w(X), Z\} - \mathbb{P}\{T(\mathbf{u}_2, Y) \leq 0 \mid w(X), Z\}| \leq l(w(X), Z)\|\mathbf{u}_1 - \mathbf{u}_2\|,$$

where $\|\mathbf{u}\| = \sqrt{\mathbf{u}^T \mathbf{u}}$. Consider the Structured set-valued function class $\mathfrak{C} = \{C(x; h) : h \in \mathcal{H}\}$ defined in (3). Let

$$\alpha(Z; h) := \mathbb{P}\{Y \notin C(X; h)\} = 1 - \mathbb{E}[\mathbb{P}\{T(h(X), Y) \leq 0 \mid w(X), Z\} \mid Z],$$

and $h^0(w(X)) = \mathbb{E}[H^0(w(X), Z) \mid w(X)]$. Then we have:

$$\begin{aligned} & \mathbb{E}[(\alpha(Z; h^0) - \alpha)^2] \\ &= \mathbb{E}\left[\left\{\mathbb{E}\left[\mathbb{P}\{T(H^0(w(X), Z), Y) \leq 0 \mid w(X), Z\} - \mathbb{P}\{T(h^0(w(X)), Y) \leq 0 \mid w(X), Z\} \mid Z\right]\right\}^2\right] \\ &\leq \kappa^2 \mathbb{E}\left[\left\{\mathbb{E}\left[\|h^0(w(X)) - H^0(w(X), Z)\| \mid Z\right]\right\}^2\right] \\ &\leq \kappa^2 \mathbb{E}\left[\left(h^0(w(X)) - H^0(w(X), Z)\right)^T \left(h^0(w(X)) - H^0(w(X), Z)\right)\right] \\ &= \kappa^2 \text{Tr}\left(\mathbb{E}\left[\mathbb{E}\left[\left(h^0(w(X)) - H^0(w(X), Z)\right) \left(h^0(w(X)) - H^0(w(X), Z)\right)^T \mid w(X)\right]\right]\right) \\ &= \kappa^2 \text{Tr}\left(\mathbb{E}\left[\text{Cov}(H^0(w(X), Z) \mid w(X))\right]\right) \\ &= \kappa^2 \text{Tr}\left(\text{Cov}(H^0(w(X), Z))\right) (1 - \rho^2), \end{aligned}$$

where the last inequality we use Jensen's inequality and $\rho^2 = \frac{\text{Tr}(\text{Cov}(h^0(w(X))))}{\text{Tr}(\text{Cov}(H^0(w(X), Z)))}$. By the definition of h^{ora} :

$$\mathbb{E}[(\alpha(Z; h^{\text{ora}}) - \alpha)^2] \leq \mathbb{E}[(\alpha(Z; h^0) - \alpha)^2] \leq \kappa^2 \text{Tr}\left(\text{Cov}(H^0(w(X), Z))\right) (1 - \rho^2).$$

□

C.4.1 Discuss of Assumption 3

For the test-conditional coverage setting in Example 2.1, Assumption 3 is required to hold with $w(X) = X$. We take $Z = X$ and consider the pretrained sublevel prediction sets in (7), then $T(h(X), Y) = s(X, Y) - h(X)$. In this case, if the distribution of $s(X, Y) | X$ is a Lipschitz function, then for any $h_1, h_2 \in \mathcal{H}$,

$$\begin{aligned} & |\mathbb{P}\{T(h_1(X), Y) \leq 0 | w(X), Z\} - \mathbb{P}\{T(h_2(X), Y) \leq 0 | w(X), Z\}| \\ &= |\mathbb{P}\{s(X, Y) \leq h_1(X) | X\} - \mathbb{P}\{s(X, Y) \leq h_2(X) | X\}| \lesssim |h_1(X) - h_2(X)|, \end{aligned}$$

Hence, Assumption 3 (1) holds. Let

$$h^0(X) = \mathbb{E} [H^0(X) | X] = H^0(X) = \inf\{t : \mathbb{P}\{s(X, Y) \leq t | X\} \geq 1 - \alpha\}.$$

Therefore, $\mathbb{P}\{s(X, Y) \leq H^0(X) | X\} = 1 - \alpha$ by the distribution of $s(X, Y) | X$ is a Lipschitz continuous and then Assumption 3 (2) holds. Then $h^0(x) \in \mathcal{H}$ provided that \mathcal{H} is sufficiently rich. For example, \mathcal{H} may be chosen as a function class capable of approximating arbitrary continuous functions, such as an RKHS with a universal kernel.

For the group-conditional coverage setting in Example 2.2, Assumption 3 is required to hold with $w(X) = (\mathbb{1}\{X \in G_1\}, \dots, \mathbb{1}\{X \in G_K\})^\top$. We take $Z = w(X)$, $\mathcal{H} = \mathcal{F} = \left\{ \sum_{Z=z} \beta_z \mathbb{1}\{Z = z\} : \beta_z \in \mathbb{R}, z \in \mathcal{Z} \right\}$ and consider the pretrained sublevel prediction sets in (7), then $T(h(X), Y) = s(X, Y) - h(X)$. If the distribution of $s(X, Y) | Z$ is a Lipschitz function, then for any $h_1, h_2 \in \mathcal{H}$,

$$\begin{aligned} & |\mathbb{P}\{T(h_1(X), Y) | w(X), Z\} - \mathbb{P}\{T(h_2(X), Y) | w(X), Z\}| \\ &= |\mathbb{P}\{s(X, Y) \leq h_1(X) | Z\} - \mathbb{P}\{s(X, Y) \leq h_2(X) | Z\}| \lesssim |h_1(X) - h_2(X)|, \end{aligned}$$

Hence, Assumption 3 (1) holds. Moreover, by letting $q_z = \inf\{t : \mathbb{P}\{s(X, Y) \leq t \mid Z = z\} \geq 1 - \alpha\}$ for $z \in \mathcal{Z}$, we have

$$h^0(w(X)) = \mathbb{E}\left[H^0(Z) \mid w(X)\right] = H^0(Z) = \sum_{z \in \mathcal{Z}} q_z \mathbb{1}\{Z = z\},$$

Therefore, $\mathbb{P}\{s(X, Y) \leq H^0(Z) \mid Z\} = 1 - \alpha$ by the distribution of $s(X, Y) \mid Z$ is a Lipschitz continuous and then Assumption 3 (2) holds. Moreover, $h^0 \in \mathcal{H}$ by the definition of \mathcal{H} and Assumption 3 (3) holds.

For the Equalized coverage setting in Example 2.3, we assume there exist a $w(x)$ that satisfies Assumption 3, then $h^0(w(X)) = \mathbb{E}[H^0(w(X), Z) \mid w(X)]$. $h^0(w(X)) \in \mathcal{H}$ if \mathcal{H} is sufficiently rich.

C.5 Proof of Theorem 4.3 and 4.4

By Theorem 4.1, the convergence rate of the MSCE is primarily governed by the critical radius $\delta_{n, \mathcal{F}_U}$ and $\delta_{n, \mathcal{G}}$ associated with the function classes \mathcal{F} and \mathcal{G} . Accordingly, the following theorem characterizes the orders of $\delta_{n, \mathcal{F}_U}$ and $\delta_{n, \mathcal{G}}$ in the setting where \mathfrak{C} is a VC class with VC dimension $d_{\mathfrak{C}}$ and \mathfrak{C} is chosen to be shape-constrained prediction set (3) and $C^{\text{ora}}(X) = \{y \in \mathcal{Y} : T(h^{\text{ora}}(X), Y) \leq 0\}$.

Theorem C.2. *Let \mathfrak{C} be VC class with VC dimension $d_{\mathfrak{C}}$ and consider the shape-constrained prediction set (3). Then we obtain following results:*

(1) *If \mathcal{F} is a VC class with VC dimension $d_{\mathcal{F}}$, then*

$$\delta_{n, \mathcal{F}_U} \asymp \sqrt{\frac{d_{\mathcal{F}}}{n}}, \quad \delta_{n, \mathcal{G}} \asymp \sqrt{\frac{d_{\mathcal{F}} \vee d_{\mathfrak{C}}}{n}}.$$

(2) If \mathcal{F} is a RKHS equipped with a Gaussian kernel and $\mathcal{Z} = [0, 1]^{d_{\mathcal{Z}}}$, then

$$\delta_{n, \mathcal{F}_U} \asymp \sqrt{\frac{d_{\mathcal{Z}} \log^{d_{\mathcal{Z}}+1}(n/d_{\mathcal{Z}})}{n}}, \quad \delta_{n, \mathcal{G}} \asymp \frac{d_{\mathcal{E}} \log\left(\frac{n}{d_{\mathcal{E}}}\right) \vee d_{\mathcal{Z}} \log^{d_{\mathcal{Z}}}\left(\frac{n}{d_{\mathcal{Z}}}\right)}{n}.$$

Proof of Theorem C.2. We bound $\delta_{n, \mathcal{F}_U}$ and $\delta_{n, \mathcal{G}}$ respectively.

Step 1: Upper bounded $\delta_{n, \mathcal{F}_U}$.

Case (a): \mathcal{F} is a VC class. Since $\mathcal{F}_U = \{f \in \mathcal{F} : \|f\|_{\mathcal{F}}^2 \leq U\}$ is a subset of \mathcal{F} , it is straightforward to verify that for any pair of function classes $\mathcal{U} \subset \mathcal{V}$, the corresponding critical radius satisfy $\delta_{n, \mathcal{U}} \leq \delta_{n, \mathcal{V}}$. Hence, it suffices to bound $\delta_{\mathcal{F}}$. Let $d_{\mathcal{F}}$ be the VC-dimension of \mathcal{F} . Using Theorem 2.6.4 in [Van Der Vaart and Wellner \(2023\)](#), we can bound the covering number of \mathcal{F} by its VC dimension $d_{\mathcal{F}}$:

$$N(\rho, \mathcal{F}, \|\cdot\|_{L_2}) \leq K d_{\mathcal{F}} (16e)^{d_{\mathcal{F}}} (1/\rho)^{2d_{\mathcal{F}}}, \quad (\text{C.17})$$

where C is a universal constant. Now use Dudley inequality, e.g., Theorem 5.22 in [Wainwright \(2019\)](#), we can bound localized Rademacher complexity $\overline{\mathcal{R}}_n(\delta; \mathcal{F})$ by

$$\overline{\mathcal{R}}_n(\delta; \mathcal{F}) = \mathbb{E} \left[\sup_{\substack{f \in \mathcal{F} \\ \|f\|_{L_2} \leq \delta}} \left| \frac{1}{n} \sum_{i=1}^n \varepsilon_i f(Z_i) \right| \right] \leq \frac{C_0}{\sqrt{n}} \int_0^\delta \sqrt{\log N(\rho, \mathcal{F}, \|\cdot\|_{L_2})} d\rho, \quad (\text{C.18})$$

where C_0 is a universal constant. Hence, plugging (C.17) into (C.18), we have

$$\begin{aligned} \overline{\mathcal{R}}_n(\delta; \mathcal{F}) &\leq \frac{C_0}{\sqrt{n}} \int_0^\delta \sqrt{\log(C d_{\mathcal{F}}) + d_{\mathcal{F}} \log 16e + 2d_{\mathcal{F}} \log(1/\rho)} d\rho \\ &\leq \frac{C_0}{\sqrt{n}} \left(\int_0^\delta \sqrt{2d_{\mathcal{F}} \log(1/\rho)} d\rho + \delta \sqrt{\log(C d_{\mathcal{F}}) + d_{\mathcal{F}} \log 16e} \right) \\ &\leq \delta \sqrt{\frac{C_1 d_{\mathcal{F}} \log(1/\delta^2)}{n}} + \delta \sqrt{\frac{C_2 (\log d_{\mathcal{F}} + d_{\mathcal{F}})}{n}} \\ &\leq \delta \sqrt{\frac{C_3 d_{\mathcal{F}} \log(1/\delta^2)}{n}}, \end{aligned} \quad (\text{C.19})$$

where the last equality hold for sufficiently small δ . Since $\delta_{\mathcal{F}}$ is an arbitrary solution of $\overline{\mathcal{R}}_n(\delta; \mathcal{F}) \lesssim \delta^2$, then we just require

$$\delta \sqrt{\frac{d_{\mathcal{F}} \log(1/\delta^2)}{n}} \lesssim \delta^2 \iff \frac{d_{\mathcal{F}} \log(1/\delta^2)}{n} \lesssim \delta^2.$$

Considering the fixed point condition, let $t = \frac{1}{\delta^2}$ and check the root of the equation $t \log t = n/d_{\mathcal{F}}$. Taking the logarithm on both sides, we have:

$$\log t + \log \log t = \log(n/d_{\mathcal{F}}).$$

By Lemma E.1 with $L_n = \log(n/d_{\mathcal{F}})$, we have

$$\frac{1}{\delta_{\mathcal{F}}^2} \asymp \exp(L_n - \log L_n) = \frac{n/d_{\mathcal{F}}}{\log(n/d_{\mathcal{F}})}.$$

Hence, it follows that $\delta_{n, \mathcal{F}_U} \lesssim \delta_{\mathcal{F}} \asymp \sqrt{\frac{d_{\mathcal{F}}}{n} \log \frac{n}{d_{\mathcal{F}}}}$.

Case (b): \mathcal{F} is a RKHS equipped with a Gaussian kernel. Since \mathcal{F} is a RKHS equipped with a Gaussian kernel and $\mathcal{F}_U = \{f \in \mathcal{F} : \|f\|_{\mathcal{F}}^2 \leq U\}$. When \mathcal{F}_U is equipped with a Gaussian kernel with $\|f\|_{\mathcal{F}} \leq U$, $Z \in [0, 1]^{d_Z}$, by Proposition 1 of Zhou (2002),

$$\log N(\rho, \mathcal{F}_U, \|\cdot\|_{L_2}) \leq 4^{d_Z} (6d_Z + 2) (\log(U/\rho))^{d_Z+1}. \quad (\text{C.20})$$

By substituting (C.20) into (C.18),

$$\begin{aligned} \overline{\mathcal{R}}_n(\delta; \mathcal{F}_U) &\leq \frac{C_0}{\sqrt{n}} \int_0^\delta \sqrt{4^{d_Z} (6d_Z + 2) (\log(U/\rho))^{d_Z+1}} d\rho \\ &\leq C_0 \delta \sqrt{\frac{(2d_Z + 1)(4 \log(U^2/\delta^2))^{d_Z+1}}{n}}. \end{aligned} \quad (\text{C.21})$$

Since $\delta_{\mathcal{F}_U}$ is an arbitrary solution of $\overline{\mathcal{R}}(\delta; \mathcal{F}_U) \lesssim \delta^2$, then we just require

$$\delta \sqrt{\frac{d_Z}{n} \log^{d_Z+1}(U^2/\delta^2)} \lesssim \delta^2 \iff \frac{d_Z}{n} \log^{d_Z+1}(U^2/\delta^2) \lesssim \delta^2.$$

Considering the fixed point condition, let $t = U^2/\delta^2$ and check the root of the equation $t(\log t)^{d_Z+1} = nB^2/d_Z$. Taking the logarithm on both sides, we have:

$$\log t + (d_Z + 1) \log \log t = \log(nU^2/d_Z).$$

By Lemma E.1 with $L_n = \log(nU^2/d_Z)$, we have

$$\frac{U^2}{\delta_{\mathcal{F}}^2} \asymp \exp \left\{ \log(nU^2/d_Z) - (d_Z + 1) \log \log(nU^2/d_Z) \right\} = \frac{nU^2/d_Z}{\log^{d_Z+1}(nU^2/d_Z)}. \quad (\text{C.22})$$

Hence, $\delta_{n, \mathcal{F}_U} \asymp \sqrt{\frac{d_Z \log^{d_Z+1}(n/d_Z)}{n}}$.

Step 2: Upper bounded $\delta_{n, \mathcal{G}}$. Since we consider sublevel set (7), by the definition of \mathcal{G} in (C.13), $g_h \in \mathcal{G}$ can be written as,

$$g_h(X, Z, Y) = f_h(Z) (\mathbb{1}\{T(h(X), Y) \leq 0\} - \mathbb{1}\{T(h^{\text{ora}}(X), Y) \leq 0\}),$$

where $f_h = \arg \min_{f \in \mathcal{F}_U} \mathbb{E}[(f - (\alpha(Z; h) - \alpha(Z; h^{\text{ora}})))^2]$. We define the function class

$$\mathcal{G}^* := \{f(Z) (\mathbb{1}\{T(h(X), Y) \leq 0\} - \mathbb{1}\{T(h^{\text{ora}}(X), Y) \leq 0\}) : f \in \mathcal{F}_U, h \in \mathcal{H}\}.$$

Note that $\mathcal{G} \subseteq \mathcal{G}^*$, then we have $\overline{\mathcal{R}}_n(\delta; \mathcal{G}) \leq \overline{\mathcal{R}}_n(\delta; \mathcal{G}^*)$. Let $\gamma_h(x, y) = \mathbb{1}\{T(h(x), y) \leq 0\} - \mathbb{1}\{T(h^{\text{ora}}(x), y) \leq 0\}$ and $\Gamma_{\mathcal{H}} = \{\gamma_h : h \in \mathcal{H}\}$. By Assumption 4, the VC-dimension of

$\Gamma_{\mathcal{H}}$ is also $O(d_{\mathfrak{E}})$. By Lemma E.5 and $\|f\|_{\infty} \leq 1$ and $\|\gamma_h\|_{\infty} \leq 1$, we have

$$\log N(\rho, \mathcal{G}^*, \|\cdot\|_{L_2}) \leq \log N(\rho/2, \mathcal{F}_U, \|\cdot\|_{L_2}) + \log N(\rho/2, \Gamma_{\mathcal{H}}, \|\cdot\|_{L_2}).$$

Together with (C.17) and (C.18), we have

$$\begin{aligned} \overline{\mathcal{R}}_n(\delta; \mathcal{G}) &\leq \overline{\mathcal{R}}_n(\delta; \mathcal{G}^*) \leq \frac{C_0}{\sqrt{n}} \int_0^{\delta} \sqrt{\log N(\rho, \mathcal{G}^*, \|\cdot\|_{L_2})} d\rho \\ &\leq 2 \int_0^{\delta/2} \sqrt{\log N(\rho, \mathcal{F}_U, \|\cdot\|_{L_2})} d\rho + 2 \int_0^{\delta/2} \sqrt{\log N(\rho, \Gamma_{\mathcal{H}}, \|\cdot\|_{L_2})} d\rho \\ &\leq 2 \int_0^{\delta/2} \sqrt{\log N(\rho, \mathcal{F}_U, \|\cdot\|_{L_2})} d\rho + \delta \sqrt{\frac{C_5 d_{\mathfrak{E}} \log(4/\delta^2)}{n}}. \end{aligned} \quad (\text{C.23})$$

Case (a): \mathcal{F} is a VC class. Combining (C.19) and (C.23), we have

$$\overline{\mathcal{R}}_n(\delta; \mathcal{G}) \leq \delta \sqrt{\frac{C_6 (d_{\mathfrak{E}} \vee d_{\mathcal{F}}) \log(4/\delta^2)}{n}}$$

Considering the fixed point condition, and let $t = \frac{2}{\delta}$, $L = \log \frac{n}{d_{\mathcal{F}} \vee d_{\mathfrak{E}}}$. By Lemma E.1,

$$\begin{aligned} \frac{1}{\delta_{\mathcal{G}}^2} &\asymp \exp(L - \log L) = \frac{n / (d_{\mathcal{F}} \vee d_{\mathfrak{E}})}{\log(n / (d_{\mathcal{F}} \vee d_{\mathfrak{E}}))} \\ \implies \delta_{n, \mathcal{G}} &\lesssim \sqrt{\frac{d_{\mathcal{F}} \vee d_{\mathfrak{E}}}{n} \log\left(\frac{n}{d_{\mathcal{F}} \vee d_{\mathfrak{E}}}\right)}. \end{aligned}$$

Case (b): \mathcal{F} is a RKHS equipped with a Gaussian kernel. Combining (C.21) and (C.23), we have

$$\overline{\mathcal{R}}_n(\delta; \mathcal{G}) \leq \delta \sqrt{\frac{C_4 \log^{dz+1}(4U^2/\delta^2)}{n}} + \delta \sqrt{\frac{C_5 d_{\mathfrak{E}} \log(4/\delta^2)}{n}}$$

Since we require $\overline{\mathcal{R}}(\delta; \mathcal{G}) \lesssim \delta^2$, then using Lemma E.1, we can have

$$\begin{cases} \frac{d_{\mathcal{Z}}}{n} \log^{d_{\mathcal{Z}}+1}(U^2/\delta^2) \lesssim \frac{1}{2}\delta^2, \\ \frac{d_{\mathfrak{C}}}{n} \log \frac{1}{\delta^2} \lesssim \frac{1}{2}\delta^2. \end{cases} \implies \delta_{n,\mathcal{G}} \asymp \sqrt{\frac{d_{\mathfrak{C}} \log\left(\frac{n}{d_{\mathfrak{C}}}\right) \vee d_{\mathcal{Z}} \log^{d_{\mathcal{Z}}+1}(n/d_{\mathcal{Z}})}{n}}.$$

□

Proof of Theorem 4.3. Since we choose $\mathcal{F} = \{\sum_{z \in \mathcal{Z}} \beta_z \mathbb{1}\{Z = z\} : \beta_z \in \mathbb{R}\}$, for any $C \in \mathfrak{C}$, the function $\alpha(z; C)$ corresponds to $Z = z$ takes at most $|\mathcal{Z}|$ distinct values which indicates that $\alpha(z; C) \in \mathcal{F}$. Therefore, by definitions of \mathcal{F} and $f_C = \arg \min_{f \in \mathcal{F}_U} \mathbb{E}[(f(Z) - (\alpha(Z; C^{\text{ora}}) - \alpha(Z; C)))^2]$, we have $\mathbb{E}[(f_C(Z) - (\alpha(Z; C^{\text{ora}}) - \alpha(Z; C)))^2] = 0$. Hence, $\eta = 0$. By Theorem 4.1 and C.2, we choose $\gamma = 0$ and then there exist $C > 0$ such that w.p. $1 - 4\zeta$:

$$\begin{aligned} & \mathbb{E}[(\alpha(Z; \widehat{C}) - \alpha)^2 \mid \mathcal{D}_n] \\ & \leq C \left(\epsilon^2 + \frac{d_{\mathcal{F}} \vee d_{\mathfrak{C}}}{n} \log\left(\frac{n}{d_{\mathcal{F}} \vee d_{\mathfrak{C}}}\right) + \frac{\log((\log n)/\zeta)}{n} \right) := A_n. \end{aligned}$$

Therefore, Let $\mathcal{E} = \{\mathbb{E}[(\alpha(Z; \widehat{C}) - \alpha)^2 \mid \mathcal{D}_n] \leq A_n\}$

$$\begin{aligned} \mathbb{E}[(\alpha(Z; \widehat{C}) - \alpha)^2] &= \mathbb{E}[\mathbb{E}[(\alpha(Z; \widehat{C}) - \alpha)^2 \mid \mathcal{D}_n]] \\ &= \mathbb{E}[\mathbb{E}[(\alpha(Z; \widehat{C}) - \alpha)^2 \mid \mathcal{D}_n] \mathbb{1}_{\mathcal{E}}] \\ &\quad + \mathbb{E}[\mathbb{E}[(\alpha(Z; \widehat{C}) - \alpha)^2 \mid \mathcal{D}_n] \mathbb{1}_{\mathcal{E}^c}] \\ &\leq A_n + 4\zeta. \end{aligned}$$

By choosing $\zeta = \frac{1}{n}$, we have

$$\mathbb{E}[(\alpha(Z; \widehat{C}) - \alpha)^2] \lesssim \epsilon^2 + \frac{d_{\mathcal{F}} \vee d_{\mathfrak{C}}}{n} \log\left(\frac{n}{d_{\mathcal{F}} \vee d_{\mathfrak{C}}}\right).$$

□

Proof of Theorem 4.4. By Theorem 4.1 and C.2, we choose $\gamma \geq 0$ s.t. $\gamma \|f\|_{\mathcal{F}}^2 \leq \|f\|_2^2$ and combining all results above, there exist $C > 0$ such that w.p. $1 - 4\zeta$:

$$\begin{aligned} & \mathbb{E} \left[(\alpha(Z; \widehat{C}) - \alpha)^2 \mid \mathcal{D}_n \right] \\ & \leq C \left(\epsilon^2 + \eta^2 + \frac{d_{\mathcal{E}} \log \left(\frac{n}{d_{\mathcal{E}}} \right) \vee d_{\mathcal{Z}} \log^{d_{\mathcal{Z}+1}} \left(\frac{n}{d_{\mathcal{Z}}} \right) + \frac{\log((\log n)/\zeta)}{n}}{n} \right) := A_n. \end{aligned}$$

Therefore, Let $\mathcal{E} = \left\{ \mathbb{E} \left[(\alpha(Z; \widehat{C}) - \alpha)^2 \mid \mathcal{D}_n \right] \leq A_n \right\}$

$$\begin{aligned} \mathbb{E} \left[(\alpha(Z; \widehat{C}) - \alpha)^2 \right] &= \mathbb{E} \left[\mathbb{E} \left[(\alpha(Z; \widehat{C}) - \alpha)^2 \mid \mathcal{D}_n \right] \right] \\ &= \mathbb{E} \left[\mathbb{E} \left[(\alpha(Z; \widehat{C}) - \alpha)^2 \mid \mathcal{D}_n \right] \mathbb{1}_{\mathcal{E}} \right] \\ &\quad + \mathbb{E} \left[\mathbb{E} \left[(\alpha(Z; \widehat{C}) - \alpha)^2 \mid \mathcal{D}_n \right] \mathbb{1}_{\mathcal{E}^c} \right] \\ &\leq A_n + 4\zeta. \end{aligned}$$

By choosing $\zeta = \frac{1}{n}$, we have

$$\mathbb{E} \left[(\alpha(Z; \widehat{C}) - \alpha)^2 \right] \lesssim \epsilon^2 + \eta^2 + \frac{d_{\mathcal{E}} \log \left(\frac{n}{d_{\mathcal{E}}} \right) \vee d_{\mathcal{Z}} \log^{d_{\mathcal{Z}+1}} \left(\frac{n}{d_{\mathcal{Z}}} \right)}{n}.$$

□

C.6 Proof of Corollary 4.1

Proof. Since $Z = (\mathbb{1}\{X \in G_1\}, \dots, \mathbb{1}\{X \in G_K\})^\top$ and $w(X) = Z$, then $h^0(w(X)) = \mathbb{E}[H^0(w(X), Z) \mid w(X)] = H^0(w(X), Z)$ is a function of Z and takes at most $|\mathcal{Z}|$ distinct values. Hence by choosing $\mathcal{H} = \mathcal{F} = \left\{ \sum_{Z=z} \beta_z \mathbb{1}\{Z = z\} : \beta_z \in \mathbb{R}, z \in \mathcal{Z} \right\}$, we have $h^0 \in \mathcal{H}$. Therefore Assumption 3 holds. By Theorem 4.2, we have $\epsilon = 0$. By the definition of Z , for any $k \in [K]$, there exist some $z_k \in \mathcal{Z}$ such that $\mathbb{1}\{X \in G_k\} = \mathbb{1}\{Z = z_k\}$. Then

for any $k \in [K]$,

$$\mathbb{P}\{Y \notin \widehat{C}(X; h) \mid X \in G_k\} = \mathbb{P}\{Y \notin \widehat{C}(X; h) \mid Z = z_k\}.$$

Note that

$$\begin{aligned} & (\mathbb{P}\{Y \notin \widehat{C} \mid X \in G_k\} - \alpha)^2 \mathbb{P}\{X \in G_k\} \\ & \leq \sum_{k=1}^K (\mathbb{P}\{Y \notin \widehat{C} \mid X \in G_k\} - \alpha)^2 \mathbb{P}\{X \in G_k\} \\ & = \sum_{k=1}^K (\mathbb{P}\{Y \notin \widehat{C} \mid Z = z_k\} - \alpha)^2 \mathbb{P}\{Z = z_k\} \\ & \stackrel{(i)}{\leq} \sum_{z \in \mathcal{Z}} (\alpha(z, \widehat{C}) - \alpha)^2 \mathbb{P}\{Z = z\} = \mathbb{E} [(\alpha(Z; \widehat{C}) - \alpha)^2], \end{aligned}$$

where (i) is because the groups G_k may overlap; when the groups are disjoint, the inequality becomes an equality. Hence,

$$\left| \mathbb{P}\{Y \notin \widehat{C} \mid X \in G_k\} - \alpha \right| \leq \sqrt{\frac{\mathbb{E} [(\alpha(Z; \widehat{C}) - \alpha)^2]}{\mathbb{P}\{X \in G_k\}}}$$

Hence by Theorem 4.3, we have

$$\left| \mathbb{P}\{Y \in \widehat{C}(X) \mid X \in G_k\} - (1 - \alpha) \right| \lesssim \sqrt{\frac{d_{\mathfrak{e}} + |\mathcal{Z}|}{n} \log \frac{n}{d_{\mathfrak{e}} + |\mathcal{Z}|}}.$$

Moreover, for pretrained sublevel set (7), $T(h(X, Y)) = s(X, Y) - h(X)$ and then $\{Y \notin C(X; h)\} = \{s(X, Y) > h(X)\}$ is a subgraph for all $h \in \mathcal{H}$. Since $\mathcal{H} = \left\{ \sum_{Z=z} \beta_z \mathbb{1}\{Z = z\} : \beta_z \in \mathbb{R}, z \in \mathcal{Z} \right\}$ and it has VC dimension $d_{\mathcal{H}} \leq |\mathcal{Z}|$, then $\{(x, y) : s(x, y) > h(x), h \in \mathcal{H}\}$ is a VC-subgraph with VC dimension $O(|\mathcal{Z}|)$. \square

C.7 Proof of Corollary 4.2

Proof. Since Assumption 3 holds for some $w(X)$, then by Theorem 4.2, we have

$$\text{MSCE}(C^{\text{ora}}) \leq \kappa^2(1 - \rho^2) \text{Tr} \left(\text{Cov} \left\{ H^0(w(X), Z) \right\} \right) \lesssim 1 - \rho^2.$$

For each $z \in \mathcal{Z}$, note that

$$\mathbb{E} \left[(\alpha(Z; \hat{C}) - \alpha)^2 \right] = \sum_{z \in \mathcal{Z}} (\alpha(z, \hat{C}) - \alpha)^2 \mathbb{P}\{Z = z\}.$$

Hence,

$$\left| \mathbb{P}\{Y \notin \hat{C} \mid Z = z\} - \alpha \right| \leq \sqrt{\frac{\mathbb{E}[(\alpha(Z; \hat{C}) - \alpha)^2]}{\mathbb{P}\{Z = z\}}}$$

Hence by Theorem 4.3, we have

$$\left| \mathbb{P}\{Y \in \hat{C}^{\text{opt}}(X) \mid Z = z\} - (1 - \alpha) \right| \lesssim \sqrt{\frac{1 - \rho^2}{\mathbb{P}\{Z = z\}}} + \sqrt{\frac{d_{\mathfrak{c}} + |\mathcal{Z}|}{n \cdot \mathbb{P}(Z = z)} \log \left(\frac{n}{d_{\mathfrak{c}} + |\mathcal{Z}|} \right)}.$$

□

C.8 Proof of Corollary 4.3

Proof. Since Assumption 3 holds for some $w(X) = X$ and $Z = X$, then by Theorem 4.2, we have $\epsilon = 0$. Moreover, since we assume $\alpha(Z; C) - \alpha(Z; C^{\text{ora}}) \in \mathcal{F}_U$, by the definition of f_C ,

$$f_C = \arg \min_{f \in \mathcal{F}} \mathbb{E} \left[(f(Z) - (\alpha(Z; C) - \alpha(Z; C^{\text{ora}})))^2 \right],$$

then we have $\eta = 0$. Hence, by Theorem 4.4, we have

$$\mathbb{E} \left[(\alpha(X_{n+1}; \hat{C}) - \alpha)^2 \right] \lesssim \frac{d_{\mathfrak{c}} \log(n/d_{\mathfrak{c}})}{n} + \frac{d_{\mathfrak{z}} \log^{d_{\mathfrak{z}}+1}(n/d_{\mathfrak{z}})}{n}.$$

□

C.9 Multi-group coverage guarantee

In addition to the MSE results, we also have the multi-group coverage guarantee for MOPI.

Theorem C.3 (Multi-group coverage). *Under the same settings of Theorem 4.1 and assume f is bounded by some constant $B > 0$ for all $f \in \mathcal{F}$, with probability at least $1 - 4\zeta$:*

$$\mathbb{E} \left[f(Z) \left(\mathbb{1}\{Y \notin \widehat{C}(X)\} - \alpha \right) \mid \mathcal{D}_n \right] \lesssim \left(\mathbb{E} \left[(\alpha(Z; \widehat{C}) - \alpha)^2 \mid \mathcal{D}_n \right] \right)^{1/2}.$$

Proof. Since $\|f\|_\infty \leq B$, then $\sup_{f \in \mathcal{F}} \|f\|_2 \leq B$. Note that $\mathbb{E} [f(Z) (\mathbb{1}\{Y \notin C(X)\} - \alpha)] = \mathbb{E} [f(Z) (\alpha(Z; C) - \alpha)]$, by Cauchy-Schwarz inequality,

$$\sup_{f \in \mathcal{F}} \mathbb{E} [f(Z) (\mathbb{1}\{Y \notin C(X)\} - \alpha)] \leq \sup_{f \in \mathcal{F}} \|f\|_2 \left(\mathbb{E} [(\alpha(Z; C) - \alpha)^2] \right)^{1/2}.$$

for all $C \in \mathfrak{C}$. □

D Infinite-dimensional set-valued function class

Now we consider the case where \mathfrak{C} is an infinite-dimensional set-valued function space, e.g., $\mathfrak{C} = \{C(x; h) : h \in \mathcal{H}\}$ and \mathcal{H} is an RKHS. In this case, let $\|\cdot\|_{\mathcal{H}}$ be the equipped norm in the space \mathcal{H} . Then, we construct the empirical MOPI prediction set via

$$\widehat{C} = \arg \min_{C \in \mathfrak{C}} \max_{f \in \mathcal{F}} \left\{ \widehat{\Psi}(C, f) - \gamma \|f\|_{\mathcal{F}} - \nu \|C\|_{\mathcal{H}} \right\}, \quad (\text{D.1})$$

where $\nu \geq 0$ is a regularization parameter for $C \in \mathfrak{C}$, and $\|C\|_{\mathcal{H}} = \|h\|_{\mathcal{H}}$ for $C(x) = C(x; h)$ for some $h \in \mathcal{H}$. Similar to Lemmas 3.1 and 3.2, we can obtain the closed forms for the inner maximization for (D.1) under the corresponding choice of \mathcal{F} .

Next, we present the upper bound of MSCE for the set-valued function class defined in (3) when \mathcal{F} and \mathcal{H} are both RKHS with a Gaussian kernel. For simplicity, we assume $\mathcal{Z} = [0, 1]^{d_{\mathcal{Z}}}$ and $\mathcal{X} = [0, 1]^{d_{\mathcal{X}}}$, where $d_{\mathcal{Z}}$ and $d_{\mathcal{X}}$ are the dimensions.

Theorem D.1. *Suppose Assumption 2 holds for the structured set-valued class \mathfrak{C} in (3). Assume the marginal density of $T(h(X), Y)$ has an upper bound for any $h \in \mathcal{H}$, and $T(\cdot, \cdot)$ is Lipschitz continuous with respect to its first variable. If the hyperparameters γ and ν in optimization problem (D.1) are chosen such that $\|f\|_{L_2}^2 \leq \gamma \|f\|_{\mathcal{F}}^2$ for all $f \in \mathcal{F}$ and $\nu \lesssim \frac{d_{\mathcal{Z}} \log^{d_{\mathcal{Z}}+1}(n/d_{\mathcal{Z}})}{n}$, then for sufficiently large n , we have*

$$\mathbb{E} \left[\left(\alpha(Z; \hat{C}) - \alpha \right)^2 \right] \lesssim \text{MSCE}(C^{\text{ora}}) + \eta^2 + \frac{m d_{\mathcal{X}} \log^{d_{\mathcal{X}}+1}(mn/d_{\mathcal{X}})}{n} + \frac{d_{\mathcal{Z}} \log^{d_{\mathcal{Z}}+1}(n/d_{\mathcal{Z}})}{n}.$$

The establishment of MSCE bound differs from that in Section 4.1 when \mathfrak{C} is finite-dimensional. When \mathfrak{C} is infinite-dimensional, its VC dimension is also infinite, so the complexity of the induced class \mathcal{G} can no longer be controlled via VC theory as we did in Section 4.3. In addition, we cannot directly apply standard contraction arguments (e.g., Proposition 5.28 of Wainwright (2019)) to \mathcal{G} because the functions in \mathcal{G} are not Lipschitz due to the presence of indicator functions. To address this challenge, we use the *margin cost functions* in the generalization theory of classification problems (Mason et al., 2000; Koltchinskii and Panchenko, 2002), which are Lipschitz continuous and can approximate indicator functions. The final bounds are determined by optimizing the margin parameter to achieve the fastest convergence rate.

D.1 Proof of Theorem D.1

In this section, we consider \mathcal{F} and \mathcal{H} are both RKHS with a Gaussian kernel and $C(x; h) = \{y \in \mathcal{Y} : T(h(x), y) \leq 0\}$. Formally, let $\mathcal{K}_{\mathcal{Z}}(\cdot, \cdot) : \mathcal{Z} \times \mathcal{Z} \rightarrow \mathbb{R}$, $\mathcal{K}_{\mathcal{X}}(\cdot, \cdot) : \mathcal{X} \times \mathcal{X} \rightarrow \mathbb{R}$ be Gaussian kernel and $\mathbb{K}_{\mathcal{K}_{\mathcal{Z}}}$, $\mathbb{K}_{\mathcal{K}_{\mathcal{X}}}$ denote RKHSs equipped with kernel $\mathcal{K}_{\mathcal{Z}}$, $\mathcal{K}_{\mathcal{X}}$ respectively.

Let $\mathcal{F} = \mathbb{K}_{\mathcal{K}_Z}$ and

$$\mathcal{H} = \{h = (h_1, \dots, h_m)^\top : h_j \in \mathbb{K}_{\mathcal{K}_X}, \|h_j\|_{\mathbb{K}_{\mathcal{K}_X}}^2 \leq U_X, j \in [m]\}. \quad (\text{D.2})$$

Consider the shape-constrained prediction set (3) and let $C^{\text{ora}}(X) = \{y \in \mathcal{Y} : T(h^{\text{ora}}(X), Y) \leq 0\}$. Align with the proof of Theorem C.1, we define the following notations. Let $\psi(h, f) = f(z)(\mathbb{1}\{y \notin C(x; h)\} - \alpha) = f(z)((1 - \mathbb{1}\{T(h(x), y) \leq 0\}) - \alpha)$, $v(h, h^{\text{ora}}) = v(C, C^{\text{ora}}) = \|\alpha(Z; C(X; h)) - \alpha(Z; C(X; h^{\text{ora}}))\|_{L_2}$ and

$$f_h = \arg \min_{f \in \mathcal{F}_U} \mathbb{E} \left[(f(Z) - \{\alpha(Z; C(X; h)) - \alpha(Z; C(X; h^{\text{ora}}))\})^2 \right].$$

For any $C \in \mathfrak{C}$, define

$$\|C\|_{\mathcal{H}}^2 := \sum_{j=1}^m \|h_j\|_{\mathbb{K}_{\mathcal{K}_X}}^2.$$

Proof. Note that

$$\begin{aligned} \mathbb{1}\{y \notin C(x; h)\} - \mathbb{1}\{y \notin C(x; h^{\text{ora}})\} &= \mathbb{1}\{T(h^{\text{ora}}(x), y) \leq 0\} - \mathbb{1}\{T(h(x), y) \leq 0\} \\ &=: D(h(x), y). \end{aligned}$$

Denote $\delta_n(\sigma_\ell) = \max\{\delta_{n, \mathcal{G}_{\varphi\sigma_\ell}^+}, \delta_{n, \mathcal{G}_{\varphi\sigma_\ell}^-}, \delta_{n, \mathcal{G}_{\varphi\sigma_\ell}^-}, \delta_{n, \mathcal{G}_{\varphi\sigma_\ell}^+}\}$ and $R_n(\sigma_\ell) = \lceil \log_2(1/\delta_n(\sigma_\ell)) \rceil + 1$. Define sequence $\sigma_\ell = 2^{-\ell+1}$ for $\ell \geq 1$. Taking $x = \log(4R_n(\sigma_\ell)/\zeta)$ for Lemma D.1, we can guarantee that w.p. $1 - \zeta$,

$$\begin{aligned} \forall h \in \mathcal{H}, \quad |(P_n - P)\{D(h)f_h\}| &\leq 2 \inf_{\ell \geq 1} \left\{ \Delta(h, \sigma_\ell) + \bar{\Delta}(h, \sigma_\ell) + \frac{2 \log(4R_n(\sigma_\ell)/\zeta)}{3n} \right. \\ &\quad \left. + 4v(h, h^{\text{ora}}) \left(2\delta_n(\sigma_\ell) + \sqrt{\frac{2 \log(4R_n(\sigma_\ell)/\zeta)}{n}} \right) \right\}, \end{aligned}$$

where we also used the fact $\|f_h\|_{L_2} \leq 2v(h, h^{\text{ora}})$. By Lemma D.2, we have

$\Delta(h, \sigma_\ell), \bar{\Delta}(h, \sigma_\ell) \lesssim \sigma_\ell$ and

$$\delta_n(\sigma_\ell) \lesssim \sqrt{\frac{d_{\mathcal{Z}} \log^{d_{\mathcal{Z}}+1}(n/d_{\mathcal{Z}})}{n}} + \sqrt{\frac{md_{\mathcal{X}} \log^{d_{\mathcal{X}}+1}\left(\frac{mn}{\sigma_i^2 d_{\mathcal{X}}}\right)}{n}}.$$

Hence, let $\ell = \lceil \log_2 n \rceil$, then $\Delta(h, \sigma_\ell), \bar{\Delta}(h, \sigma_\ell) \lesssim \frac{1}{n}$,

$$\delta_n(\sigma_\ell) \lesssim \sqrt{\frac{d_{\mathcal{Z}} \log^{d_{\mathcal{Z}}+1}(n/d_{\mathcal{Z}})}{n}} + \sqrt{\frac{md_{\mathcal{X}} \log^{d_{\mathcal{X}}+1}\left(\frac{mn}{d_{\mathcal{X}}}\right)}{n}} := \delta_{n,\mathcal{G}},$$

and $R_n(\sigma_\ell) \lesssim \log_2 n$. Thus, $\forall h \in \mathcal{H}$, w.p. $1 - \zeta$,

$$|(P_n - P)\{D(h)f_h\}| \leq O(1) \left\{ \frac{1}{n} + \frac{\log(\log_2 n/\zeta)}{n} + v(h, h^{\text{ora}}) \left(\delta_{n,\mathcal{G}} + \sqrt{\frac{\log(\log_2 n/\zeta)}{n}} \right) \right\}. \quad (\text{D.3})$$

Similar to (C.14), using (D.3) we have

$$\begin{aligned} & \sup_{f \in \mathcal{F}} \left\{ P_n \psi(\hat{h}, f) - P_n \psi(h^{\text{ora}}, f) - 2 \left(P_n f^2 + \gamma \|f\|_{\mathcal{F}}^2 \right) \right\} \\ & \geq r P_n \psi(\hat{h}, f_{\hat{h}}) - r P_n \psi(h^{\text{ora}}, f_{\hat{h}}) - 2r^2 \left(P_n f_{\hat{h}}^2 + \gamma \|f_{\hat{h}}\|_{\mathcal{F}}^2 \right) \\ & \geq r(v(\hat{h}, h^{\text{ora}}) - 2\eta) \|f_{\hat{h}}\|_{L_2} - 2r^2 \left(\gamma \|f_{\hat{h}}\|_{\mathcal{F}}^2 + \frac{7}{4} \|f_{\hat{h}}\|_{L_2}^2 + \frac{\tilde{\delta}_{n,\mathcal{F}}^2}{2} \right) \\ & - rO(1) \left\{ \frac{1}{n} + \frac{\log(\log_2 n/\zeta)}{n} + v(h, h^{\text{ora}}) \left(\delta_{n,\mathcal{G}} + \sqrt{\frac{\log(\log_2 n/\zeta)}{n}} \right) \right\}. \end{aligned}$$

If $2\delta_{n,\mathcal{G}} + \sqrt{\frac{2\log(\log_2 n/\zeta)}{n}} \geq \|f_{\hat{h}}\|_{L_2}/2$, we have

$$v(\hat{h}, h^{\text{ora}}) \leq \|f_{\hat{h}}\|_{L_2} + \eta \lesssim \delta_{n,\mathcal{G}} + \sqrt{\frac{\log(\log_2 n/\zeta)}{n}} + \eta.$$

Otherwise, i.e., $2\delta_{n,\mathcal{G}} + \sqrt{\frac{2\log(\log_2 n/\zeta)}{n}} \leq \|f_{\hat{h}}\|_{L_2}/2$, using (C.10), w.p. $1 - 4\zeta$, we get

$$\begin{aligned} v(\hat{h}, h^{\text{ora}}) &\lesssim \frac{1}{r\|f_{\hat{h}}\|_{L_2}} \left(\epsilon^2 + \tilde{\delta}_{n,\mathcal{F}}^2 + \nu\|C^{\text{ora}}\|_{\mathcal{H}}^2 \right) + \eta \\ &\quad + \frac{1}{n\|f_{\hat{h}}\|_{L_2}} + \frac{\log(\log_2 n/\zeta)}{n\|f_{\hat{h}}\|_{L_2}} + \frac{r}{\|f_{\hat{h}}\|_{L_2}} \left(\gamma\|f_{\hat{h}}\|_{\mathcal{F}}^2 + \|f_{\hat{h}}\|_{L_2}^2 + \tilde{\delta}_{n,\mathcal{F}}^2 \right), \end{aligned}$$

If $\|f_{\hat{h}}\|_{L_2} \geq \tilde{\delta}_{n,\mathcal{F}} \geq \sqrt{\frac{\log(c_1/\zeta)}{c_2 n}}$, choosing $r = \max\{\epsilon, \tilde{\delta}_{n,\mathcal{F}}\}/\|f_{\hat{C}}\|_{L_2}$, by $\gamma\|f\|_{\mathcal{F}}^2 \leq \|f\|_{L_2}^2$, we have

$$\begin{aligned} v(\hat{h}, h^{\text{ora}}) &\lesssim \epsilon + \tilde{\delta}_{n,\mathcal{F}} + \frac{\nu\|C^{\text{ora}}\|_{\mathcal{H}}^2}{\tilde{\delta}_{n,\mathcal{F}}} + \eta + \sqrt{\frac{\log(\log_2 n/\zeta)}{n}} + \tilde{\delta}_{n,\mathcal{F}} + \tilde{\delta}_{n,\mathcal{F}} + \tilde{\delta}_{n,\mathcal{F}} \\ &\lesssim \epsilon + \tilde{\delta}_{n,\mathcal{F}} + \frac{\nu\|C^{\text{ora}}\|_{\mathcal{H}}^2}{\tilde{\delta}_{n,\mathcal{F}}} + \eta + \sqrt{\frac{\log(\log_2 n/\zeta)}{n}}. \end{aligned}$$

Therefore,

$$v(\hat{h}, h^{\text{ora}}) \lesssim \epsilon + \tilde{\delta}_{n,\mathcal{F}} + \eta + \sqrt{\frac{\log(\log_2 n/\zeta)}{n}} + \frac{\nu\|C^{\text{ora}}\|_{\mathcal{H}}^2}{\tilde{\delta}_{n,\mathcal{F}}}. \quad (\text{D.4})$$

Otherwise, i.e. $\|f_{\hat{h}}\|_{L_2} \leq \tilde{\delta}_{n,\mathcal{F}}$, we have

$$v(\hat{h}, h^{\text{ora}}) \leq \|f_{\hat{h}}\|_{L_2} + \eta \lesssim \tilde{\delta}_{n,\mathcal{F}} + \eta.$$

Combining the relations above, we can conclude that

$$v(\hat{h}, h^{\text{ora}}) \lesssim \epsilon + \delta_{n,\mathcal{F}_U} + \delta_{n,\mathcal{G}} + \eta + \frac{\nu\|C^{\text{ora}}\|_{\mathcal{H}}^2}{\tilde{\delta}_{n,\mathcal{F}}} + \sqrt{\frac{\log(\log_2 n/\zeta)}{n}},$$

where we used the definition of $\tilde{\delta}_{n,\mathcal{F}}$. Hence there exist $C > 0$ such that w.p. $1 - 4\zeta$:

$$\begin{aligned} &\mathbb{E} \left[(\alpha(Z; \hat{C}) - \alpha)^2 \mid \mathcal{D}_n \right] \\ &\leq C \left(\epsilon^2 + \eta^2 + \delta_{n,\mathcal{F}_U}^2 + \delta_{n,\mathcal{G}}^2 + \frac{\nu^2\|C^{\text{ora}}\|_{\mathcal{H}}^4}{\delta_{n,\mathcal{F}_U}^2} + \frac{\log((\log_2 n)/\zeta)}{n} \right) := A_n. \end{aligned}$$

Therefore, Let $\mathcal{E} = \left\{ \mathbb{E} \left[(\alpha(Z; \widehat{C}) - \alpha)^2 \mid \mathcal{D}_n \right] \leq A_n \right\}$

$$\begin{aligned} \mathbb{E} \left[(\alpha(Z; \widehat{C}) - \alpha)^2 \right] &= \mathbb{E} \left[\mathbb{E} \left[(\alpha(Z; \widehat{C}) - \alpha)^2 \mid \mathcal{D}_n \right] \right] \\ &= \mathbb{E} \left[\mathbb{E} \left[(\alpha(Z; \widehat{C}) - \alpha)^2 \mid \mathcal{D}_n \right] \mathbb{1}_{\mathcal{E}} \right] \\ &\quad + \mathbb{E} \left[\mathbb{E} \left[(\alpha(Z; \widehat{C}) - \alpha)^2 \mid \mathcal{D}_n \right] \mathbb{1}_{\mathcal{E}^c} \right] \\ &\leq A_n + 4\zeta. \end{aligned}$$

By choosing $\zeta = \frac{1}{n}$, we have

$$\mathbb{E} \left[(\alpha(Z; \widehat{C}) - \alpha)^2 \right] \lesssim \epsilon^2 + \eta^2 + \delta_{n, \mathcal{F}_U}^2 + \delta_{n, \mathcal{G}}^2 + \frac{\nu^2 \|C^{\text{ora}}\|_{\mathcal{H}}^4}{\delta_{n, \mathcal{F}_U}^2} + \frac{\log(n \log_2 n)}{n}.$$

Since $\mathcal{F} = \mathbb{K}_{\mathcal{K}_Z}$, by Theorem C.2, we have $\delta_{n, \mathcal{F}_U} \lesssim \sqrt{\frac{d_Z \log^{d_Z+1}(n/d_Z)}{n}}$. By the definition of \mathcal{H} in (D.2), $\|C^{\text{ora}}\|_{\mathcal{H}}^2 \leq mU_{\mathcal{X}}$. Then by choosing $\nu \lesssim \frac{d_Z \log^{d_Z+1}(n/d_Z)}{n}$, we have

$$\mathbb{E} \left[(\alpha(Z; \widehat{C}) - \alpha)^2 \right] \lesssim \epsilon^2 + \eta^2 + \frac{md_{\mathcal{X}} \log^{d_{\mathcal{X}+1}}(mn/d_{\mathcal{X}})}{n} + \frac{d_Z \log^{d_Z+1}(n/d_Z)}{n}.$$

□

D.1.1 Margin concentration lemma

Lemma D.1. *Define sequence $\sigma_\ell = 2^{-\ell+1}$ for $\ell \geq 1$. For any $x > 0$, w.p. $1 - (\lceil \log_2(1/\delta_{n, \widetilde{\mathcal{G}}_\varphi^-} \rceil) + \lceil \log_2(1/\delta_{n, \mathcal{G}_\varphi^-} \rceil) + 2)e^{-x} - (\lceil \log_2(1/\delta_{n, \widetilde{\mathcal{G}}_\varphi^+} \rceil) + \lceil \log_2(1/\delta_{n, \mathcal{G}_\varphi^+} \rceil) + 2)e^{-x}$,*

$$\begin{aligned} \forall h \in \mathcal{H}, \quad |(P_n - P) \{D(h) f_h\}| &\leq \inf_{\ell \geq 1} \left\{ \overline{\Delta}(h, \sigma_\ell) + \|f_h\|_{L_2} \left(2\delta_{n, \mathcal{G}_{\varphi^+}^{\sigma_\ell}} + \sqrt{\frac{2 \log x}{n}} \right) + \frac{\log x}{3n} \right\} \\ &\quad + \inf_{\ell \geq 1} \left\{ \Delta(h, \sigma_\ell) + \|f_h\|_{L_2} \left(2\delta_{n, \mathcal{G}_{\varphi^+}^{\sigma_\ell}} + \sqrt{\frac{2 \log x}{n}} \right) + \frac{\log x}{3n} \right\} \\ &\quad + \inf_{\ell \geq 1} \left\{ \overline{\Delta}(h, \sigma_\ell) + \|f_h\|_{L_2} \left(2\delta_{n, \mathcal{G}_{\varphi^-}^{\sigma_\ell}} + \sqrt{\frac{2 \log x}{n}} \right) + \frac{\log x}{3n} \right\} \end{aligned}$$

$$+ \inf_{\ell \geq 1} \left\{ \Delta(h, \sigma_\ell) + \|f_h\|_{L_2} \left(2\delta_{n, \mathcal{G}_{\varphi\sigma_\ell}^-} + \sqrt{\frac{2 \log x}{n}} \right) + \frac{\log x}{3n} \right\},$$

where $g_{\varphi\sigma_\ell}^+(h) \in \mathcal{G}_{\varphi\sigma_\ell}^+$, $g_{\varphi\sigma_\ell}^+(h) \in \mathcal{G}_{\varphi\sigma_\ell}^+$ are defined in (D.5) and (D.6); $g_{\varphi\sigma_\ell}^-(h) \in \mathcal{G}_{\varphi\sigma_\ell}^-$, $g_{\varphi\sigma_\ell}^-(h) \in \mathcal{G}_{\varphi\sigma_\ell}^-$ are defined in (D.10) and (D.11); $\bar{\Delta}(h, \sigma_\ell)$ and $\Delta(h, \sigma_\ell)$ are defined in (D.7) and (D.8).

Proof. For any function f , we write $[f]^+ = f\mathbb{1}\{f \geq 0\}$ and $[f]^- = -f\mathbb{1}\{f < 0\}$. We first notice that

$$(P_n - P)D(h)f_h = \underbrace{(P_n - P) \left\{ D_+(h)[f_h]^+ \right\}}_{\text{(I)}} - \underbrace{(P_n - P) \left\{ D(h)[f_h]^- \right\}}_{\text{(II)}}.$$

Assumption D.1. The Lipschitz functions $\bar{\varphi}$ and φ satisfy $0 \leq \varphi(u) \leq \mathbb{1}\{u \leq 0\} \leq \bar{\varphi}(u) \leq 1$.

Bounding the term (I). Given $\bar{\varphi}$ and φ , we define two function classes

$$\mathcal{G}_{\bar{\varphi}}^+ = \{g_{\bar{\varphi}}^+(h) = [f_h]^+ (\bar{\varphi} \circ T(h) - (1 - \mathbb{1}\{T(h^{\text{ora}}) \leq 0\})) : h \in \mathcal{H}\}, \quad (\text{D.5})$$

$$\mathcal{G}_{\varphi}^+ = \{g_{\varphi}^+(h) = [f_h]^+ (\varphi \circ T(h) - (1 - \mathbb{1}\{T(h^{\text{ora}}) \leq 0\})) : h \in \mathcal{H}\}. \quad (\text{D.6})$$

Using Lemma E.7, w.p. $1 - (\lceil \log_2(1/\delta_{n, \tilde{\mathcal{G}}_{\bar{\varphi}}^+}) \rceil + 1)e^{-x}$, we have

$$\begin{aligned} \forall h \in \mathcal{H} \in \mathcal{G}_{\bar{\varphi}}^+, \quad |(P_n - P)g_{\bar{\varphi}}^+(h)| &\leq \|g_{\bar{\varphi}}^+(h)\|_{L_2} \left(2\delta_{n, \mathcal{G}_{\bar{\varphi}}^+} + \sqrt{\frac{2 \log x}{n}} \right) + \frac{\log x}{3n} \\ &\leq \|f_h\|_{L_2} \left(2\delta_{n, \mathcal{G}_{\bar{\varphi}}^+} + \sqrt{\frac{2 \log x}{n}} \right) + \frac{\log x}{3n}. \end{aligned}$$

And, w.p. $1 - (\lceil \log_2(1/\delta_{n, \mathcal{G}_\varphi^+}) \rceil + 1)e^{-x}$, we have

$$\begin{aligned} \forall h \in \mathcal{H}, \quad |(P_n - P)g_\varphi^+(h)| &\leq \|g_\varphi^+(h)\|_{L_2} \left(2\delta_{n, \mathcal{G}_\varphi^+} + \sqrt{\frac{2 \log x}{n}} \right) + \frac{\log x}{3n} \\ &\leq \|fh\|_{L_2} \left(2\delta_{n, \mathcal{G}_\varphi^+} + \sqrt{\frac{2 \log x}{n}} \right) + \frac{\log x}{3n}. \end{aligned}$$

For any $\sigma \in [0, 1]$, we take the Lipschitz continuous function as

$$\bar{\varphi}_\sigma(u) = \begin{cases} 1, & u < -\sigma, \\ -u/\sigma, & -\sigma \leq u \leq 0, \\ 0, & u \geq 0. \end{cases}, \quad \varphi_\sigma(u) = \begin{cases} 1, & u < 0, \\ -u/\sigma, & 0 \leq u < \sigma, \\ 0, & u \geq \sigma. \end{cases}$$

which satisfies Assumption [D.1](#). In addition, we know $L_{\bar{\varphi}_\sigma}, L_{\varphi_\sigma} \leq 1/\sigma$. Define Lipschitz constants $\sigma_\ell = 2^{-\ell+1}$ for $\ell \geq 1$. Denote the quantities

$$\bar{\Delta}(h, \sigma_\ell) := P\{\bar{\varphi}_{\sigma_\ell} \circ T(h) \neq \mathbb{1}\{T(h) \leq 0\}\}, \quad (\text{D.7})$$

$$\Delta(h, \sigma_\ell) := P\{\varphi_{\sigma_\ell} \circ T(h) \neq \mathbb{1}\{T(h) \leq 0\}\}. \quad (\text{D.8})$$

Then, w.p. $1 - R_n \sum_{\ell=1}^{\infty} e^{-(x+2 \log \ell)} \geq 1 - 2R_n e^{-x}$, we have

$$\begin{aligned} \forall h \in \mathcal{H}, \quad P_n \{D(h)[fh]^+\} &\leq \inf_{\ell \geq 1} \left\{ P_n g_{\bar{\varphi}_{\sigma_\ell}}^+(h) \right\} \\ &\leq \inf_{\ell \geq 1} \left\{ P g_{\bar{\varphi}_{\sigma_\ell}}^+(h) + \left| (P_n - P) g_{\bar{\varphi}_{\sigma_\ell}}^+(h) \right| \right\} \\ &\leq P \{D(h)[fh]^+\} + \inf_{\ell \geq 1} \left\{ \bar{\Delta}(h, \sigma_\ell) + \|fh\|_{L_2} \left(2\delta_{n, \mathcal{G}_{\bar{\varphi}_{\sigma_\ell}}^+} + \sqrt{\frac{2 \log x}{n}} \right) + \frac{\log x}{3n} \right\}, \end{aligned}$$

and

$$\forall h \in \mathcal{H}, \quad P_n \{D(h)[fh]^+\} \geq \sup_{\ell \geq 1} \left\{ P_n g_{\varphi_{\sigma_\ell}}^+(h) \right\}$$

$$\begin{aligned}
&\geq \sup_{\ell \geq 1} \left\{ P g_{\varphi_{\sigma_\ell}}^+(h) - |(P_n - P)g_{\varphi_{\sigma_\ell}}^+(h)| \right\} \\
&\geq P \left\{ D(h)[f_h]^+ \right\} + \sup_{\ell \geq 1} \left\{ -\Delta(h, \sigma_\ell) - \|f_h\|_{L_2} \left(2\delta_{n, \mathcal{G}_{\varphi_{\sigma_\ell}}^+} + \sqrt{\frac{2 \log x}{n}} \right) - \frac{\log x}{3n} \right\}.
\end{aligned}$$

It follows that w.p. $1 - (\lceil \log_2(1/\delta_{n, \tilde{\mathcal{G}}_\varphi^+}) \rceil + \lceil \log_2(1/\delta_{n, \mathcal{G}_\varphi^+}) \rceil + 2)e^{-x}$

$$\begin{aligned}
\forall h \in \mathcal{H}, \quad & |(P_n - P) \left\{ D(h)[f_h]^+ \right\}| \\
&\leq \inf_{\ell \geq 1} \left\{ \bar{\Delta}(h, \sigma_\ell) + \|f_h\|_{L_2} \left(2\delta_{n, \mathcal{G}_{\varphi_{\sigma_\ell}}^+} + \sqrt{\frac{2 \log x}{n}} \right) + \frac{\log x}{3n} \right\} \\
&+ \inf_{\ell \geq 1} \left\{ \Delta(h, \sigma_\ell) + \|f_h\|_{L_2} \left(2\delta_{n, \mathcal{G}_{\varphi_{\sigma_\ell}}^+} + \sqrt{\frac{2 \log x}{n}} \right) + \frac{\log x}{3n} \right\}. \quad (\text{D.9})
\end{aligned}$$

Bounding the term (II). Similarly, given $\bar{\varphi}$ and φ , we define another two function classes

$$\mathcal{G}_{\bar{\varphi}}^- = \{ [f_h]^- (\bar{\varphi} \circ T(h) - (1 - \mathbb{1}\{T(h^{\text{ora}}) \leq 0\})) : h \in \mathcal{H} \}, \quad (\text{D.10})$$

$$\mathcal{G}_{\varphi}^- = \{ [f_h]^- (\varphi \circ T(h) - (1 - \mathbb{1}\{T(h^{\text{ora}}) \leq 0\})) : h \in \mathcal{H} \}. \quad (\text{D.11})$$

Recalling the definition of $D(h)$, we have

$$P\{g_{\bar{\varphi}_{\sigma_\ell}}^- \neq D(h)[f_h]^- \} = P\{\bar{\varphi}_{\sigma_\ell} \circ T(h) \neq \mathbb{1}\{T(h) \leq 0\}\} = \bar{\Delta}(h, \sigma_\ell),$$

$$P\{g_{\varphi_{\sigma_\ell}}^+ \neq D(h)[f_h]^- \} = P\{\varphi_{\sigma_\ell} \circ T(h) \neq \mathbb{1}\{T(h) \leq 0\}\} = \Delta(h, \sigma_\ell).$$

We can show that w.p. $1 - (\lceil \log_2(1/\delta_{n, \tilde{\mathcal{G}}_\varphi^-}) \rceil + \lceil \log_2(1/\delta_{n, \mathcal{G}_\varphi^-}) \rceil + 2)e^{-x}$,

$$\begin{aligned}
\forall h \in \mathcal{H}, \quad & |(P_n - P) \left\{ D(h)[f_h]^- \right\}| \\
&\leq \inf_{\ell \geq 1} \left\{ \bar{\Delta}(h, \sigma_\ell) + \|f_h\|_{L_2} \left(2\delta_{n, \mathcal{G}_{\bar{\varphi}_{\sigma_\ell}}^-} + \sqrt{\frac{2 \log x}{n}} \right) + \frac{\log x}{3n} \right\} \\
&+ \inf_{\ell \geq 1} \left\{ \Delta(h, \sigma_\ell) + \|f_h\|_{L_2} \left(2\delta_{n, \mathcal{G}_{\varphi_{\sigma_\ell}}^-} + \sqrt{\frac{2 \log x}{n}} \right) + \frac{\log x}{3n} \right\}. \quad (\text{D.12})
\end{aligned}$$

Combining Eqs. (D.9) and (D.12), we can prove the conclusion. \square

Lemma D.2. *Suppose the marginal density of $T := T(h(X), Y)$ is bounded, i.e. $p_T(t) \leq \bar{C}_T$ with some constant $\bar{C}_T > 0$ and assume for any $\mathbf{u}_1, \mathbf{u}_2 \in \mathbb{R}^m$, $|T(\mathbf{u}, y) - T(\mathbf{u}, y)| \leq \bar{L}_T \|\mathbf{u}_1 - \mathbf{u}_2\|$ with some constant $\bar{L}_T > 0$. If we choose $\mathcal{F} = \mathbb{K}_{\mathcal{K}_Z}$ and \mathcal{H} is defined in (D.2), then we have $\bar{\Delta}(h, \sigma_\ell), \Delta(h, \sigma_\ell) \leq \bar{C}_T \sigma_\ell$, and*

$$\delta_{n, \mathcal{G}_{\bar{\varphi}}^+}, \delta_{n, \mathcal{G}_{\bar{\varphi}}^-}, \delta_{n, \mathcal{G}_{\varphi}^+}, \delta_{n, \mathcal{G}_{\varphi}^-} \lesssim \frac{1}{\sqrt{n}} \cdot \sqrt{d_Z \log^{d_Z+1}(n/d_Z) \vee m d_{\mathcal{X}} \log^{d_{\mathcal{X}}+1}\left(\frac{mn}{\sigma_l^2 d_{\mathcal{X}}}\right)}.$$

Proof. By definition of Δ and $\bar{\Delta}$ in (D.8) and (D.8) and the assumption,

$$\begin{aligned} \bar{\Delta}(h, \sigma_\ell) &= P\{-\sigma_\ell \leq T(h) \leq 0\} = \int_{-\sigma_\ell}^0 f_T(t) dt \leq \bar{C}_T \sigma_\ell, \\ \Delta(h, \sigma_\ell) &= P\{0 \leq T(h) \leq \sigma_\ell\} = \int_0^{\sigma_\ell} f_T(t) dt \leq \bar{C}_T \sigma_\ell, \end{aligned}$$

The critical part is to calculate the rate of $\mathcal{G}_{\bar{\varphi}}^+, \mathcal{G}_{\bar{\varphi}}^-, \mathcal{G}_{\varphi}^+, \mathcal{G}_{\varphi}^-$. We first consider the $\mathcal{G}_{\bar{\varphi}}^+$ in (D.5). Since for any $\mathbf{u}_1, \mathbf{u}_2 \in \mathbb{R}^m$, $|T(\mathbf{u}, y) - T(\mathbf{u}, y)| \leq \bar{L}_T \|\mathbf{u}_1 - \mathbf{u}_2\|$, then $\bar{\varphi} \circ T(\mathbf{u}, y)$ is a Lipschitz function w.r.t. \mathbf{u} with Lipschitz constant \bar{L}_T/σ_l . For fixed $h^{\text{ora}} \in \mathcal{H}$, define

$$\tilde{\mathcal{G}}_{\bar{\varphi}}^+ = \{g_{\bar{\varphi}}^+(h) = [f]^+(\bar{\varphi} \circ T(h) - (1 - \mathbb{1}\{T(h^{\text{ora}}) \leq 0\})) : h \in \mathcal{H}, f \in \mathcal{F}_{U_Z}\}.$$

Here we denote $U_Z := U$ to distinguish it from $U_{\mathcal{X}}$. Note that $\mathcal{G}_{\bar{\varphi}}^+ \subseteq \tilde{\mathcal{G}}_{\bar{\varphi}}^+$, then we only need to bound the covering number of $\tilde{\mathcal{G}}_{\bar{\varphi}}^+$. By Lemma E.2, E.3 and E.5, we have

$$\log N(\rho, \tilde{\mathcal{G}}_{\bar{\varphi}}^+, \|\cdot\|_{L_2}) \leq \log N(\rho/2, \mathcal{F}_{U_Z}, \|\cdot\|_{L_2}) + \log N\left(\frac{\sigma_l \rho}{2\bar{L}_T}, \mathcal{H}, \|\cdot\|_{L_2}\right).$$

Let $\mathcal{K}_Z(\cdot, \cdot) : \mathcal{Z} \times \mathcal{Z} \rightarrow \mathbb{R}$, $\mathcal{K}_{\mathcal{X}}(\cdot, \cdot) : \mathcal{X} \times \mathcal{X} \rightarrow \mathbb{R}$ be Gaussian kernel and $\mathbb{K}_{\mathcal{K}_Z}, \mathbb{K}_{\mathcal{K}_{\mathcal{X}}}$ denote RKHSs equipped with kernel $\mathcal{K}_Z, \mathcal{K}_{\mathcal{X}}$ respectively. Let $\mathcal{F} = \mathbb{K}_{\mathcal{K}_Z}$ and $\mathcal{H} = \{h =$

$(h_1, \dots, h_m)^\top : h_j \in \mathbb{K}_{\mathcal{K}_X}, \|h_j\|_{\mathbb{K}_{\mathcal{K}_X}}^2 \leq U_X, j \in [m]\}$. By Lemma E.4 and (C.20), we have

$$\begin{aligned}\log N(\rho, \mathcal{F}_{U_Z}, \|\cdot\|_{L_2}) &\leq 4^{d_Z} (6d_Z + 2) (\log(U_Z/\rho))^{d_Z+1}, \\ \log N(\rho, \mathcal{H}, \|\cdot\|_{L_2}) &\leq m4^{d_X} (6d_Z + 2) (\log(mU_X/\rho))^{d_X+1}.\end{aligned}$$

$$\begin{aligned}\bar{\mathcal{R}}_n(\delta; \mathcal{G}_\varphi^+) &\leq \bar{\mathcal{R}}_n(\delta; \tilde{\mathcal{G}}_\varphi^+) \leq \frac{C_0}{\sqrt{n}} \int_0^\delta \sqrt{\log N(\rho, \tilde{\mathcal{G}}_\varphi^+, \|\cdot\|_{L_2})} d\rho \\ &\leq \frac{2}{\sqrt{n}} \int_0^{\delta/2} \sqrt{\log N(\rho, \mathcal{F}_{U_Z}, \|\cdot\|_{L_2})} d\rho + \frac{2\bar{L}_T}{\sigma_l \sqrt{n}} \int_0^{\sigma_l \delta / (2\bar{L}_T)} \sqrt{\log N(\rho, \mathcal{H}, \|\cdot\|_{L_2})} d\rho \\ &\lesssim \delta \sqrt{\frac{(2d_Z + 1)(4 \log(U_Z^2/\delta^2))^{d_Z+1}}{n}} \\ &\quad + \delta \sqrt{\frac{m(2d_X + 1)(4 \log\{(mU_X \bar{L}_T)^2 / (\sigma_l \delta)^2\})^{d_X+1}}{n}}.\end{aligned}\tag{D.13}$$

Similar with the proof of Theorem C.2, since we require $\bar{\mathcal{R}}(\delta; \tilde{\mathcal{G}}_\varphi^+) \lesssim \delta^2$, we can have

$$\begin{cases} \frac{d_Z}{n} \log^{d_Z+1}(U_Z^2/\delta^2) \lesssim \frac{1}{2}\delta^2, \\ \frac{md_X}{n} \log^{d_X+1}((mU_X \bar{L}_T)^2 / (\sigma_l \delta)^2) \lesssim \frac{1}{2}\delta^2. \end{cases}$$

For the first inequality, using (C.22) we get $\delta \asymp \sqrt{\frac{d_Z \log^{d_Z+1}(n/d_Z)}{n}}$. For the second inequality, using Lemma E.1, let $t = \frac{(mU_X \bar{L}_T)^2}{\sigma_l^2 \delta^2}$ and check the root of the equation $t(\log t)^{d_X+1} = \frac{nm(U_X \bar{L}_T)^2}{\sigma_l^2 d_X}$. Taking the logarithm on both sides, we have:

$$\log t + (d_X + 1) \log \log t = \log\left(\frac{nm(U_X \bar{L}_T)^2}{\sigma_l^2 d_X}\right).$$

By Lemma E.1 with $L_n = \log\left(\frac{nm(U_X \bar{L}_T)^2}{\sigma_l^2 d_X}\right)$, we have

$$\frac{(mU_X \bar{L}_T)^2}{\sigma_l^2 \delta^2} \asymp \exp\left\{\log\left(\frac{nm(U_X \bar{L}_T)^2}{\sigma_l^2 d_X}\right) - (d_X + 1) \log \log\left(\frac{nm(U_X \bar{L}_T)^2}{\sigma_l^2 d_X}\right)\right\}$$

$$= \frac{\frac{nm(U_X \bar{L}_T)^2}{\sigma_l^2 d_X}}{\log^{d_X+1} \left(\frac{nm(U_X \bar{L}_T)^2}{\sigma_l^2 d_X} \right)}.$$

Hence,

$$\delta_{n, \mathcal{G}_\varphi^+} \lesssim \delta_{n, \tilde{\mathcal{G}}_\varphi^+} \asymp \frac{1}{\sqrt{n}} \cdot \sqrt{d_Z \log^{d_Z+1}(n/d_Z) \vee m d_X \log^{d_X+1} \left(\frac{mn}{\sigma_l^2 d_X} \right)}.$$

The above derivation applies equally to $\mathcal{G}_{\bar{\varphi}}^-, \mathcal{G}_\varphi^+, \mathcal{G}_{\bar{\varphi}}^-$ since φ and $\bar{\varphi}$, $[f]^+$ and $[f]^-$ share the same Lipschitz constant. Similarly, we can bound $\delta_{n, \mathcal{G}_{\bar{\varphi}}^-}$, $\delta_{n, \mathcal{G}_\varphi^+}$, and $\delta_{n, \mathcal{G}_{\bar{\varphi}}^-}$ in the same manner. Therefore,

$$\delta_{n, \mathcal{G}_{\bar{\varphi}}^-}, \delta_{n, \mathcal{G}_\varphi^+}, \delta_{n, \mathcal{G}_{\bar{\varphi}}^-}, \delta_{n, \mathcal{G}_\varphi^+} \lesssim \frac{1}{\sqrt{n}} \cdot \sqrt{d_Z \log^{d_Z+1}(n/d_Z) \vee m d_X \log^{d_X+1} \left(\frac{mn}{\sigma_l^2 d_X} \right)}.$$

□

D.2 Proof of Theorem 4.5

Lemma D.3. *Let $\tilde{\mathbb{1}}\{a < b\}$ be the smoothed indicator function defined by*

$$\tilde{\mathbb{1}}\{a < b\} = \frac{1}{2} \left(1 + \operatorname{erf} \left(\frac{b-a}{\sqrt{2}r} \right) \right)$$

where $\operatorname{erf}(x)$ is the error function, defined as $\operatorname{erf}(x) = \frac{2}{\sqrt{\pi}} \int_0^x e^{-t^2} dt$, and $r > 0$ is the smoothing parameter. The error between the smoothed indicator function $\tilde{\mathbb{1}}\{a < b\}$ and the actual indicator function $\mathbb{1}\{a < b\}$, integrated over all a , is given by

$$E = \int_{-\infty}^{\infty} |\tilde{\mathbb{1}}\{a < b\} - \mathbb{1}\{a < b\}| da = \sqrt{\frac{\pi}{2}} r.$$

Proof. Let $x = a - b$. Note

$$\tilde{\mathbb{1}}\{a < b\} = \frac{1}{2} \left(1 + \operatorname{erf} \left(\frac{b-a}{\sqrt{2}r} \right) \right) = \Phi \left(\frac{b-a}{r} \right) = \Phi \left(-\frac{x}{r} \right),$$

where Φ is the standard normal CDF and φ its density.

$$E = \int_{-\infty}^{\infty} |\Phi(-x/r) - \mathbb{1}\{x < 0\}| dx = \int_{-\infty}^0 (1 - \Phi(-x/r)) dx + \int_0^{\infty} \Phi(-x/r) dx.$$

By symmetry,

$$E = 2 \int_0^{\infty} \Phi(-x/r) dx = 2r \int_0^{\infty} \Phi(-u) du = 2r \int_0^{\infty} (1 - \Phi(u)) du.$$

Since $1 - \Phi(u) = \int_u^{\infty} \varphi(t) dt$, Fubini gives

$$\int_0^{\infty} (1 - \Phi(u)) du = \int_0^{\infty} \int_u^{\infty} \varphi(t) dt du = \int_0^{\infty} t\varphi(t) dt = \frac{1}{\sqrt{2\pi}}.$$

Therefore $E = 2r \cdot \frac{1}{\sqrt{2\pi}} = r\sqrt{\frac{2}{\pi}}$. □

Lemma D.4. *Let $f(x, b) = \tilde{\mathbb{1}}\{x < b\} = \frac{1}{2} \left(1 + \operatorname{erf}\left(\frac{b-x}{\sqrt{2r}}\right)\right)$, where $\operatorname{erf}(x) = \frac{2}{\sqrt{\pi}} \int_0^x e^{-t^2} dt$ and $r > 0$ is the smoothing parameter. Then $f(x, b)$ is Lipschitz continuous with respect to x with a Lipschitz constant $\frac{1}{\sqrt{2\pi r}}$.*

Proof. Since

$$\left| \frac{\partial}{\partial x} f(x, b) \right| = \left| \frac{1}{2} \frac{\partial}{\partial x} \left(1 + \frac{2}{\sqrt{\pi}} \int_0^{(b-x)/\sqrt{2r}} e^{-t^2} dt \right) \right| = \frac{1}{\sqrt{2\pi r}} e^{-\frac{(b-x)^2}{2r^2}} \leq \frac{1}{\sqrt{2\pi r}},$$

$f(x, b)$ is Lipschitz continuous with respect to x with Lipschitz constant $\frac{1}{\sqrt{2\pi r}}$. □

Proof of Theorem 4.5. For $f \in \mathcal{F}$, $h \in \mathcal{H}$, we denote the function

$$\begin{aligned} \tilde{\psi}(h, f)(X, Z, Y) &= f(Z) \left(\tilde{\mathbb{1}}\{T(h(X), Y) > 0\} - \alpha \right), \\ \psi(h, f)(X, Z, Y) &= f(Z) \left(\mathbb{1}\{T(h(X), Y) > 0\} - \alpha \right), \end{aligned}$$

and assume $\sup_{f \in \mathcal{F}} \|f\|_\infty \leq \bar{C}_\mathcal{F}$ and the density of $T(h(X), Y) \mid Z$, $p_{T \mid Z}$ is upper bounded by \bar{C}_T . Consider

$$\begin{aligned}
\sup_{f \in \mathcal{F}} \left\{ P\tilde{\psi}(h, f) - P\psi(h, f) \right\} &= \sup_{f \in \mathcal{F}} \mathbb{E} \left[f(Z) \left(\tilde{\mathbb{1}}\{T(h(X), Y) > 0\} - \mathbb{1}\{T(h(X), Y) > 0\} \right) \right] \\
&\leq \sup_{f \in \mathcal{F}} \|f\|_\infty \mathbb{E} \left[\left| \tilde{\mathbb{1}}\{T(h(X), Y) > 0\} - \mathbb{1}\{T(h(X), Y) > 0\} \right| \right] \\
&\leq \bar{C}_\mathcal{F} \mathbb{E}_Z \left[\mathbb{E} \left[\left| \mathbb{1}\{T(h(X), Y) > 0\} - \tilde{\mathbb{1}}\{T(h(X), Y) > 0\} \right| \mid Z \right] \right] \\
&\leq \sqrt{\frac{2}{\pi}} \bar{C}_\mathcal{F} \bar{C}_T r, \tag{D.14}
\end{aligned}$$

where we use Lemma D.3. Recall that $\tilde{\delta}_{n, \mathcal{F}} = \delta_{n, \mathcal{F}_U} + \sqrt{\frac{\log(c_1/\zeta)}{c_2 n}}$ for some positive constants c_1 and c_2 . Since $\tilde{\psi}(h, f)$ is 1-Lipschitz w.r.t. f , using Lemma 14 in Foster and Syrgkanis (2023), we also have

$$\mathbb{P} \left(\forall f \in \mathcal{F}, |(P_n - P)\tilde{\psi}(h^{\text{ora}}, f)| \leq 18 \left(\tilde{\delta}_{n, \mathcal{F}} \|f\|_{L_2} + \left(1 \vee \frac{\|f\|_\mathcal{F}}{\sqrt{U}} \right) \tilde{\delta}_{n, \mathcal{F}}^2 \right) \right) \geq 1 - \zeta. \tag{D.15}$$

Define $\tilde{\Psi}_\gamma(h, f) = P_n \tilde{\psi}(h, f) - P_n f^2 - \gamma \|f\|_\mathcal{F}^2$ for any $h \in \mathcal{H}$, $f \in \mathcal{F}$ and recall that $\Psi_\lambda(h, f) = P\psi(h, f) - \lambda P f^2$. Since $\tilde{h} = \arg \min_{h \in \mathcal{H}} \max_{f \in \mathcal{F}} \tilde{\Psi}_\gamma(h, f)$, by the optimality of \hat{h} ,

$$\sup_{f \in \mathcal{F}} \tilde{\Psi}_\gamma(\tilde{h}, f) \leq \sup_{f \in \mathcal{F}} \tilde{\Psi}_\gamma(h^{\text{ora}}, f). \tag{D.16}$$

Combining (C.5) and (D.15), we can get w.p. $1 - 2\zeta$:

$$\begin{aligned}
\sup_{f \in \mathcal{F}} \tilde{\Psi}_\gamma(h^{\text{ora}}, f) &= \sup_{f \in \mathcal{F}} \left\{ P_n \tilde{\psi}(h^{\text{ora}}, f) - P_n f^2 - \gamma \|f\|_\mathcal{F}^2 \right\} \\
&\leq \sup_{f \in \mathcal{F}} \left\{ P_n \tilde{\psi}(h^{\text{ora}}, f) - \left(\gamma \|f\|_\mathcal{F}^2 + \frac{1}{4} \|f\|_{L_2}^2 - \frac{\tilde{\delta}_{n, \mathcal{F}}^2}{2} \right) \right\} \\
&\leq \sup_{f \in \mathcal{F}} \left\{ P\tilde{\psi}(h^{\text{ora}}, f) + 18 \left(\tilde{\delta}_{n, \mathcal{F}} \|f\|_{L_2} + \left(1 \vee \frac{\|f\|_\mathcal{F}}{\sqrt{U}} \right) \tilde{\delta}_{n, \mathcal{F}}^2 \right) - \left(\gamma \|f\|_\mathcal{F}^2 + \frac{1}{4} \|f\|_{L_2}^2 - \frac{\tilde{\delta}_{n, \mathcal{F}}^2}{2} \right) \right\}
\end{aligned}$$

$$\begin{aligned}
&\stackrel{(i)}{\leq} \sup_{f \in \mathcal{F}} \left\{ P\psi(h^{\text{ora}}, f) - \frac{1}{8}Pf^2 \right\} + \sup_{f \in \mathcal{F}} \left\{ 36\tilde{\delta}_{n,\mathcal{F}}\|f\|_{L_2} - \frac{1}{8}\|f\|_{L_2}^2 \right\} + 18\tilde{\delta}_{n,\mathcal{F}}^2 + \frac{\tilde{\delta}_{n,\mathcal{F}}^2}{2} \\
&+ \sup_{f \in \mathcal{F}} \left\{ P\tilde{\psi}(h^{\text{ora}}, f) - P\psi(h^{\text{ora}}, f) \right\} \\
&\leq \sup_{f \in \mathcal{F}} \Psi_{\frac{1}{8}}(h^{\text{ora}}, f) + 2 \cdot 36^2\tilde{\delta}_{n,\mathcal{F}}^2 + 18\tilde{\delta}_{n,\mathcal{F}}^2 + \frac{\tilde{\delta}_{n,\mathcal{F}}^2}{2} + \sqrt{\frac{2}{\pi}}\bar{C}_{\mathcal{F}}\bar{C}_{Tr}, \tag{D.17}
\end{aligned}$$

where (i) we used the assumption $\tilde{\delta}_{n,\mathcal{F}}\|f\|_{\mathcal{F}} \leq \sqrt{\frac{U}{2}}\|f\|_{L_2}$ and $\gamma \geq 0$. In addition, we also have the lower bound

$$\begin{aligned}
\sup_{f \in \mathcal{F}} \tilde{\Psi}_{\gamma}(\tilde{h}, f) &= \sup_{f \in \mathcal{F}} \left\{ P_n\tilde{\psi}(\tilde{h}, f) - P_n\tilde{\psi}(h^{\text{ora}}, f) + P_n\tilde{\psi}(h^{\text{ora}}, f) - P_nf^2 - \gamma\|f\|_{\mathcal{F}}^2 \right\} \\
&\geq \sup_{f \in \mathcal{F}} \left\{ P_n\tilde{\psi}(\tilde{h}, f) - P_n\tilde{\psi}(h^{\text{ora}}, f) - 2(P_nf^2 + \gamma\|f\|_{\mathcal{F}}^2) \right\} \\
&\quad + \inf_{f \in \mathcal{F}} \left\{ P_n\tilde{\psi}(h^{\text{ora}}, f) + P_nf^2 + \gamma\|f\|_{\mathcal{F}}^2 \right\} \\
&= \sup_{f \in \mathcal{F}} \left\{ P_n\tilde{\psi}(\tilde{h}, f) - P_n\tilde{\psi}(h^{\text{ora}}, f) - 2(P_nf^2 + \gamma\|f\|_{\mathcal{F}}^2) \right\} - \sup_{f \in \mathcal{F}} \tilde{\Psi}_{\gamma}(h^{\text{ora}}, f),
\end{aligned}$$

where we used the fact that \mathcal{F} is symmetric. It follows that w.p. $1 - 2\zeta$:

$$\begin{aligned}
&\sup_{f \in \mathcal{F}} \left\{ P_n\tilde{\psi}(\tilde{h}, f) - P_n\tilde{\psi}(h^{\text{ora}}, f) - 2(P_nf^2 + \gamma\|f\|_{\mathcal{F}}^2) \right\} \\
&\leq \left\{ \sup_{f \in \mathcal{F}} \tilde{\Psi}_{\gamma}(\tilde{h}, f) + \sup_{f \in \mathcal{F}} \tilde{\Psi}_{\gamma}(h^{\text{ora}}, f) \right\} \\
&\stackrel{(i)}{\leq} 2 \sup_{f \in \mathcal{F}} \tilde{\Psi}_{\gamma}(h^{\text{ora}}, f) \\
&\stackrel{(ii)}{\leq} 2 \sup_{f \in \mathcal{F}} \Psi_{\frac{1}{8}}(h^{\text{ora}}, f) + 4 \cdot 36^2\tilde{\delta}_{n,\mathcal{F}}^2 + 36\tilde{\delta}_{n,\mathcal{F}}^2 + \tilde{\delta}_{n,\mathcal{F}}^2 + 2\sqrt{\frac{2}{\pi}}\bar{C}_{\mathcal{F}}\bar{C}_{Tr} \\
&\stackrel{(iii)}{\leq} 4\epsilon^2 + 4 \cdot 36^2\tilde{\delta}_{n,\mathcal{F}}^2 + 36\tilde{\delta}_{n,\mathcal{F}}^2 + \tilde{\delta}_{n,\mathcal{F}}^2 + 2\sqrt{\frac{2}{\pi}}\bar{C}_{\mathcal{F}}\bar{C}_{Tr}, \tag{D.18}
\end{aligned}$$

where (i) holds due to (D.16), (ii) holds due to (D.17) and (iii) holds due to Lemma C.1 and the assumption $\mathbb{E}[(\alpha(Z; h^{\text{ora}}) - \alpha)^2] \leq \epsilon^2$.

Define $\tilde{\alpha}(Z; h) = \mathbb{E}[\tilde{\mathbb{1}}\{T(h(X), Y) > 0\} | Z]$ and note that

$$\begin{aligned}
& \|(\alpha(Z; h) - \tilde{\alpha}(Z; h)) - (\alpha(Z; h^{\text{ora}}) - \tilde{\alpha}(Z; h^{\text{ora}}))\|_{L_2} \\
& \leq \|\alpha(Z; h) - \tilde{\alpha}(Z; h)\|_{L_2} + \|\alpha(Z; h^{\text{ora}}) - \tilde{\alpha}(Z; h^{\text{ora}})\|_{L_2} \\
& \leq \left(\mathbb{E} \left[\left(\mathbb{E} \left[\tilde{\mathbb{1}}\{T(h(X), Y) > 0\} - \mathbb{1}\{T(h(X), Y) > 0\} \mid Z \right]^2 \right) \right] \right)^{1/2} \\
& + \left(\mathbb{E} \left[\left(\mathbb{E} \left[\tilde{\mathbb{1}}\{T(h^{\text{ora}}(X), Y) > 0\} - \mathbb{1}\{T(h^{\text{ora}}(X), Y) > 0\} \mid Z \right]^2 \right) \right] \right)^{1/2} \\
& \leq 2\sqrt{\frac{2}{\pi}} \bar{C}_{Tr}.
\end{aligned}$$

Recall that

$$f_h = \arg \min_{f \in \mathcal{F}_U} \mathbb{E} \left[(f(Z) - (\alpha(Z; h^{\text{ora}}) - \alpha(Z; h)))^2 \right],$$

and we assume that $\mathbb{E}[(f_h(X) - (\alpha(X; h^{\text{ora}}) - \alpha(X; h)))^2] \leq \eta^2$ holds for any $h \in \mathcal{H}$. Notice that

$$\begin{aligned}
P\tilde{\psi}(h, f_h) - P\tilde{\psi}(h^{\text{ora}}, f_h) &= \mathbb{E}[f_h(Z)(\tilde{\alpha}(Z; h) - \tilde{\alpha}(Z; h^{\text{ora}}))] \\
&= \mathbb{E}[f_h^2(Z)] + \mathbb{E}[f_h(Z)(\alpha(Z; h) - \alpha(Z; h^{\text{ora}}) - f_h(Z))] \\
&+ \mathbb{E}[f_h(Z)(\{\tilde{\alpha}(Z; h) - \tilde{\alpha}(Z; h^{\text{ora}})\} - \{\alpha(Z; h) - \alpha(Z; h^{\text{ora}})\})] \\
&\geq \|f_h\|_{L_2}^2 - \|f_h\|_{L_2} \|\alpha(Z; h) - \alpha(Z; h^{\text{ora}}) - f_h(Z)\|_{L_2} \\
&- \|f_h\|_{L_2} \|\{\tilde{\alpha}(Z; h) - \tilde{\alpha}(Z; h^{\text{ora}})\} - \{\alpha(Z; h) - \alpha(Z; h^{\text{ora}})\}\|_{L_2} \\
&\geq \|f_h\|_{L_2}^2 - \|f_h\|_{L_2} (\eta + 2\sqrt{\frac{2}{\pi}} \bar{C}_{Tr}).
\end{aligned}$$

Note that

$$\begin{aligned}
\|\alpha(Z; h) - \alpha(Z; h^{\text{ora}})\|_{L_2} &\leq \|\tilde{\alpha}(Z; h) - \tilde{\alpha}(Z; h^{\text{ora}})\|_{L_2} \\
&+ \|(\alpha(Z; h) - \tilde{\alpha}(Z; h)) - (\alpha(Z; h^{\text{ora}}) - \tilde{\alpha}(Z; h^{\text{ora}}))\|_{L_2}
\end{aligned}$$

$$\leq \|\tilde{\alpha}(Z; h) - \tilde{\alpha}(Z; h^{\text{ora}})\|_{L_2} + 2\sqrt{\frac{2}{\pi}}\bar{C}_T r.$$

Therefore, by symmetry we have

$$\left| \|\alpha(Z; h) - \alpha(Z; h^{\text{ora}})\|_{L_2} - \|\tilde{\alpha}(Z; h) - \tilde{\alpha}(Z; h^{\text{ora}})\|_{L_2} \right| \leq 2\sqrt{\frac{2}{\pi}}Mr. \quad (\text{D.19})$$

Then we have

$$\begin{aligned} \frac{P\tilde{\psi}(h, f_h) - P\tilde{\psi}(h^{\text{ora}}, f_h)}{\|f_h\|_{L_2}} &\geq \|f_h\|_{L_2} - \eta - 2\sqrt{\frac{2}{\pi}}\bar{C}_T r \\ &\geq \|\alpha(Z; h) - \alpha(Z; h^{\text{ora}})\|_{L_2} - 2\sqrt{\frac{2}{\pi}}\bar{C}_T r - 2\eta, \end{aligned} \quad (\text{D.20})$$

where the last inequity we use (D.19). Let $r \in [0, 1]$, then $rf_{\tilde{h}} \in \mathcal{F}_U$ since \mathcal{F}_U is star-shaped.

Recall that $v^2(h, h^{\text{ora}}) = \mathbb{E}[|\alpha(Z; h) - \alpha(Z; h^{\text{ora}})|^2]$ and define

$$\tilde{\mathcal{G}} = \left\{ \tilde{\psi}(h, f_h) - \tilde{\psi}(h^{\text{ora}}, f_h) : h \in \mathcal{H} \right\}.$$

By the optimality of f_h , $\|f_h - (\alpha(X; h^{\text{ora}}) - \alpha(X; h))\|_{L_2} \leq \|0 - (\alpha(X; h^{\text{ora}}) - \alpha(X; h))\|_{L_2} = v(h, h^{\text{ora}})$, for all $h \in \mathcal{H}$. Thus

$$\|\tilde{\psi}(h, f_h) - \tilde{\psi}(h^{\text{ora}}, f_h)\|_{L_2} \leq \|f_h\|_{L_2} \leq 2v(h, h^{\text{ora}}). \quad (\text{D.21})$$

Then we have w.p. $1 - 2\zeta$:

$$\begin{aligned} &\sup_{f \in \mathcal{F}} \left\{ P_n \psi(\tilde{h}, f) - P_n \psi(h^{\text{ora}}, f) - 2 \left(P_n f^2 + \gamma \|f\|_{\mathcal{F}}^2 \right) \right\} \\ &\geq r P_n \tilde{\psi}(\tilde{h}, f_{\tilde{h}}) - r P_n \tilde{\psi}(h^{\text{ora}}, f_{\tilde{h}}) - 2r^2 \left(P_n f_{\tilde{h}}^2 + \gamma \|f_{\tilde{h}}\|_{\mathcal{F}}^2 \right) \\ &\stackrel{(i)}{\geq} r P_n \tilde{\psi}(\tilde{h}, f_{\tilde{h}}) - r P_n \tilde{\psi}(h^{\text{ora}}, f_{\tilde{h}}) - 2r^2 \left(\gamma \|f_{\tilde{h}}\|_{\mathcal{F}}^2 + \frac{7}{4} \|f_{\tilde{h}}\|_{L_2}^2 + \frac{\tilde{\delta}_{n, \mathcal{F}}^2}{2} \right) \end{aligned}$$

$$\begin{aligned}
&\stackrel{\text{(ii)}}{\geq} r \left(P\tilde{\psi}(\tilde{h}, f_{\tilde{h}}) - P\tilde{\psi}(h^{\text{ora}}, f_{\tilde{h}}) - v(\tilde{h}, h^{\text{ora}}) \left(4\delta_{n,\tilde{\mathcal{G}}} + 2\sqrt{\frac{2\log(R_n/\zeta)}{n}} \right) \right) \\
&\quad - \frac{r \log(R_n/\zeta)}{3n} - 2r^2 \left(\gamma \|f_{\tilde{h}}\|_{\mathcal{F}}^2 + \frac{7}{4} \|f_{\tilde{h}}\|_{L_2}^2 + \frac{\tilde{\delta}_{n,\mathcal{F}}^2}{2} \right) \\
&\stackrel{\text{(iii)}}{\geq} r \left((v(\tilde{h}, h^{\text{ora}}) - 2\sqrt{\frac{2}{\pi}} \bar{C}_T r - 2\eta) \|f_{\tilde{h}}\|_{L_2} - v(\tilde{h}, h^{\text{ora}}) \left(4\delta_{n,\tilde{\mathcal{G}}} + 2\sqrt{\frac{2\log(R_n/\zeta)}{n}} \right) \right) \\
&\quad - \frac{r \log(R_n/\zeta)}{3n} - 2r^2 \left(\gamma \|f_{\tilde{h}}\|_{\mathcal{F}}^2 + \frac{7}{4} \|f_{\tilde{h}}\|_{L_2}^2 + \frac{\tilde{\delta}_{n,\mathcal{F}}^2}{2} \right), \tag{D.22}
\end{aligned}$$

where (i) use (C.6); (ii) holds due to Lemma E.7 and (D.21); and (iii) holds due to (D.20).

$R_n = \lceil \log_2(1/\delta_{n,\tilde{\mathcal{G}}}) \rceil$. If $4\delta_{n,\tilde{\mathcal{G}}} + 2\sqrt{\frac{2\log(R_n/\zeta)}{n}} \geq \|f_{\tilde{h}}\|_{L_2}/2$, we have

$$v(\tilde{h}, h^{\text{ora}}) \leq \|f_{\tilde{h}}\|_{L_2} + \eta + 2\sqrt{\frac{2}{\pi}} \bar{C}_T r \lesssim \delta_{n,\tilde{\mathcal{G}}} + \sqrt{\frac{\log(R_n/\zeta)}{n}} + \eta + r.$$

Otherwise, i.e. $4\delta_{n,\tilde{\mathcal{G}}} + 2\sqrt{\frac{2\log(R_n/\zeta)}{n}} \leq \|f_{\tilde{h}}\|_{L_2}/2$, using the upper bound in (D.18), by (D.22)

w.p. $1 - 4\zeta$ we get

$$\begin{aligned}
v(\tilde{h}, h^{\text{ora}}) &\leq \frac{2}{r \|f_{\tilde{h}}\|_{L_2}} \left(4\epsilon^2 + 4 \cdot 36^2 \tilde{\delta}_{n,\mathcal{F}}^2 + 36\tilde{\delta}_{n,\mathcal{F}}^2 + \tilde{\delta}_{n,\mathcal{F}}^2 + 2\sqrt{\frac{2}{\pi}} \bar{C}_{\mathcal{F}} \bar{C}_T r \right) \\
&\quad + \frac{2 \log(R_n/\zeta)}{3n \|f_{\tilde{h}}\|_{L_2}} + \frac{4r}{\|f_{\tilde{h}}\|_{L_2}} \left(\gamma \|f_{\tilde{h}}\|_{\mathcal{F}}^2 + \frac{7}{4} \|f_{\tilde{h}}\|_{L_2}^2 + \frac{\tilde{\delta}_{n,\mathcal{F}}^2}{2} \right) + 2\sqrt{\frac{2}{\pi}} \bar{C}_T r + 2\eta.
\end{aligned}$$

If $\|f_{\tilde{h}}\|_{L_2} \geq \tilde{\delta}_{n,\mathcal{F}} \geq \sqrt{\frac{\log(c_1/\zeta)}{c_2 n}}$, choosing $r = \max\{\epsilon, \tilde{\delta}_{n,\mathcal{F}}\}/\|f_{\tilde{h}}\|_{L_2}$, by $\gamma \|f\|_{\mathcal{F}}^2 \leq \|f\|_{L_2}^2$ for all $f \in \mathcal{F}$, we have

$$v(\tilde{h}, h^{\text{ora}}) \lesssim \epsilon + \tilde{\delta}_{n,\mathcal{F}} + \eta + \sqrt{\frac{\log(R_n/\zeta)}{n}} + \frac{\nu \|h^{\text{ora}}\|_{\mathcal{H}}^2}{\tilde{\delta}_{n,\mathcal{F}}} + (1 + \tilde{\delta}_{n,\mathcal{F}}) \frac{r}{\tilde{\delta}_{n,\mathcal{F}}}.$$

Otherwise, i.e. $\|f_{\tilde{h}}\|_{L_2} \leq \tilde{\delta}_{n,\mathcal{F}}$, we have

$$v(\tilde{h}, h^{\text{ora}}) \leq \|f_{\tilde{h}}\|_{L_2} + \eta + 2\sqrt{\frac{2}{\pi}} \bar{C}_T r \lesssim \tilde{\delta}_{n,\mathcal{F}} + \eta + r.$$

Combining the relations above, we can conclude that

$$v(\tilde{h}, h^{\text{ora}}) \lesssim \epsilon + \delta_{n, \mathcal{F}_U} + \delta_{n, \tilde{\mathcal{G}}} + \eta + \frac{\nu \|h^{\text{ora}}\|_{\mathcal{H}}^2}{\tilde{\delta}_{n, \mathcal{F}}} + \frac{r}{\tilde{\delta}_{n, \mathcal{F}}} + \sqrt{\frac{\log(R_n/\zeta)}{n}},$$

where we used the definition of $\tilde{\delta}_{n, \mathcal{F}}$.

□

E Auxiliary Lemmas

Lemma E.1. *Let $\log t + d \log \log t = L_n$ be a equation w.r.t. t with $d > 0$ and $L_n \rightarrow \infty$ as $n \rightarrow \infty$. Then the solution t^* of the equation satisfies $t^* \asymp \exp\{L_n - d \log L_n\}$.*

Proof. Consider $\log t = L - d \log L + \Delta$ and we prove $\Delta = o(1)$. Using $\log(1+u) = u + O(u^2)$, we have

$$\begin{aligned} & (L - d \log L + \Delta) + d \log(L - d \log L + \Delta) = L \\ \iff & (L - d \log L + \Delta) + d \log L + d \log \left(1 - d \frac{\log L}{L} + \frac{\Delta}{L}\right) = L \\ \iff & \Delta + d \left(-\frac{d \log L}{L} + O\left(\frac{(\log L)^2}{L^2}\right) + \frac{\Delta}{L}\right) = 0 \\ \iff & \Delta \left(1 + \frac{d}{L}\right) = d^2 \frac{\log L}{L} + O\left(\frac{(\log L)^2}{L^2}\right). \end{aligned} \tag{E.1}$$

As $n \rightarrow \infty$, $L \rightarrow \infty$, the right hand side of (E.1) converge to 0, therefore $\Delta = o(1)$. Therefore, solution $t^* \asymp \exp\{L_n - d \log L_n\}$. □

Lemma E.2. *Let \mathcal{F} be a function class with ρ -covering number $N(\rho, \mathcal{F}, \|\cdot\|_{L_2})$, and g be any measurable function. Let $\mathcal{F} - g := \{f - g : f \in \mathcal{F}\}$, then for any $\rho > 0$, $N(\rho, \mathcal{F}, \|\cdot\|_{L_2}) = N(\rho, \mathcal{F} - g, \|\cdot\|_{L_2})$.*

Proof. Let $\{f_\ell\}_{\ell=1}^{N(\rho, \mathcal{F}, \|\cdot\|_{L_2})}$ be a ρ -covering of \mathcal{F} under the L_2 norm. For any $h \in \mathcal{F} - g$,

there exists $f \in \mathcal{F}$ such that $h = f - g$. By the definition of the covering number, there exists some f_{ℓ_1} satisfying

$$\|(f - g) - (f_{\ell_1} - g)\|_{L_2} = \|f - f_{\ell_1}\|_{L_2} \leq \rho.$$

Hence, the collection $\{f_\ell - g\}_{\ell=1}^{N(\rho, \mathcal{F}, \|\cdot\|_{L_2})}$ forms a ρ -covering of $\mathcal{F} - g$, which implies $N(\rho, \mathcal{F} - g, \|\cdot\|_{L_2}) \leq N(\rho, \mathcal{F}, \|\cdot\|_{L_2})$. Conversely, observe that $\mathcal{F} = (\mathcal{F} - g) + g$. Applying the above argument with $-g$ in place of g yields $N(\rho, \mathcal{F}, \|\cdot\|_{L_2}) \leq N(\rho, \mathcal{F} - g, \|\cdot\|_{L_2})$. Combining the two inequalities completes the proof. \square

Lemma E.3. *Let \mathcal{F} be a function class with ρ -covering number $N(\rho, \mathcal{F}, \|\cdot\|_{L_2})$, and φ be a L -Lipschitz function. Let $\varphi \circ \mathcal{F} := \{\varphi \circ f : f \in \mathcal{F}\}$, then for any $\rho > 0$, $N(\rho, \varphi \circ \mathcal{F}, \|\cdot\|_{L_2}) \leq N(\rho/L, \mathcal{F}, \|\cdot\|_{L_2})$.*

Proof. Let $\{f_\ell\}_{\ell=1}^{N(\rho/L, \mathcal{F}, \|\cdot\|_{L_2})}$ be a ρ/L -covering of \mathcal{F} under the L_2 norm. By the definition of the covering number, there exists some f_{ℓ_1} satisfying $\|f - f_{\ell_1}\|_{L_2} \leq \rho/L$. For any $\varphi \circ f \in \varphi \circ \mathcal{F}$,

$$\begin{aligned} \|\varphi(f) - \varphi(f_{\ell_1})\|_{L_2}^2 &= \int (\varphi(f)) - \varphi(f_{\ell_1})^2 dP \\ &\leq L^2 \int (f - f_{\ell_1})^2 dP = L^2 \|f - f_{\ell_1}\|_{L_2}^2 \leq \rho^2 \end{aligned}$$

Hence, the collection $\{\varphi \circ f_\ell\}_{\ell=1}^{N(\rho/L, \mathcal{F}, \|\cdot\|_{L_2})}$ forms a ρ -covering of $\varphi \circ \mathcal{F}$, which implies $N(\rho, \varphi \circ \mathcal{F}, \|\cdot\|_{L_2}) \leq N(\rho/L, \mathcal{F}, \|\cdot\|_{L_2})$. \square

Lemma E.4. *Let \mathcal{F} be a function class with ρ -covering number $N(\rho, \mathcal{F}, \|\cdot\|_{L_2})$, and let $\mathfrak{F} = \{\mathbf{f} = (f_1, \dots, f_m)^\top : f_1, \dots, f_m \in \mathcal{F}\}$, then for any $\rho > 0$, $N(\rho, \mathfrak{F}, \|\cdot\|_{L_2(P, \mathbb{R}^m)}) \leq \left(N(\rho/\sqrt{m}, \mathcal{F}, \|\cdot\|_{L_2(P, \mathbb{R})})\right)^m$.*

Proof. Let $\{f_\ell\}_{\ell=1}^{N(\rho/\sqrt{m}, \mathcal{F}, \|\cdot\|_{L_2})}$ be a ρ/\sqrt{m} -covering of \mathcal{F} under the L_2 norm. By the definition

of the covering number, there exists some f_{ℓ_i} satisfying $\|f - f_{\ell_i}\|_{L_2} \leq \rho/\sqrt{m}$. Let

$$\bar{\mathfrak{F}} = \{(f_{\ell_1}, \dots, f_{\ell_m})^\top : \ell_1, \dots, \ell_m \in [N(\rho/\sqrt{m}, \mathcal{F}, \|\cdot\|_{L_2})]\}$$

For any $\mathbf{f} \in \mathfrak{F}$, there exist some $\bar{\mathbf{f}} \in \bar{\mathfrak{F}}$ such that

$$\|\mathbf{f} - \bar{\mathbf{f}}\|_{L_2}^2 = \int \sum_{i=1}^m (f_i - \bar{f}_{\ell_i})^2 dP \leq m \cdot \frac{\rho^2}{m} = \rho^2$$

Hence, the collection $\bar{\mathfrak{F}}$ forms a ρ -covering of \mathfrak{F} , which implies $N(\rho, \mathfrak{F}, \|\cdot\|_{L_2}) \leq |\bar{\mathfrak{F}}| \leq (N(\rho/\sqrt{m}, \mathcal{F}, \|\cdot\|_{L_2}))^m$. \square

Lemma E.5. *Let \mathcal{F}, \mathcal{G} be two function classes with the ρ -covering number $N(\rho, \mathcal{F}, \|\cdot\|_{L_2})$ and $N(\rho, \mathcal{G}, \|\cdot\|_{L_2})$, respectively. In addition, $\sup_{f \in \mathcal{F}} \|f\|_\infty \leq B_{\mathcal{F}}$ and $\sup_{g \in \mathcal{G}} \|g\|_\infty \leq B_{\mathcal{G}}$. Then the product function class $\mathcal{M} = \{fg : f \in \mathcal{F}, g \in \mathcal{G}\}$ satisfies*

$$N(\rho, \mathcal{M}, \|\cdot\|_{L_2}) \leq N(\rho/(2B_{\mathcal{G}}), \mathcal{F}, \|\cdot\|_{L_2}) \cdot N(\rho/(2B_{\mathcal{F}}), \mathcal{G}, \|\cdot\|_{L_2}).$$

Proof. We first notice that for any $f_1, f_2 \in \mathcal{F}$ and $g_1, g_2 \in \mathcal{G}$, it holds that

$$\begin{aligned} \|f_1 g_1 - f_2 g_2\|_{L_2} &\leq \|(f_1 - f_2)g_1\|_{L_2} + \|(g_1 - g_2)f_2\|_{L_2} \\ &\leq B_{\mathcal{G}}\|f_1 - f_2\|_{L_2} + B_{\mathcal{F}}\|g_1 - g_2\|_{L_2}. \end{aligned}$$

Let $\{f_\ell\}_{\ell=1}^{N(\rho/(2B_{\mathcal{G}}), \mathcal{F}, \|\cdot\|_{L_2})}$ and $\{g_\ell\}_{\ell=1}^{N(\rho/(2B_{\mathcal{F}}), \mathcal{G}, \|\cdot\|_{L_2})}$ be $\rho/(2B_{\mathcal{G}})$ -covering of \mathcal{F} and $\rho/(2B_{\mathcal{F}})$ -covering \mathcal{G} , respectively. It means that for any $f \in \mathcal{F}$ and $g \in \mathcal{G}$, there exist some f_{ℓ_1} and g_{ℓ_2} such that $\|f - f_{\ell_1}\|_{L_2} \leq \rho/(2B_{\mathcal{G}})$ and $\|g - g_{\ell_2}\|_{L_2} \leq \rho/(2B_{\mathcal{F}})$. Hence we have

$$\|fg - f_{\ell_1}g_{\ell_2}\|_{L_2} \leq \rho.$$

Therefore, $\{f_{\ell_1 g_{\ell_2}} : \ell_1 \in [N(\rho/(2B_{\mathcal{G}}), \mathcal{F}, \|\cdot\|_{L_2})], \ell_2 \in [N(\rho/(2B_{\mathcal{F}}), \mathcal{G}, \|\cdot\|_{L_2})]\}$ is a ρ -covering for \mathcal{M} , then the conclusion follows immediately. \square

Lemma E.6 (Theorem 14.1, [Wainwright \(2019\)](#)). *Given a star-shaped function class \mathcal{F} , suppose $\|f\|_{\infty} \leq 1$ holds for any $f \in \mathcal{F}$. Let δ_n be any positive solution of the inequality*

$$\mathbb{E} \left[\sup_{f \in \mathcal{F}, \|f\|_{L_2} \leq \delta} \left| \frac{1}{n} \varepsilon_i f(X_i) \right| \right] \leq \delta^2,$$

where $\{\varepsilon_i\}_{i=1}^n$ are i.i.d. Rademacher variables. For any $t \geq \delta_n$, we have

$$|(P_n - P)f^2| \leq \frac{1}{2} P f^2 + \frac{t^2}{2}, \quad \forall f \in \mathcal{F},$$

with probability at least $1 - c_1 e^{-c_2 n \delta_n^2 / b^2}$. If in addition $n \delta_n^2 \geq \frac{2}{c_2} \log(4 \log(1/\delta_n))$, then

$$|P_n f^2 - P f^2| \leq c_0 \delta_n, \quad \forall f \in \mathcal{F},$$

with probability at least $1 - c'_1 e^{-c'_2 n \delta_n^2 / b^2}$.

Lemma E.7. *Let \mathcal{G} be a star-shaped function class. Denote the critical radius of \mathcal{G} as $\delta_{n,\mathcal{G}}$. If $\sup_{g \in \mathcal{G}} \|g\|_{\infty} \leq 1$, with probability at least $1 - \zeta$, we have*

$$|(P_n - P)g| \leq \|g\|_{L_2} \left(2\delta_{n,\mathcal{G}} + \sqrt{\frac{2 \log(R_n/\zeta)}{n}} \right) + \frac{\log(R_n/\zeta)}{3n}$$

simultaneously holds for any $g \in \mathcal{G}$, where $R_n = \lceil \log_2(1/\delta_{n,\mathcal{G}}) \rceil$.

Proof. Define the following function space

$$\mathcal{G}(r) = \{g \in \mathcal{G} : \|g\|_{L_2} \leq r\},$$

where $r > 0$. Denote the random variable $Z_n(r) = \sup_{g \in \mathcal{G}(r)} |(P_n - P)g|$. Applying the

functional version of Bennett's inequality (e.g., Theorem 7.3 in [Bousquet \(2003\)](#)), we have

$$\mathbb{P} \left\{ Z_n(r) \geq \mathbb{E}[Z_n(r)] + r\sqrt{\frac{2x}{n}} + \frac{x}{3n} \right\} \leq e^{-x}. \quad (\text{E.2})$$

Let $\varepsilon_i \sim \text{Uniform}\{\pm 1\}$ be i.i.d Rademacher variables. Using the standard symmetrization technique (e.g., Lemma A.5 in [Bartlett et al. \(2005\)](#)), for any $r \geq \delta_{n,\mathcal{G}}$ we have

$$\mathbb{E}[Z_n(r)] \leq 2 \mathbb{E} \left[\sup_{g \in \mathcal{G}(r)} \left| \frac{1}{n} \sum_{i=1}^n \varepsilon_i g(X_i) \right| \right] = 2\overline{\mathcal{R}}(r; \mathcal{G}) \leq 2r\delta_{n,\mathcal{G}}, \quad (\text{E.3})$$

where we used the fact $\overline{\mathcal{R}}(r; \mathcal{G})/r$ is non-increasing and the definition of critical radius, then for any $r \geq \delta_{n,\mathcal{G}}$,

$$\frac{\overline{\mathcal{R}}(r; \mathcal{G})}{r} \leq \frac{\overline{\mathcal{R}}(\delta_{n,\mathcal{G}}; \mathcal{G})}{\delta_{n,\mathcal{G}}} \leq \delta_{n,\mathcal{G}}.$$

Substituting (E.3) into (E.2), we can have

$$\mathbb{P} \left\{ Z_n(r) \geq 2r\delta_{n,\mathcal{G}} + r\sqrt{\frac{2x}{n}} + \frac{x}{3n} \right\} \leq e^{-x}. \quad (\text{E.4})$$

Next, we employ the peeling argument by defining $\mathcal{G}^{(0)} = \{g \in \mathcal{G} : \|g - g^*\|_{L_2} \leq \delta_{n,\mathcal{G}}\}$ and

$$\mathcal{G}^{(k)} = \left\{ g \in \mathcal{G} : 2^{k-1}\delta_{n,\mathcal{G}}^2 \leq \|g\|_{L_2} \leq 2^k\delta_{n,\mathcal{G}} \right\}, k \geq 1.$$

Let $R_n = \lceil \log_2(1/\delta_{n,\mathcal{G}}) \rceil + 1$, then it holds that $\cup_{k=0}^{R_n} \mathcal{G}^{(k)} = \mathcal{G}$. Letting $r_k = 2^k\delta_{n,\mathcal{G}}$ and using (E.4), we can guarantee that

$$\mathbb{P} \left\{ \forall k \in [K], Z_n(r_k) \geq 2r_k\delta_{n,\mathcal{G}} + r_k\sqrt{\frac{2x}{n}} + \frac{x}{3n} \right\} \leq R_n e^{-x}.$$

And we also have

$$\mathbb{P} \left\{ Z_n(r_0) \geq 2\delta_{n,\mathcal{G}} + \delta_{n,\mathcal{G}} \sqrt{\frac{2x}{n}} + \frac{x}{3n} \right\} \leq e^{-x}.$$

Notice that $g \in \mathcal{G}^{(k)}$ implies that $\|g\|_{L_2} \leq r_k$ for $k \geq 1$ and $g \in \mathcal{G}^{(0)}$ implies that $\|g\|_{L_2} \leq \delta_{n,\mathcal{G}}$.

Hence we can conclude that, for any $g \in \mathcal{G}$ such that $\|g\|_{L_2} \geq \delta_{n,\mathcal{G}}$,

$$\mathbb{P} \left\{ \sup_{g \in \mathcal{G}} |(P_n - P)g| \geq 2\|g\|_{L_2} \delta_{n,\mathcal{G}} + \|g\|_{L_2} \sqrt{\frac{2x}{n}} + \frac{x}{3n} \right\} \leq R_n e^{-x}. \quad (\text{E.5})$$

Taking $x = \log(R_n/\zeta)$ in (E.5) and denoting $v(g, g^*) = \|g - g^*\|_{L_2}$, we can prove that with probability at least $1 - \zeta$,

$$|(P_n - P)g| \leq \|g\|_{L_2} \left(2\delta_{n,\mathcal{G}} + \sqrt{\frac{2 \log(R_n/\zeta)}{n}} \right) + \frac{\log(R_n/\zeta)}{3n},$$

simultaneously holds for any $g \in \mathcal{G}$. □

Lemma E.8. *Let \mathcal{G} be the function class defined in (C.13), $R_n = \lceil \log_2(1/\delta_{n,\mathcal{G}}) \rceil + 1$ and $v(C, C^{\text{ora}}) = \|\alpha(C) - \alpha(C^{\text{ora}})\|_{L_2}$, then with probability at least $1 - \delta$, we have*

$$|(P_n - P)(\psi(C, f_C) - \psi(C^{\text{ora}}, f_C))| \leq v(C, C^{\text{ora}}) \left(4\delta_{n,\mathcal{G}} + 2\sqrt{\frac{2 \log(R_n/\zeta)}{n}} \right) + \frac{\log(R_n/\zeta)}{3n},$$

simultaneously holds for any $C \in \mathfrak{C}$.

Proof. By the definition of f_C in (C.11) and

$$\mathcal{G} = \{(x, z, y) \mapsto f_C(z)(\mathbb{1}\{y \notin C(x)\} - \mathbb{1}\{y \notin C^{\text{ora}}(x)\}) : C \in \mathfrak{C}\},$$

we know $\sup_{g \in \mathcal{G}} \|g\|_{\infty} \leq \sup_{C \in \mathfrak{C}} \|f_C\|_{\infty} \leq 1$. Applying Lemma E.7 on \mathcal{G} , we can prove the conclusion by using the fact $\|g\|_{L_2} \leq \|f_C\|_{L_2} \leq 2v(C, C^{\text{ora}})$ due to the definition

$f_C = \arg \min_{f \in \mathcal{F}} \|f - (\alpha(C) - \alpha(C^{\text{ora}}))\|_{L_2}^2$ and $\|f_C\|_{L_2} \leq \|f - (\alpha(C) - \alpha(C^{\text{ora}}))\|_{L_2} + \|\alpha(C) - \alpha(C^{\text{ora}})\|_{L_2}$. \square

F Additional Synthetic Data Results

F.1 Experiment details of Section 5.1

To obtain a reliable estimate of the MSCE, we set $|\mathcal{D}_{\text{test}}| = 10,000$. The **CC** method [Gibbs et al. \(2025\)](#) is a full conformal procedure that requires recomputation for each test point and therefore cannot be efficiently implemented with matrix operations, resulting in substantial computational cost. In our experiments, its runtime is approximately 10–100 times larger than that of **CC(non-full)**, which only performs quantile regression using \mathcal{D}_{cal} (see [Appendix B.2](#)). To mitigate the excessive computational burden caused by the large number of test samples, we therefore adopt **CC(non-full)** as the **CC** baseline in this section.

In this experiment, we set the number of equidistant partition sets to $|\mathcal{J}| = 100$ when computing $\sqrt{\text{MSCE}}$ and the number of balls to $n_B = 50$ when evaluating worst-case coverage. For the metric *Set Size*, we compute the set size $|\widehat{C}(x)|$ in closed form for both ellipsoidal and box prediction sets.

Ellipsoidal sets. For the baseline methods, the prediction set takes the form $\widehat{C}(x) = \{y \in \mathbb{R}^{d_y} : (y - \mu_0(x))^\top \Sigma_0^{-1} (y - \mu_0(x)) \leq q(x)\}$, whose volume is given by

$$|\widehat{C}(x)| = \frac{\pi^{d_y/2}}{\Gamma\left(\frac{d_y}{2} + 1\right)} q(x)^{d_y/2} \det(\Sigma_0)^{1/2},$$

where $\Gamma(\cdot)$ is the standard Gamma function. For our **MOPI**, the volume of prediction set is

$$|\widehat{C}(x)| = \frac{\pi^{d_y/2}}{\Gamma\left(\frac{d_y}{2} + 1\right)} \det(\Sigma_0 \Sigma(x))^{1/2}.$$

Box sets. For the baseline methods, the prediction set is defined as $\widehat{C}(x) = \{y \in \mathbb{R}^{d_y} : \|(y - \mu_0(X))/\sigma_0(X)\|_\infty \leq q(x)\}$, which corresponds to an axis-aligned box with side lengths $2q(x)\sigma_{0,j}(x)$ along each coordinate. Its volume is

$$|\widehat{C}(x)| = \prod_{j=1}^{d_y} 2q(x)\sigma_{0,j}(x).$$

For our MOPI, the volume of prediction set is

$$|\widehat{C}(x)| = \prod_{j=1}^{d_y} 2\sigma_{0,j}(x)\sigma_j(x).$$

For each method, all tuning parameters are selected by minimizing the average $\sqrt{\text{MSCE}}$ over 10 replications of the entire experiment with different random seeds. These seeds are distinct from those used in the reported experiments.

F.2 Experiment details of Section 5.2

We first describe Setting 2 in detail: $Y_i \mid \{X_i, Z_i = z\} \sim N(\mu_z(X_i), \sigma_z^2(X_i))$, $Z_i \mid X_i \sim \text{Cat}(\pi_1(X_i), \dots, \pi_4(X_i))$, where Cat is the categorical distribution. The mixing weights $\{\pi_z(X_i)\}_{k=1}^4$ are defined through a softmax model

$$\pi_z(X_i) = \frac{\exp(X_i^\top \gamma_z)}{\sum_{\ell=1}^4 \exp(X_i^\top \gamma_\ell)}, \quad z = 1, \dots, 4,$$

with coefficient vectors $\gamma_z \in \mathbb{R}^{d_x}$.

$$\mu_z(X_i) = X_i^\top a_z + 0.5 \sin^2(X_{i,1}), \quad \sigma_z(X_i) = |X_i^\top \delta_z| + c_z.$$

Here, $a_z, \delta_z \in \mathbb{R}^{d_x}$ are fixed coefficient vectors and $c_z > 0$ are component-specific constants.

In this experiment, since the support of Z is relatively small, we set the test sample size

to $|\mathcal{D}_{\text{test}}| = 500$. Due to the relatively small $|\mathcal{D}_{\text{test}}|$, we can adopt the full conformal version of the CC method in this section, following [Gibbs et al. \(2025\)](#). All tuning parameters are selected by minimizing the average $\sqrt{\text{MSCE}}$ over 10 replications of the entire experiment with different random seeds, which are distinct from those used in the reported experiments. Here,

$$\sqrt{\text{MSCE}} = \left\{ |\mathcal{Z}|^{-1} \sum_{z \in \mathcal{Z}} \left(n_z^{-1} \sum_{i \in \mathcal{D}_{\text{test}}} \mathbb{1}\{Z_i = z, Y_i \notin \hat{C}(X_i)\} - \alpha \right)^2 \right\}^{1/2},$$

where $n_z = \sum_{i \in \mathcal{D}_{\text{test}}} \mathbb{1}\{Z_i = z\}$. Since Z is a sensitive variable, our simulation setting restricts its usage as follows: Z is not available during pretraining or when constructing prediction intervals. It is only used in the calibration stage, where it helps learn a more accurate threshold function $h(x)$. In our framework, we can leverage the sensitive variable Z by solving (8). However, since Z is unobservable for the test samples, algorithms such as CC, SCP, and RLCP cannot leverage Z in their calibration procedures. Hence, for CC, SCP, and RLCP, prediction sets can only be constructed using X .

F.3 Simulation results for one-dimensional label

In this section, we consider the sublevel set (7) for all baseline methods and MOPI. In each replication, we independently generate pretraining, calibration, and test datasets from the same distribution. We use a pretraining set of size $|\mathcal{D}_{\text{pre}}| = 3,000$ to train $\hat{\mu}$ via linear regression with score $s(x, y) = |y - \hat{\mu}(x)|$, a calibration set of size $|\mathcal{D}_{\text{cal}}| = 1,500$ to construct prediction sets, and a test set of size $|\mathcal{D}_{\text{test}}| = 5,000$ for evaluation.

F.3.1 Test-conditional coverage

We first focus on test-conditional coverage, that is $Z = X = (X_1, \dots, X_6)^\top$. Consider a heteroscedastic regression model $Y = \sum_{j=1}^6 \frac{1}{\sqrt{6}} X_j + e(X)$ with X_1 independently drawn from

$\text{Unif}(0, 5)$, and X_2, \dots, X_6 independently drawn from $N(0, 1)$. The noise term is generated as $e(X) \sim N(0, \sigma^*(X)^2)$ and we consider the following three different settings:

- **Setting 1**(x): $\sigma^*(X)^2 = 1 + X_1^2 + 0.5 \times \sin\left(\sum_{j=2}^6 X_j\right)$;
- **Setting 2**(x): $\sigma^*(X)^2 = 1 + 0.2 \times \sum_{j=1}^6 \sin^2(X_j) + \sum_{j=1}^6 X_j^2 \cdot \mathbb{1}\left\{\sum_{j=1}^6 X_j > 3\right\}$.
- **Setting 3**(x): $\sigma^2(X_i) = 2 - \mathbb{1}\{X_{i,1} < 1.2\} + 5\mathbb{1}\{X_{i,1} > 3\} + 2\mathbb{1}\{X_{i,3} > 0\} + 3\mathbb{1}\{X_{i,5} > 0.5\}$.

In Setting 1(x), the variance depends only on the first coordinate X_1 , whereas in Setting 2(x), it depends on all coordinates. In Setting 3(x), the variance follows a discrete structure. We choose \mathcal{F} and \mathcal{H} as the same RKHS. All tuning parameters are selected by minimizing the average $\sqrt{\text{MSCE}}$ over 10 replications of the entire experiment with different random seeds. These seeds are distinct from those used in the reported experiments.

Computation of evaluation metrics. In our simulation studies, when computing the worst-case coverage, we set the number of random balls to $|\mathcal{B}| = 50$ and the radius to $r = \sqrt{2d_{\mathcal{X}}}$, where $d_{\mathcal{X}}$ denotes the dimension of the covariates X . For the multi-dimensional settings with $d_{\mathcal{X}} = 6$ or 11, the $\sqrt{\text{MSCE}}$ is approximated using equidistant partition sets constructed only along the first coordinate X_1 . This choice is motivated by two considerations: first, $X_1 \sim U(0, 5)$, and from the variance expressions in simulation scenarios Setting 1(x), 2(x), and 3(x), it is clear that the variance contribution from X_1 dominates. Second, constructing equidistant partition sets over the full feature space would result in an extremely large number of partitions, rendering the computation prohibitively expensive.

Table F.1 shows that MOPI basically maintains marginal coverage validity while achieving the highest worst-case coverage and the lowest MSCE. Figure F.1 presents prediction intervals for the one-dimensional X . Compared with CC, MOPI yields intervals that more

closely align with the oracle, exhibit fewer uncovered cases, as highlighted in the zoomed-in region of Figure F.1. Compared with RLCP, MOPI and CC produce smoother intervals as x varies, enhancing practical usability.

Table F.1: Coverage metrics and set size under different variance settings with $d_{\mathcal{X}} = 6$.

Methods	Setting 1(x)				Setting 2(x)				Setting 3(x)			
	<i>Marginal</i>	<i>Worst-case</i>	$\sqrt{\text{MSCE}}$	<i>Set size</i>	<i>Marginal</i>	<i>Worst-case</i>	$\sqrt{\text{MSCE}}$	<i>Set size</i>	<i>Marginal</i>	<i>Worst-case</i>	$\sqrt{\text{MSCE}}$	<i>Set size</i>
MOPI	0.888	0.865	0.050	4.492	0.891	0.865	0.049	3.046	0.888	0.865	0.054	4.075
CC	0.883	0.858	0.056	4.480	0.883	0.857	0.055	3.005	0.882	0.859	0.062	4.069
RLCP	0.900	0.815	0.094	4.955	0.901	0.811	0.076	3.320	0.900	0.846	0.066	4.249
SCP	0.900	0.796	0.113	5.090	0.900	0.788	0.095	3.351	0.899	0.831	0.075	4.251

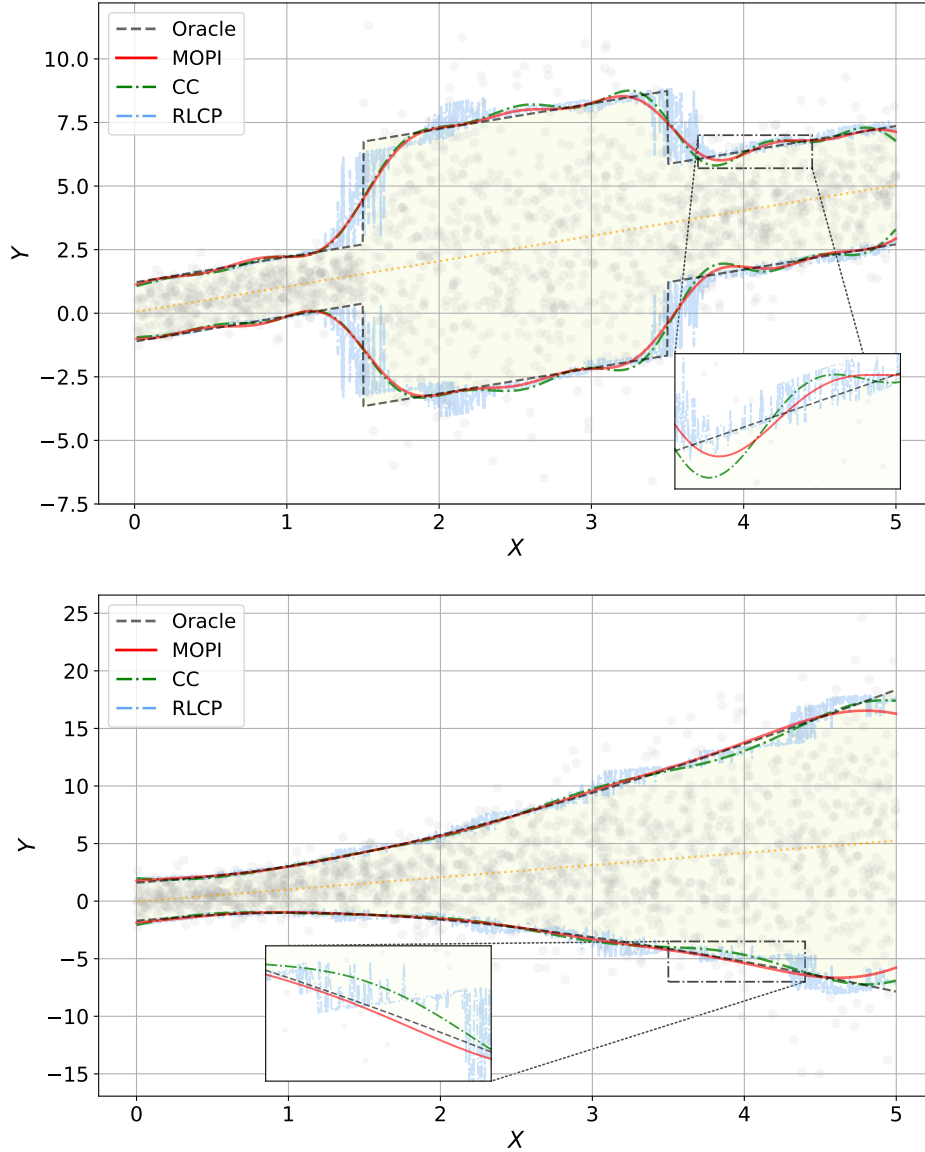


Figure F.1: Prediction intervals produced by each method under the univariate settings. We generate $X \sim U(0, 5)$ and $Y | X \sim N(X, \sigma^2(X))$. Up: $\sigma^2(X) = 0.5 \cdot \mathbb{1}\{X < 1.5\} + 10 \cdot \mathbb{1}\{1.5 \leq X < 3.5\} + 2 \cdot \mathbb{1}\{3.5 \leq X\}$; Down: $\sigma^2(X) = 1 + X^3/2$. The orange solid line represents the linear regression model $\hat{\mu}$ fitted on the training data; the colored dashed lines denote the prediction intervals constructed by the different methods; and the black dashed line corresponds to the oracle prediction interval.

Additionally, we consider Setting 1(x), Setting 2(x) and Setting 3(x) with $d_{\mathcal{X}} = 11$. From Tables F.2, we observe that MOPI achieves the highest worst-case coverage and the smallest MSCE while maintaining basically valid marginal coverage. These results indicate that, for the settings studied in our experiments, MOPI provides improved test-conditional coverage

performance under heterogeneous variance structures and varying covariate dimensions.

Table F.2: Coverage metrics and set size for $d_{\mathcal{X}} = 11$ under Settings 1(x), 2(x), and 3(x).

Methods	Setting 1(x)				Setting 2(x)				Setting 3(x)			
	<i>Marginal</i>	<i>Worst-case</i>	$\sqrt{\text{MSCE}}$	<i>Set size</i>	<i>Marginal</i>	<i>Worst-case</i>	$\sqrt{\text{MSCE}}$	<i>Set size</i>	<i>Marginal</i>	<i>Worst-case</i>	$\sqrt{\text{MSCE}}$	<i>Set size</i>
MOPI	0.896	0.884	0.056	4.546	0.896	0.885	0.053	3.159	0.895	0.885	0.054	4.155
CC	0.885	0.868	0.056	4.466	0.882	0.870	0.056	3.033	0.888	0.875	0.057	4.067
RLCP	0.901	0.823	0.100	5.027	0.900	0.836	0.069	3.313	0.901	0.852	0.068	4.263
SCP	0.900	0.813	0.112	5.099	0.900	0.826	0.078	3.332	0.900	0.844	0.075	4.258

F.3.2 Group-conditional coverage

Align with the simulation of test-conditional coverage, we investigate Setting 1(x) and Setting 2(x). To evaluate group-conditional coverage, we consider a collection of overlapping complex groups $\mathcal{G} = \{G_1, \dots, G_4\}$, where $G_1 = \{x : x_1 + x_6 \geq 3\}$, $G_2 = \{x : \sin(x_5) + x_1^2 \geq 3.5\}$, $G_3 = \{x : |x_2| + 3|x_4| + |x_6| + 2|x_3| \leq 3\sqrt{x_1}\}$, and $G_4 = \{x : 4x_3^2 + x_5^2 + 2x_2^2 - x_1^2 \leq x_1\}$. Let $Z = (\mathbb{1}\{X \in G_1\}, \dots, \mathbb{1}\{X \in G_4\})^T$. For a fair comparison, we choose the solving space of CC, \mathcal{F} and \mathcal{H} of MOPI to be $\{\sum_{z \in \mathcal{Z}} \beta_z \mathbb{1}\{Z = z\} : \beta_z \in \mathbb{R}, z \in \{0, 1\}^{2^{|\mathcal{G}|}}\}$. For RLCP, we also choose the Gaussian kernel. From Figure F.2, F.3 and F.4, we observe that both MOPI and CC achieve accurate group-conditional coverage under both the disjoint and overlapping group structures, whereas RLCP and SCP exhibit comparatively inferior performance.

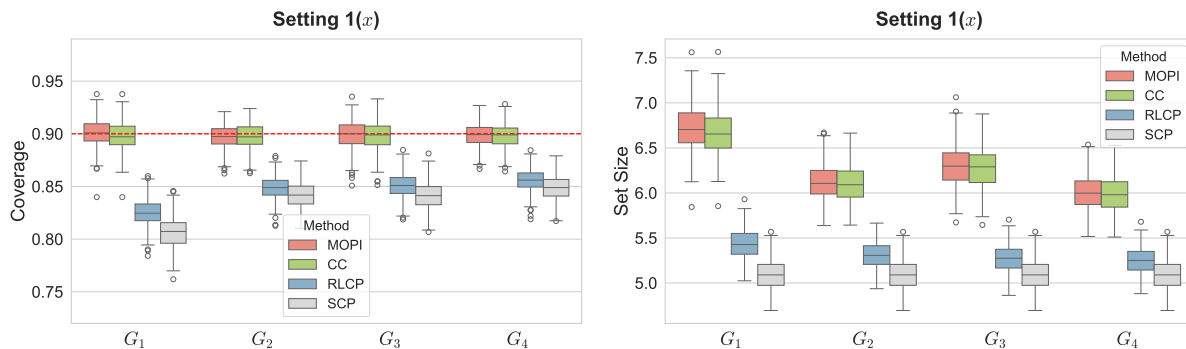


Figure F.2: Group-conditional coverage and set size under Setting 1(x) with $d_{\mathcal{X}} = 6$.

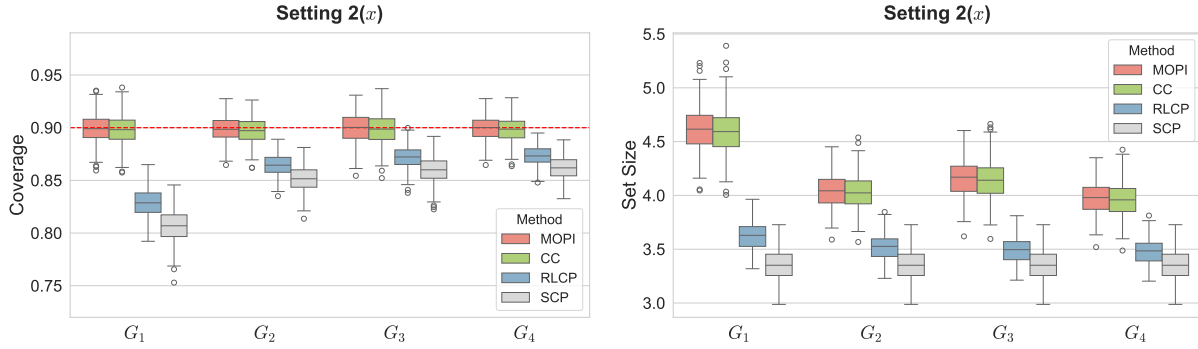


Figure F.3: Group-conditional coverage and set size under Setting $2(x)$ with $d_{\mathcal{X}} = 6$.

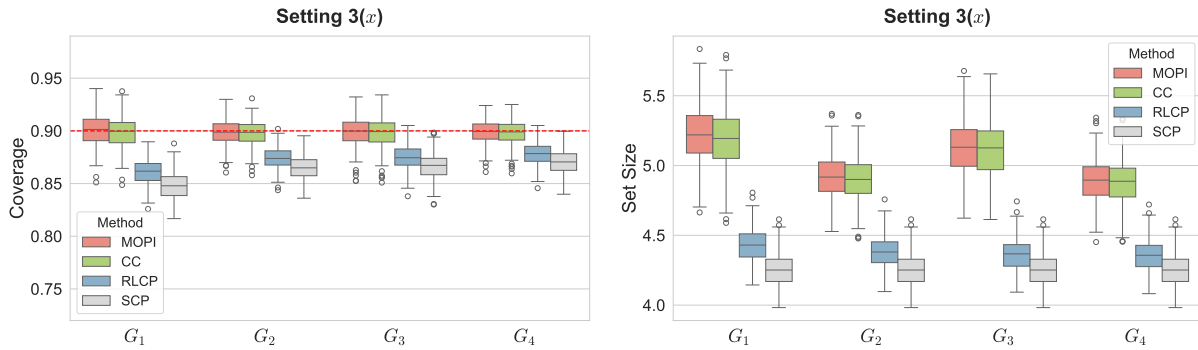


Figure F.4: Group-conditional coverage and set size under Setting $3(x)$ with $d_{\mathcal{X}} = 6$.

G Additional Real Data Results

G.1 Experiment details of Section 6.1

Pretrained models. For *ellipsoidal sets*, SCP, CC, and RLCP use the score $s(x, y) = (y - \mu_0(x))^\top \Sigma_0^{-1}(x)(y - \mu_0(x))$ and prediction sets of the form $\hat{C}(x) = \{y : s(x, y) \leq \hat{h}(x)\}$. Here the regression function $\mu_0(x)$ is pretrained using a random forest, while $\Sigma_0^{-1}(x) = L_0(x)L_0(x)^\top$ is obtained from a neural network that predicts the Cholesky factor $L^*(x)$ of $(\Sigma^*)^{-1}(x)$. The network takes x as input and outputs the lower-triangular entries of $L_0(x)$, with positivity of the diagonal enforced via a Softplus transformation. The network L_0 is

pretrained by minimizing the Gaussian negative log-likelihood

$$\min_L \frac{1}{n_{\text{pre}}} \sum_{i=1}^{n_{\text{pre}}} \left[\frac{1}{2} (Y_i - \mu_0(X_i))^\top (L(X_i)L(X_i)^\top) (Y_i - \mu_0(X_i)) - \frac{1}{2} \log \det(L(X_i)L(X_i)^\top) \right],$$

where $\log \det(L(x)L(x)^\top) = 2 \sum_j \log L_{jj}(x)$ since $L(x)$ is lower triangular.

G.2 Additional results for Communities and Crime dataset

We report additional group-conditional coverage results. We focus on subpopulations with high racial representation, defining a community as “high-representation” for a given racial group if that group’s share in the community exceeds the 70th percentile. As shown in Figure G.1, in both the masked and unmasked cases, MOPI attains more accurate and more equitable coverage across these “high-representation” subpopulations compared with the baseline methods.

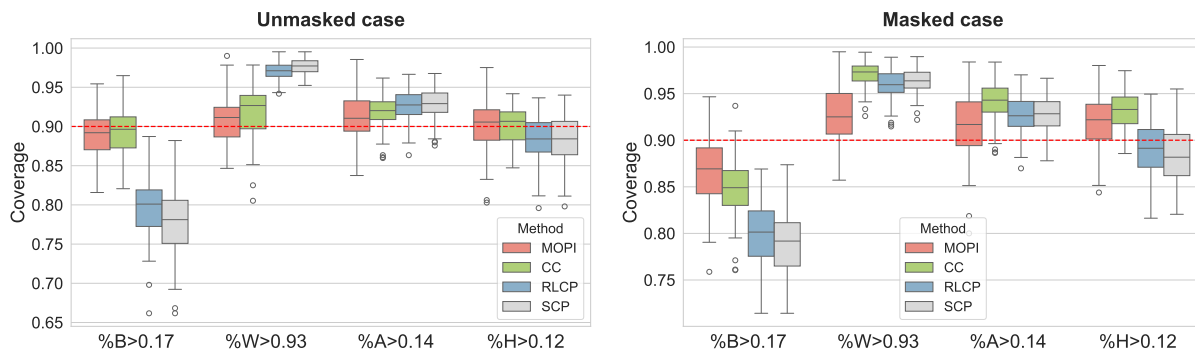


Figure G.1: Group-conditional coverage for communities and crime dataset. The letters B, W, A, and H refer to the racial categories “Black”, “White”, “Asian”, and “Hispanic”, respectively.

G.3 Medical Insurance Dataset

This dataset ¹ contains 3,630 records of medical charges and demographic attributes (age, BMI, number of children, sex, and smoking status). We use $Y = \log(\text{charges})$ as the label

¹<https://www.kaggle.com/datasets/rajgupta2019/medical-insurance-dataset>

variable and take $X_{\text{all}} = (X_{\text{age}}, X_{\text{BMI}}, X_{\text{children}}, X_{\text{sex}}, X_{\text{smoking}})$ as the feature vector. We consider the sublevel set (7) for all baseline methods and MOPI and split the data into three parts. The first 2000 samples are used to pretrain a random forest predictor μ , and we define the score function as $s(x, y) = |y - \mu(x)|$. The second 1080 samples are used to construct the prediction set and the rest 550 samples are used as test data. Here, we consider two experimental settings, the *unmasked* case and the *masked* case. The experiment is repeated 100 times with random train-calibration-test splits, and the target coverage level is $1 - \alpha = 0.9$.

In the *unmasked* case, all features are available at prediction time, corresponding to $X = Z = X_{\text{all}}$. In this case, we evaluate whether each demographic subgroup achieves the target coverage level. For a fair comparison, we set the function classes \mathcal{H} , \mathcal{F} in MOPI, and the search space in CC as RKHS with a Gaussian kernel. To avoid uninformative intervals in RLCP, we tune the kernel bandwidth such that their proportion is below 10%, and exclude these intervals when reporting lengths. We consider marginal coverage and group-conditional coverage, which include two simple groups and two complex groups: (1) *Smoker*: $X_{\text{smoking}} = 1$; (2) *Male*: $X_{\text{sex}} = 1$; (3) *BFR > 40%*: individuals with a body fat ratio (BFR) exceeding 40%, corresponding to the extremely obese group. $\text{BFR} = (1.2 \cdot X_{\text{BMI}} + 0.23 \cdot X_{\text{age}} - 10.8 \cdot X_{\text{sex}} - 5.4) \%$, see [Deurenberg et al. \(1991\)](#); (4) *Male, BFR > 24%*: obese males, defined as those with $X_{\text{sex}} = 1$ and $\text{BFR} > 24\%$. Figure G.2 shows that MOPI achieves near-perfect coverage guarantees with reasonable set sizes.

In the *masked* case, the gender attribute is treated as a sensitive variable that is unavailable for the test points. Here, we let $Z = X_{\text{sex}}$ and $X = X_{\text{all}} \setminus X_{\text{sex}}$, and assess whether the methods achieve *equalized coverage* across the two gender groups despite the sensitive attribute being unobserved at prediction time. Figure G.3 reports the coverage for the **Male** and **Female** groups under both experimental settings. Our MOPI method achieves nearly perfect coverage in both the unmasked and the masked settings, whereas the other

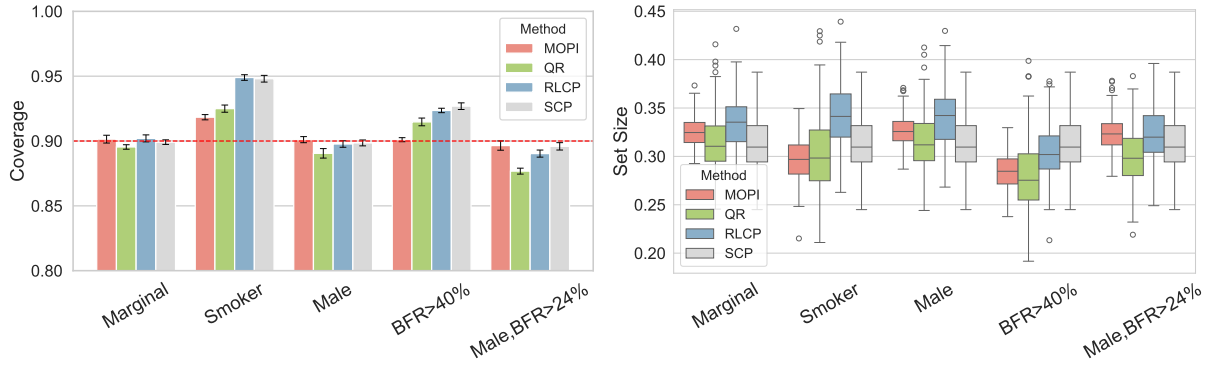


Figure G.2: Performance comparison under medical insurance charges dataset. Left: marginal and group-conditional coverage; Right: corresponding set size.

baselines exhibit noticeable coverage gaps when the sensitive attributes are masked.

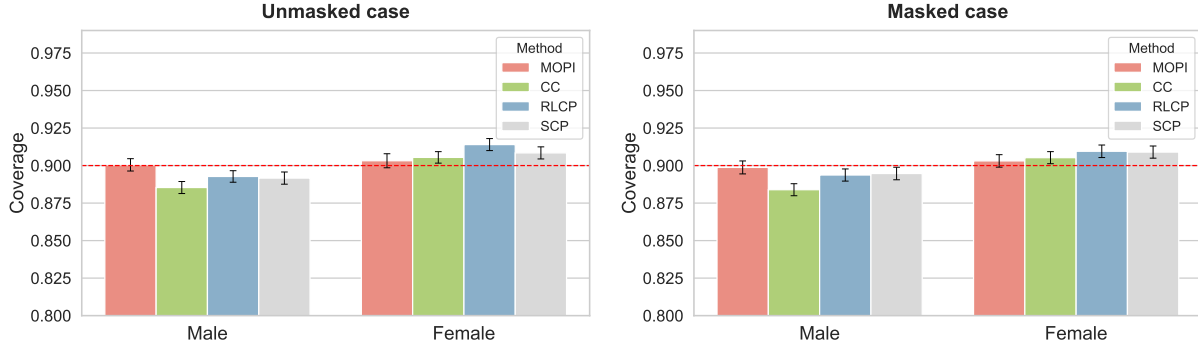


Figure G.3: Coverage on the Male and Female groups for Medical Insurance Dataset.

G.4 FashionMNIST Dataset

The dataset (Xiao et al., 2017) contains 70,000 grayscale images of clothing items (28×28 pixels), evenly distributed across ten categories such as T-shirts, shoes, and bags. We consider the sublevel set (7) for all baseline methods and MOPI. The data are partitioned into training, calibration, and test sets in a ratio of 4 : 1 : 1. We train a convolutional neural network (CNN) $\pi(x) : \mathcal{X} \mapsto [0, 1]^{|D|}$, consisting of two convolutional layers (each followed by max-pooling, ReLU, and dropout), and two fully connected layers of sizes $320 \rightarrow 20$ and $20 \rightarrow 10$, mapping the flattened features to 10 logits for classification. The 20-dimensional output of the penultimate layer is used as the feature representation. We use the adaptive prediction sets (APS) score (Romano et al., 2019), $S(x, y) := \sum_{i: \pi_i(x) > \pi_y(x)} \pi_i(x)$.

We set \mathcal{H} , \mathcal{F} in MOPI, and the solve space in CC to be RKHSs with a Gaussian kernel. For PLCP proposed by Kiyani et al. (2024a), the prediction set is obtained by solving

$$g^*, \mathbf{q}^* = \underset{\mathbf{q} \in \mathbb{R}^m}{\operatorname{argmin}} \frac{1}{n} \sum_{g \in \mathcal{G}} \sum_{j=1}^n \sum_{i=1}^m g_i(X_j) \cdot \ell_\alpha(q_i, S_j), \quad (\text{G.1})$$

where $\ell_\alpha(\cdot, \cdot)$ is pinball loss. Following the PLCP setting in Kiyani et al. (2024a), we parameterize g with $m = 8$ groups using a CNN with three convolutional layers and two fully connected layers. In addition to marginal coverage and worst-case conditional coverage, we also evaluate the absolute cluster-conditional coverage gap (*Cluster-cond-gap*) and the absolute predicted-class conditional coverage gap (*Class-cond-gap*). For *Cluster-cond-gap*, we apply k -means clustering (with $k = 5$) to the feature representations and compute the average absolute coverage gap across the resulting clusters. For *Class-cond-gap*, we measure coverage within each predicted class and then take the mean of the average absolute coverage gap over all predicted classes. From Table G.1 and the Figure G.4, our method achieves marginal validity while attaining the best performance across all metrics that reflect conditional coverage.

Table G.1: Coverage metrics comparison under FashionMNIST dataset.

Methods	<i>Marginal</i>	<i>Worst-case</i>	<i>Cluster-cond-gap</i>	<i>Class-cond-gap</i>	<i>Set size</i>
MOPI	0.910	0.851	0.021	0.036	2.294
CC	0.893	0.814	0.028	0.048	1.922
PLCP	0.907	0.825	0.021	0.050	2.049
SCP	0.894	0.802	0.036	0.053	1.928

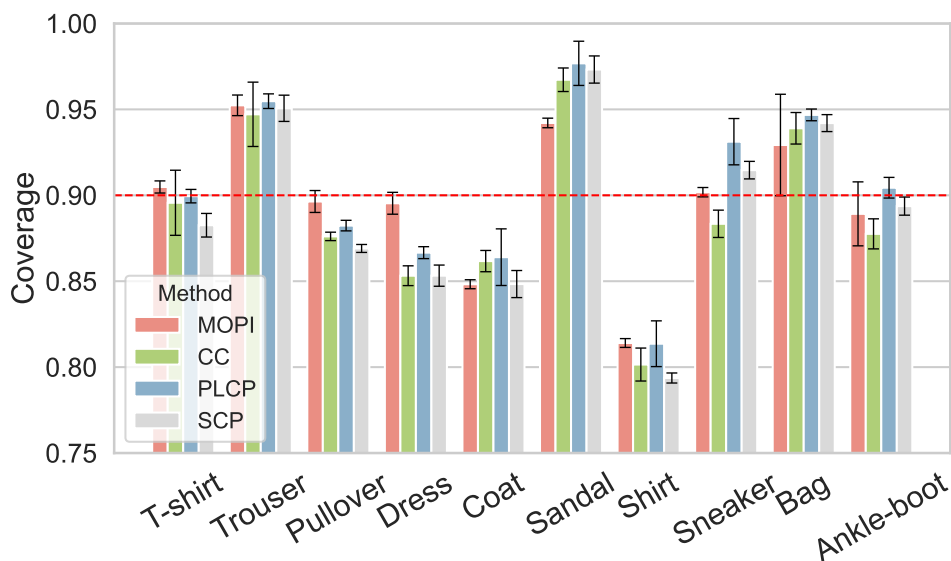


Figure G.4: Predicted class-conditional coverage of the FashionMNIST dataset.

References

- Bartlett, P. L., Bousquet, O., and Mendelson, S. (2005), “Local Rademacher complexities,” *The Annals of Statistics*, 33, 1497 – 1537.
- Bousquet, O. (2003), “Concentration inequalities for sub-additive functions using the entropy method,” in *Stochastic Inequalities and Applications*, Springer, pp. 213–247.
- Deurenberg, P., Weststrate, J. A., and Seidell, J. C. (1991), “Body mass index as a measure of body fatness: age-and sex-specific prediction formulas,” *British Journal of Nutrition*, 65, 105–114.
- Duchi, J. (2025), “Sample-Conditional Coverage in Split-Conformal Prediction,” in *The Thirty-ninth Annual Conference on Neural Information Processing Systems*.
- Foster, D. J. and Syrgkanis, V. (2023), “Orthogonal statistical learning,” *The Annals of Statistics*, 51, 879–908.
- Gibbs, I., Cherian, J. J., and Candès, E. J. (2025), “Conformal prediction with conditional guarantees,” *Journal of the Royal Statistical Society Series B: Statistical Methodology*, 87, 1100–1126.
- Kiyani, S., Pappas, G. J., and Hassani, H. (2024), “Conformal prediction with learned features,” in *International Conference on Machine Learning*, PMLR, pp. 24749–24769.
- Redmond, M. and Baveja, A. (2002), “A data-driven software tool for enabling cooperative information sharing among police departments,” *European Journal of Operational Research*, 141, 660–678.
- Romano, Y., Patterson, E., and Candès, E. (2019), “Conformalized quantile regression,” *Advances in Neural Information Processing Systems*, 32, 1–11.

- Schölkopf, B., Herbrich, R., and Smola, A. J. (2001), “A generalized representer theorem,” in *International Conference on Computational Learning Theory*, Springer, pp. 416–426.
- Van Der Vaart, A. W. and Wellner, J. A. (2023), *Weak Convergence and Empirical Processes: With Applications to Statistics*, Springer Nature.
- Wainwright, M. J. (2019), *High-Dimensional Statistics: A Non-Asymptotic Viewpoint*, vol. 48, Cambridge University Press.
- Xiao, H., Rasul, K., and Vollgraf, R. (2017), “Fashion-mnist: a novel image dataset for benchmarking machine learning algorithms,” *arXiv preprint arXiv:1708.07747*.
- Zhou, D.-X. (2002), “The covering number in learning theory,” *Journal of Complexity*, 18, 739–767.